AFOSC USER MANUAL

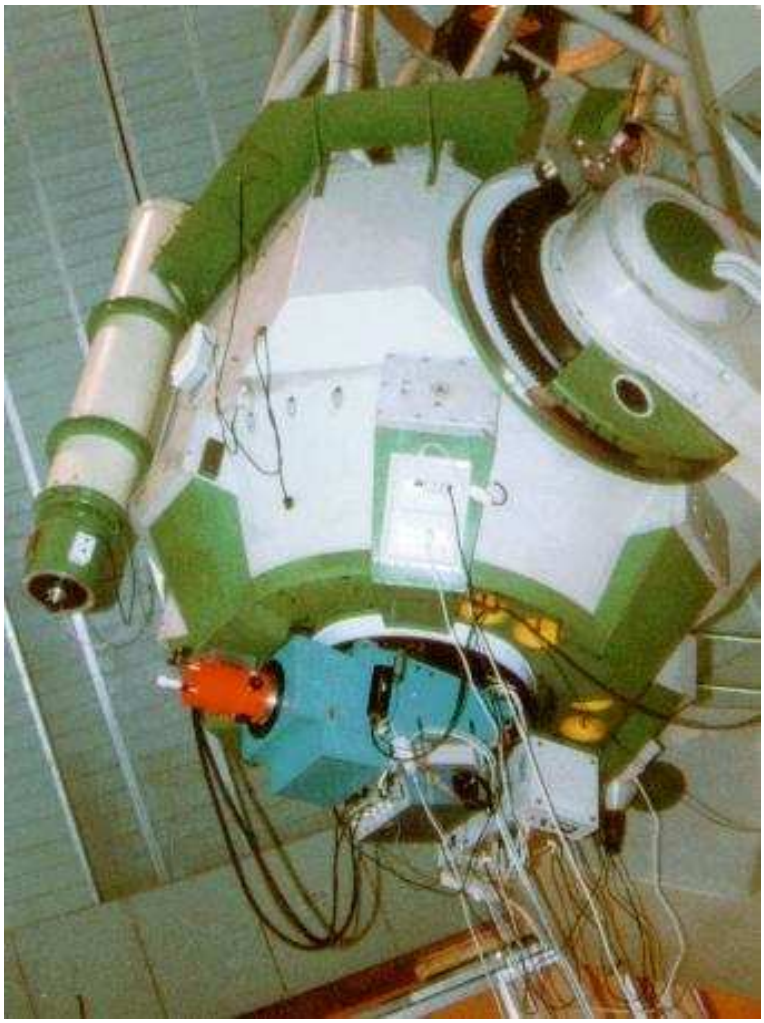

S. Desidera, D. Fantinel, E. Giro, H. Navasardyan

Osservatorio Astronomico di Padova

Version 1.2

July 2003

Introduction

This manual describes the Asiago Faint Object Spectrograph and Camera (AFOSC) mounted at the 1.82 m M. Ekar Telescope.

It is intended as a general guide for the observer, both during the preparation of the observations and during an observing run.

Chapter 1 briefly describes the 1.82 m telescope; Chapter 2 presents the AFOSC instrument with all its components; Chapter 3 gives the instrument performances; Chapter 4 describes the Graphical User Interface (GUI); Chapter 5 introduces the quick look analysis tools; Chapter 6 overviews some possible problems that might occur during observations and the ways to overcome them. The efficiency curves for the grisms, the atlas for wavelength calibration, the instructions for the preparation of the instrument set–up, and an example of FITS header are reported as appendices. The version1.1 includes the description of the Volume Phase Holographic Gratings (VPH) recently installed and partially tested at the telescope, the performances of the guide camera after the change of its position, and some minor modification with respect to the version1.0 (January 2002). In July - August 2002 a refurbishment of AFOSC control system is being performed. The main difference of this version is the updated part of the detector characteristics due to the replacement of CCD (1 July 2003). Some of the calibration presented here (e.g. AFOSC camera focus, etc.) need an update.

Asiago, July 2003

Abbreviations and Acronyms

AFOSC	Asiago Faint Object Spectrograph and Camera
ALFOSC	AndaLusian Faint Object Spectrograph and Camera
B&C	Boller and Chievens Spectrograph
BFOSC	Bologna Faint Object Spectrograph and Camera
CD	Cross Disperser
DFOSC	Danish Faint Object Spectrograph and Camera
DG	Differential Guiding
ES	Echelle Slit
FITS	Flexible Image Transport System
FM	Folding Mirror
GSC	Guide Star Catalog
GUI	Graphical User Interface
IDL	Interactive Data Language
IRAF	Image Reduction and Analysis Facility
M1	Primary Mirror (of the telescope)
M2	Secondary Mirror (of the telescope)
MF	Mask Focus (pinhole)
MIDAS	Munich Image Data Analysis System
OS	Order Separator
PM	Polarimetric Mask
TNG	Telescopio Nazionale Galileo
ToO	Target of Opportunity
VME	Versa Module Europa
VPH	Volume Phase Holographic

Contents

Chapter 1

The 1.82 m. Ekar Telescope

1.1 Introduction

The 182 cm telescope is the major instrument at the observing station of Cima Ekar (1350 m). The telescope is located at East Longitude +00h 46m 17.13s (± 0.03s) and Latitude +45d 50' 36.2" (± 0.03") (Barbieri & Galazzi 1973).

Its construction was completed in 1973. On 1997 November the observatory at Cima Ekar has been dedicated to prof. Leonida Rosino (Treviso 1915–Padova 1997).

Fig. 1.1– 1.2 show the dome and the telescope in 1980 pictures.

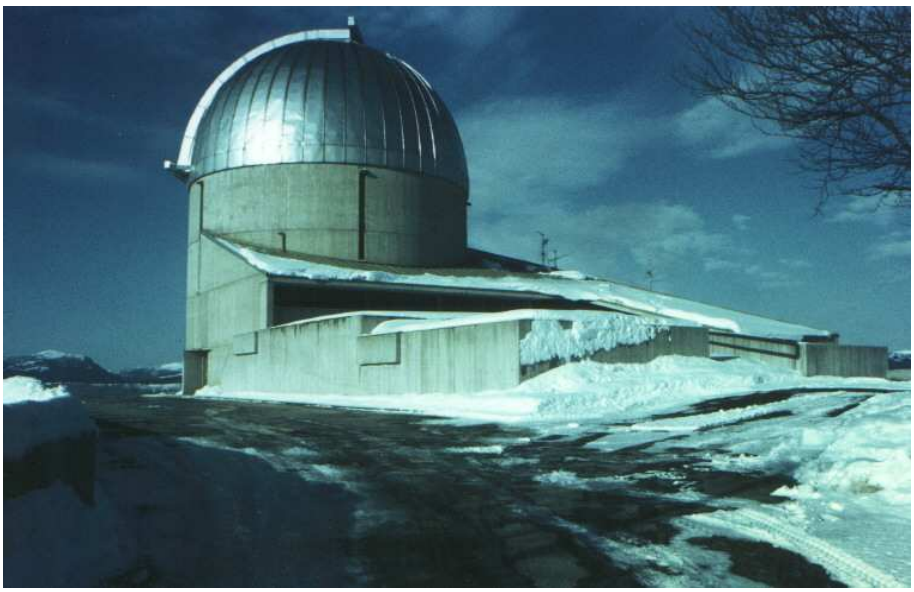

Figure 1.1: The dome of 1.82 m telescope at M. Ekar.

Figure 1.2: The 1.82 m telescope at M. Ekar.

1.2 Telescope characteristics

1.2.1 Opto-mechanical characteristics

Table 1.1 lists the basic optical parameters of the telescope (from Barbieri & Galazzi 1973). The mounting of the telescope is equatorial. The secondary mirror can be moved for the focusing, decentering and tilting to fine optical alignment (Sect. 1.4).

1.2.2 Movements

The telescope can be moved at three velocities:

- Large: 3000 arcsec/s
- Medium: 200 arcsec/s
- Micro: 2 arcsec/s

The pointing is performed by moving the telescope until the required position is reached. The telescope is in tracking when MICRO or MEDIUM movements are inserted.

Parameter	Value
Mounting	Equatorial
M1 Diameter	1820 mm
Central Hole Diameter	383 mm
Material	Schott Glass Duran 50
Thickness (at edges)	300 mm
Weight	1500 kg
Curvature Radius	10840 mm
Focal Ratio	f/3
M1 Clear Area	$\sim$ 2300000 mm^2
M2 Diameter	580 mm
Material	Schott Glass Duran 50
Thickness (at edges)	110 mm
Weight	67 kg
Curvature Radius	4592 mm
Focal Ratio	f/9
Scale	12.6 arcsec/mm

Table 1.1: Characteristics of the 1.82 m. Ekar telescope.

1.2.3 The Rotator-Adapter

The Rotator Adapter represents the interface between the telescope and the instrumentation. Furthermore, it hosts the guide probe and the calibration arm.

The rotator adapter can be rotated at any angle, allowing to observe an object at any position angle. A 90 degrees rotation is performed in less than 1 minute. The accuracy of the positioning is within 1 arcmin.

The rotation, the guide probe and the calibration arm can be controlled from the AFOSC GUI (see Sect. 4.7–4.10).

The Guide Probe

The guide probe is the system carrying on the guide camera. A folding mirror (FM1) at 45 deg with respect to the optical axis of the telescope re-directs the beam toward the guide camera on the rotator adapter plane.

The probe can be moved along two axes, covering a horse–shoe shaped area around the optical axis of the telescope.

When the calibration arm is inserted, the probe is parked in a corner to avoid collisions.

The Calibration Arm

The lamps for the wavelength calibration are attached to the integrating sphere, that ensure the homogeneity of the beam. The integrating sphere is positioned below the rotator adapter. The optical system of the calibration arm consists of the following elements:

- The light from the integrating sphere is directed toward the calibration arm by a folding mirror (FM4)
- A lens (focal length 8 cm) transforms the beam in f/9 (as that of the telescope)
- A folding mirror (FM5) redirects the beam toward AFOSC

When a calibration sequence is completed, the calibration arm is parked in a position far from the telescope optical axis, avoiding collisions with the probe.

1.2.4 The Guide Camera

Auto-Guiding is achieved by using a star outside the instrument field of view. A folding mirror inside the rotator adapter re-directs the light toward the guide camera. The useful area is horse-shoe shaped around the scientific field (see Fig 4.6) (25 x 45 arcmin). The repeatability in positioning a star in the guide camara focal plane is about 0.1 arcsec. The main characteristics of the guide camera are listed in Table 1.2. Limiting magnitude (~ 17) was estimated by identification of stars using GSC. The whole field of view of the guide camera is useful for guiding, being free of strong optical aberrations. The orientation of the guide camera as appers on the monitor in the control room is North up and West left.

The procedure to find the guide star and to start auto–guide is described in Sect. 4.7–4.8.

Parameter	Value
Type	MCP + *Fosfori* + CCD
Array size	256 x 256
Pixel scale	arcsec/pix
Useful field	2.0 x 2.3 arcmin
Limiting magnitude	~ 17
Integration time	≥ 5 ms

Table 1.2: Guide Camera characteristics.

1.2.5 Instrumentation

Two instruments are currently offered: the imager and low resolution spectrograph AFOSC, described in this manual, and the high resolution ECHELLE spectrograph (Munari 1988, Munari & Zwitter 1994).

Both instruments are mounted at the Cassegrain focus of the telescope. AFOSC is usually offered during lunar dark and grey times and the echelle spectrograph during lunar bright time.

Mounting users instrumentation at the Cassegrain focus, using the adapter of the decommissioned CCD camera, can be admitted in special cases.

1.3 Telescope Performances

1.3.1 Pointing

The typical pointing error of the telescope is about 2–3 arcmin (Fig. 1.3-1.6), after the set–point procedure has been done at the beginning of the night. This estimate does not include any correction for the atmospheric refraction or telescope flexures. The support system of the secondary mirror shows remarkable mechanical flexures depending on the pointing direction[1].

Performing set–point at the beginning of the night is strongly recommended in order to improve the pointing performances. This can be done using the OFFSET and TELESCOPE windows of the AFOSC GUI (see Sect. 4.12).

The resolution of the encoders is of about 4 arcsec. Therefore it is not possible to point the telescope with a precision better than this using the encoders.

[1] At the present a pointing model is not yet available.

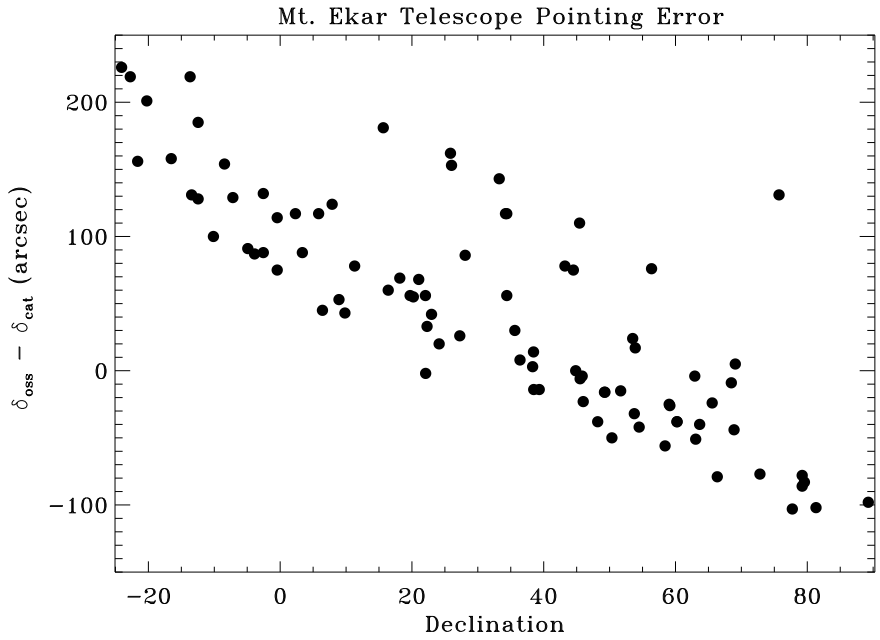

Figure 1.3: Pointing errors in declination as a function of the declination of the target, after set–point has been performed at beginning of the night.

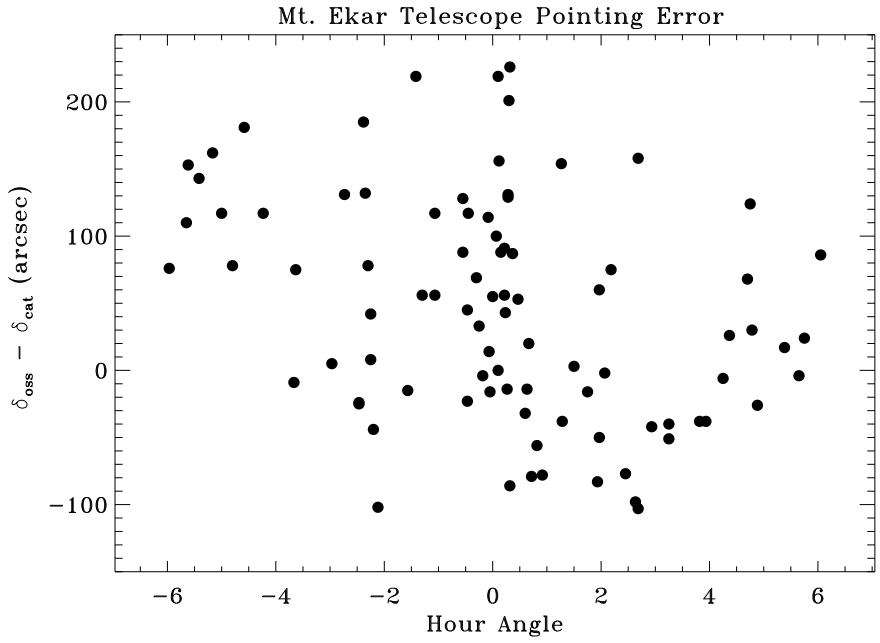

Figure 1.4: Pointing errors in declination as a function of hour angle of the target, after set–point has been performed at beginning of the night.

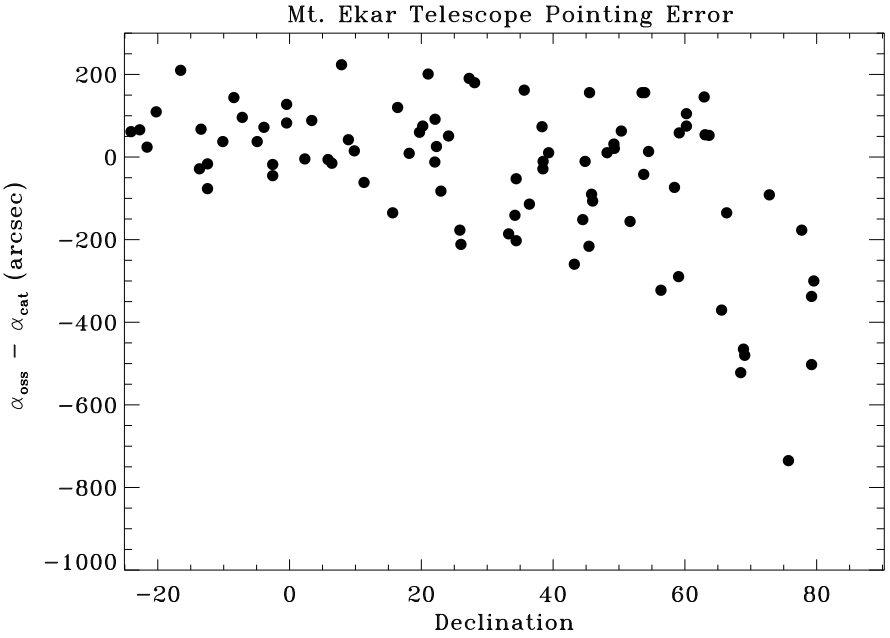

Figure 1.5: Pointing errors in right ascension as a function of the declination of the target, after set–point has been performed at beginning of the night.

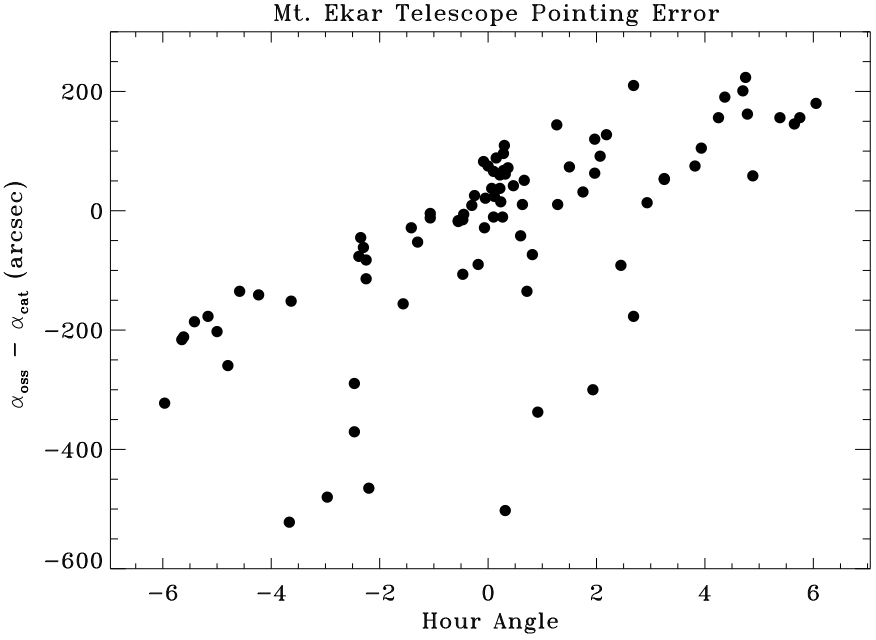

Figure 1.6: Pointing errors in right ascension as a function of hour angle of the target, after set–point has been performed at beginning of the night.

1.3.2 Tracking and Guiding

The telescope is automatically in tracking mode when MICRO or MEDIUM movements are inserted. Tracking performances make auto–guiding mandatory for exposure times longer than 1 minute in typical working conditions.

Auto–Guiding

The auto–guiding procedure is based on the calculation of the centroid of the guide star on the camera images. No significant periodism is detected in the auto-guide corrections.

If the flux from the guiding star becomes less than 5 times the background (for example for intervening clouds or obscuration due to the insertion of the calibration arm), the autoguide stops to send corrections (acoustic messages are provided). When the guide star is detected again, the autoguide starts taking as reference the same position as before the guide star was lost, so that no shifts of the science target on the detector occur.

Differential Guiding

It is possible to guide on objects with large proper motion (e.g. comets, asteroids). This is technically achieved by moving the first folding mirror of the probe at the pre–set velocity of the target. In this way, when autoguide is active, the telescope is forced to follow this movement. The maximum allowed velocity is 180 arcsec/h.

The Differential Guiding (DG) can be activated using the AFOSC GUI. Its use is described in detail in Sect. 4.15.

The use of DG implies always some degradation of the image quality, Infact, when the probe moves at the velocity requested for DG, the guide star lies off–center of the selected guide box for a few seconds, until the autoguide corrects such shift by moving the telescope of the same amount. The resulting degradation of the FWHM of stellar images can be estimated as follows:

$$FWHM = \sqrt{FWHM_{seeing}^2 + (20 * v/3600)^2} \tag{1.1}$$

where $FWHM$ is the FWHM of a stellar image, $FWHM_{seeing}$ is the seeing, v the velocity in arcsec/hr and 20 sec is the effective timescale of autoguide correction. Fig. 1.7 shows the expected degradation in the case of 1.0, 2.0 and 3.0 arcsec seeing conditions. In typical observing conditions (seeing 2–3 arcsec), the degradation is negligible for velocities up to 100-150 arcsec/hr, while during optimal seeing conditions it becomes significant at 70-80 arcsec/hr.

Eq. 1.1 represents the theorical image degradation due to differential guiding. In real cases, random errors make the degradation about twice than these limits while the elongation along the direction of the motion is not so severe as calculated.

The maximum timelength of use of differential guiding using the same guide star is limited by the the probe bounds.

Differential Tracking

Differential tracking without autoguiding in order to observe targets with velocity exceeding the limit of differential guiding working (180 arcsec/hr) showed some random behaviour

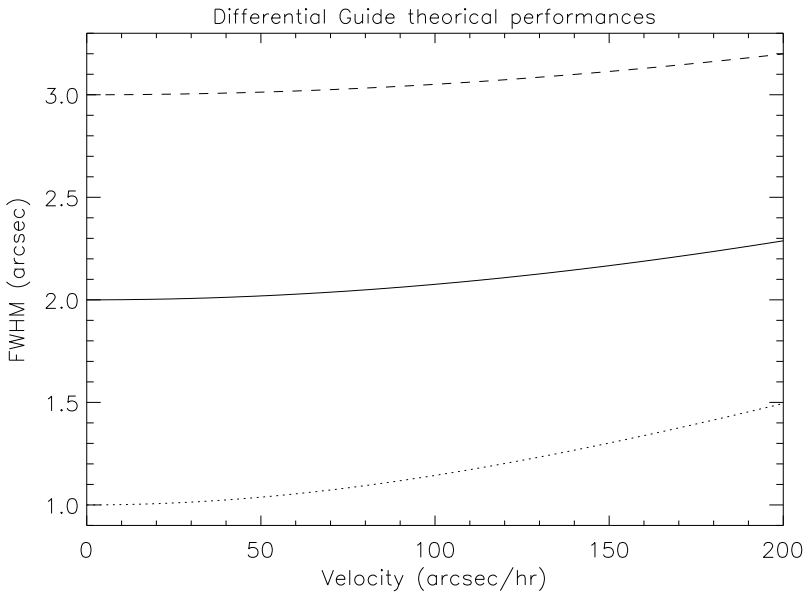

Figure 1.7: Theorical image quality degradation due to insertion of differential guiding as a function of the velocity. Continuous line: seeing 2.0 arcsec; dotted line seeing 1.0 arcsec; dashed line: seeing 3.0 arcsec.

during the initial phase of working, likely due to mechanical problems. Work aimed to understand its origin and possibly to eliminate it is in progress.

1.3.3 Image quality

Typical seeing at M. Ekar is typically 2-2.5 arcsec. Fig. 1.8 shows the distribution of seeing measured from 1993 to 1997.

Improving the seeing can be often achieved by opening the windows and the doors of the dome.

Stellar images with FWHM down to 1.0 arcsec are obtained on January 2002 in exceptional seeing conditions, indicating that with the current status of the optics and alignment image degradations due to optics is well below 1 arcsec.

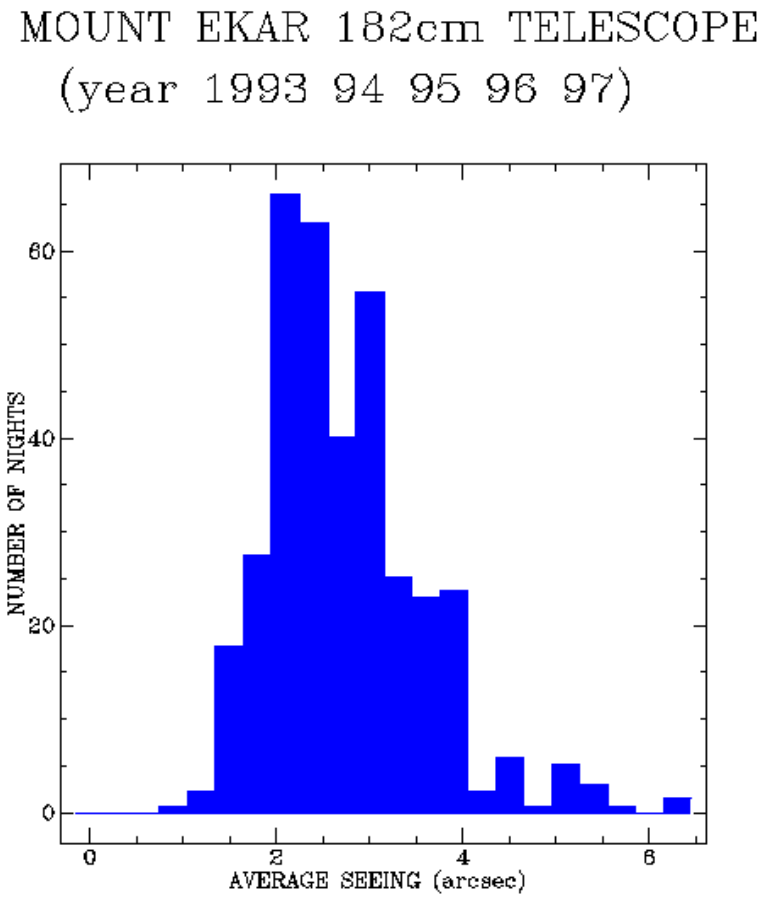

Figure 1.8: Distribution of seeing at M. Ekar from 1993 to 1997, measured with the CCD Camera.

Axis	Direction	Range	Default value
X	North-South	$-1 \div 16$ mm	6.6
Y	East-West	$-1 \div 19$ mm	5.5
Z	Height	$-1 \div 68$ mm	~ 6
α	Tilt along X	$-30 \div 30$ arcsec	0
β	Tilt along Y	$-30 \div 30$ arcsec	0

Table 1.3: Movements of the secondary mirror. The default values refer to the alignment after mirrors aluminization performed in November 2001 and the changes in the positioning of the camera (Febraury 2002). The focus position Z refers to AFOSC. When the Echelle spectrograph is used the telescope focus is about Z=25.

1.4 Focusing the telescope

Focusing of the telescope is performed by moving the secondary mirror along Z axis. The secondary mirror can also be decentered and tilted to correct for the coma (Table 1.3).

Determination of the best focus can be performed by the comparison of several images of point sources obtained at different focus position (for example using the procedure *seeing* of tool EKAR in IRAF; Sect. 5.2). Alternatively one can secure a single image using the pyramid focus of AFOSC (Sect. 2.9 and 4.14).

1.5 Using the telescope

The telescope is usually controlled by the night assistant. The observer therefore does not need to know the telescope operations. Nevertheless he/she should be aware of the basic information on telescope operation and the constraints for the observation, reported in this manual.

Fig. 1.9 shows the control room of M. Ekar Observatory. During a standard observing run, both the telescope and the instruments are fully controlled from the control room.

Figure 1.9: The Control Room at M. Ekar Observatory. From left to right, identified by letters on the picture: *A*: the workstation *alphek*, dedicated to quick look analysis of data (see Chap. 5); *B*: the workstation *wusche*, that controls AFOSC; *C*: the monitor on which the images are visualised during CCD readout (currently not in use); *D*: the Guide Camera; *E*: the Coordinate Monitor; *F*: the VME Console; *G*: the monitor of the video camera placed in the telescope room; *H*: the PC that controls M1 and M2 movements. A monitor to display the data from the meteo station was recently inserted between *wusche* and the monitor that displaies the images.

1.6 The Ekar Meteo Station

The Ekar meteo station is located in the balcony of the telescope (direction NW) and it includes sensors for temperature, humidity and light flux.

A set of temperature and humidity sensors monitor the conditions in different points of the dome and of the telescope.

Meteorological conditions are continuously updated at the web page http://alphek.pd.astro.it/meteo/index.php (Fig. 1.10), that shows also a plot with the evolution of the last 12 hours, and they can be visualised also within the AFOSC GUI (METEO window, see Sect. 4.16).

1.7 Requirements for observations

1.7.1 Telescope limits

It is not possible to observe targets with elevation over the horizon smaller than 10 degrees. However, it is stronlgly recommended to not observe targets at heights smaller than 20 degrees to avoid disalignment of the telescope optics. There are not position limits in in hour angle. However, it is possible to do at most 1.25 turns in a given direction. If the limits are reached, a block stops the movement.

1.7.2 Weather

When humidity exceeds **90%**, it is not possible to start the observations. If humidity increases during the observations, the dome has to be closed for humidity above **95%**. The telescope site is not significantly limited by windy conditions, therefore the wind speed is not measured by the meteo station. In case of strong wind, the night assistant can decide to interrupt the observations. Humidity data are written in the FITS header of the images.

Mount Ekar Observing Station

Padova Astronomical Observatory

weather and telescope parameters

Page auto updated every 60 seconds.

Current date and time: Tue, 24 Apr 2001 00:01:21 +0200

Weather

Outdoor temperature: **3.2** °C
Outdoor humidity: **67.0** %
Pyranometer: **10.0** W/m²
Dew point: **-2.33** °C

Telescope

Last update: 23 4 2001 22:55:13

Indoor temperature: **4.9** °C
Indoor humidity: **50.0** %
M1 Temperature - East: **6.8** °C
M1 Temperature - West: **6.1** °C
M2 Temperature: **4.6** °C
Top Ring Temperature: **7.0** °C
Mirror Cell Temperature: **5.8** °C
Telescope Basement Temperature: **14.9** °C
Dome Floor Temperature: **7.3** °C
AFOSC Temperature: **8.1** °

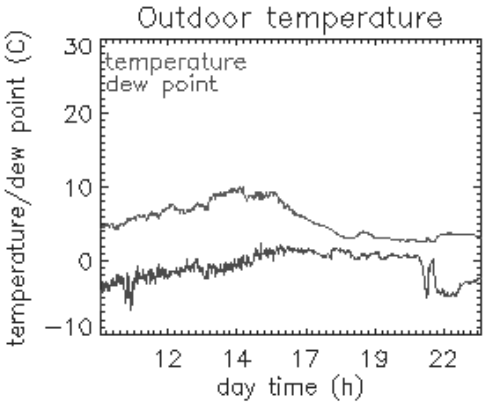

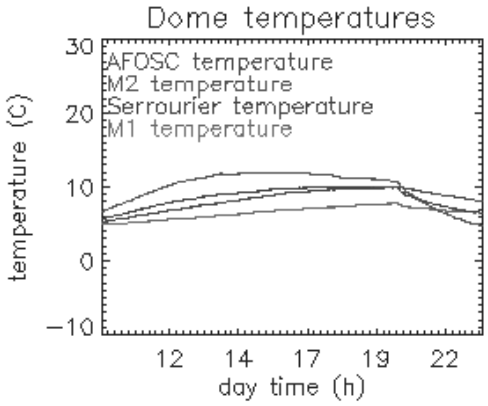

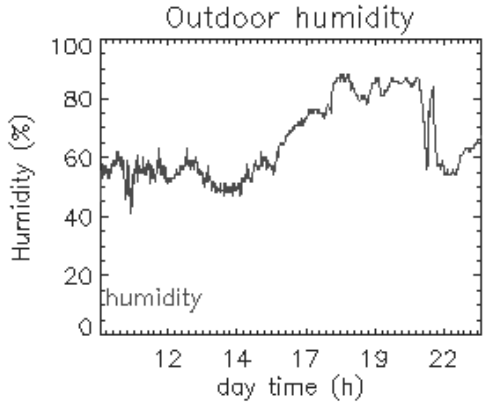

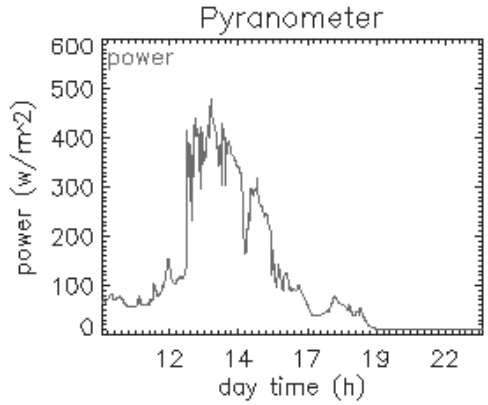

Figure 1.10: The web page showing in real time the meteorological data and instrument temperatures.

Chapter 2

AFOSC

2.1 Introduction

The Asiago Faint Object Spectrograph and Camera (AFOSC) is a focal reducer instrument. It allows wide field (8.1×8.1 arcmin field of view) imaging, low–medium resolution grism spectroscopy, polarimetry, and spectropolarimetry observations. Three wheels allow a selection of slits, filters, and grisms. The available grisms give resolutions up to 7300 (using the Volume Phase Holographic gratings and the 0.7 arcsec slit).

The instrument was provided by the Astronomical Observatory of Copenhagen. Similar instruments are DFOSC at Danish Telescope in La Silla [1], ALFOSC at NOT[2], BFOSC at Loiano[3].
The full list of the FOSC instruments is available at www.astro.ku.dk/∼per/fosc/index.html
Fig. 2.1 shows AFOSC mounted on the 1.82 telescope at M. Ekar Observatory.

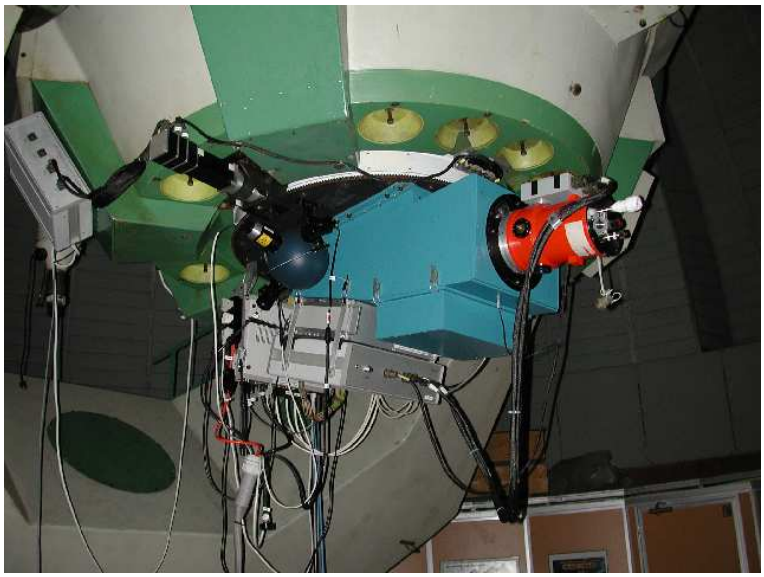

Figure 2.1: AFOSC mounted on the 1.82 m telescope at M. Ekar Observatory.

[1] www.ls.eso.org/lasilla/Telescopes/2p2T/D1p5M/#Dover
[2] www.not.iac.es
[3] www.bo.astro.it/loiano/new-bfosc.htm

2.2 Optical layout

Fig. 2.2 shows the optical layout of the instrument. Briefly, the light coming from the telescope passes through the slit (spectrographic mode) or the hole (imaging mode) in the slits wheel, it is re-directed by a total reflection prism, and it is gathered by the collimator. In the collimated beam, between the collimator and the camera, the light passes through the filter wheel and the grism wheel where a re–imaged exit pupil of the telescope is positioned. Finally the light is imaged by the camera on the detector.

Table 2.1 lists the basic optical parameters of AFOSC.

Parameter	Value
Collimator focal length	252.1 mm
Collimator linear field	52.9 × 52.9 mm^2
Beam diameter	27.8 mm
Camera focal length	146.3 mm
Camera linear field	24.58 × 24.58 mm^2
Reduction ratio	0.58
Input f-number	f/9
Output f-number	
Input scale	12.6 "/mm
Output scale	21.70 "/mm
Field of view	8.1' × 8.1'
CCD Pixel scale	0."473/pixel
Wavelength coverage	330–1100 nm
Limiting spectral resolution	7350

Table 2.1: AFOSC optical characteristics.

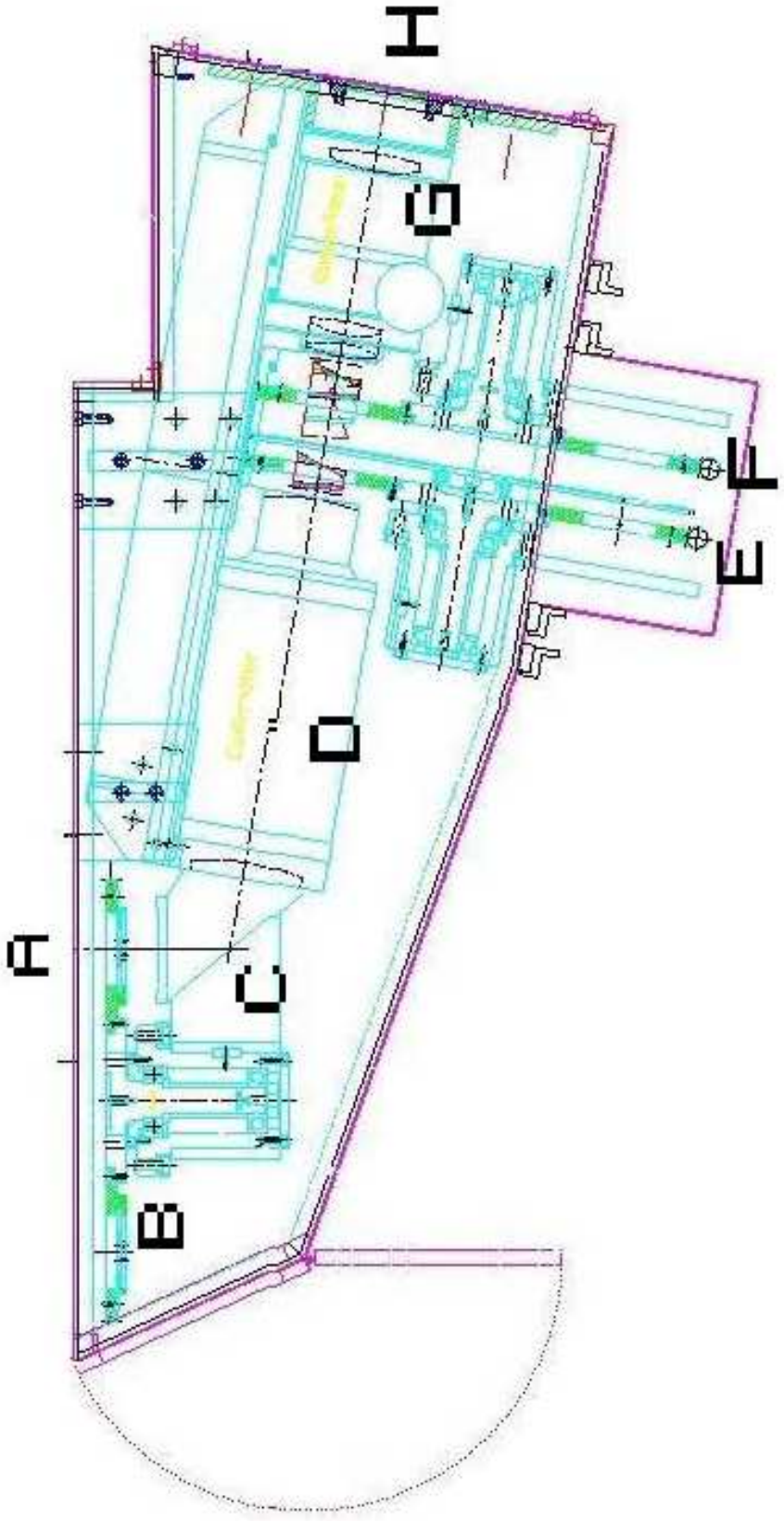

Figure 2.2: Optical layout AFOSC. Light from the telescope enters AFOSC in A, then it pass through the slit wheel (B); it is redirected by the total reflection prims (C) toward the collimator (D); it pass through the filter (E) and grism (F) wheels; and it is focalized by the camera (G). The location of the CCD dewar, not shown in the Figure, is marked by H.

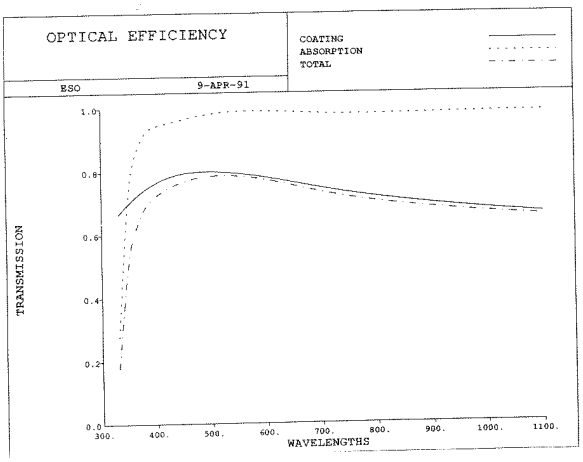

Figure 2.3: Computed efficiency for DFOSC collimator and camera, excluding the CCD field lens, from DFOSC User Manual. The actual efficieny of AFOSC should be similar.

2.3 Observing modes

One of most interesting features of AFOSC is the high grade of flexibility in performing different kinds of observations. It can be used for imaging, low–medium resolution grism spectroscopy, echelle spectroscopy, polarimetry and spectropolarimetry. Switching from different observing modes can be performed in a few seconds (just the time to move the wheels), if the appropriate instrument set–up was mounted. Table 2.2 shows the instrument set–up for the various observing modes. Filters can be positioned also in the grism wheel and grisms also in the filter wheel, since these wheels are located in a collimated beam. This allows to perform both polarimetric imaging and spectropolarimetry without changes in the instrument set up, mounting the polarimeter on the filter wheel and moving the filters to be used for polarimetric imaging in the grism wheel. The number of slits, filters and grisms is larger than the number of positions in the wheels. Therefore the observer has to define the instrument set-up well in advance of its observations (see App. A).

Mode	Slit Wheel	Filter Wheel	Grism Wheel
Imaging	hole	filter	hole
Spectroscopy	slit	hole	grism
Echelle Spectroscopy	ES	grism (cross disperser)	grism
Polarimetry	PM	filter (or POL)	POL (or filter)
Spectropolarimetry	SP	POL	grism

Table 2.2: AFOSC observing modes. ES: Echelle Slit; PM: Polarimetric Mask; SP: Spectropolarimetric Slit; POL: polarimeter.

2.4 Slits

Table 2.3 lists the available slits and the corresponding resolution achieved for the AFOSC grisms. All the slits are 50 mm long, allowing to cover the whole field of view across dispersion. In grism echelle and spectropolarimetric modes such slit length causes spectral orders or polarimeter channels superposition. To avoid this, short slits have to be used. A slit for echelle mode (width: 2.5 arcsec; length: 5 arcsec) and a slit for spectropolarimetry (5 strips 2.5 arcsec wide and 22 arcsec long) were recently prepared (Table 2.4).

The efficiency of the slits as a function of seeing is shown in Fig. 2.4.

Slit width arcsec	Slit width mm	Res. Gr #2	Res. Gr #3	Res. Gr #4	Res. Gr #6	Res. Gr #7	Res. Gr #8	Res. Gr #9	Res. Gr #10	Res. Gr #13
0.68	0.054	354	948	902	1403	1707	2769	5316	303	5028
0.84	0.067	287	768	730	1136	1382	2242	4304	245	4070
1.26	0.100	191	512	486	757	921	1494	2869	163	2713
1.69	0.134	143	382	363	565	687	1114	2139	122	2023
2.10	0.167	115	307	292	454	553	897	1721	98	1628
3.02	0.240									
4.22	0.335	57	153	145	226	275	446	857	49	810
8.44	0.670	29	76	73	113	138	223	428	24	405
16.87	1.34	14	38	36	57	69	112	214	12	203

Table 2.3: AFOSC long slits

Slit width arcsec	Slit width mm	Slit length arcsec	Slit length mm	Remarks
2.5	0.2	5.0	0.4	Echelle
2.5	0.2	22.7	1.8	Spectropolarimetry (5 slits)
1.6		1.6		Pinhole

Table 2.4: AFOSC short slits (for echelle and spectropolarimetry) and pinhole

Table 2.5 reports the position of the slits on the CCD (Y axis), that is different for the various slits. This implies some small changes in the wavelength range of the spectra taken using different slits. The typical stability of the slit positioning is within 2–3 pixels.

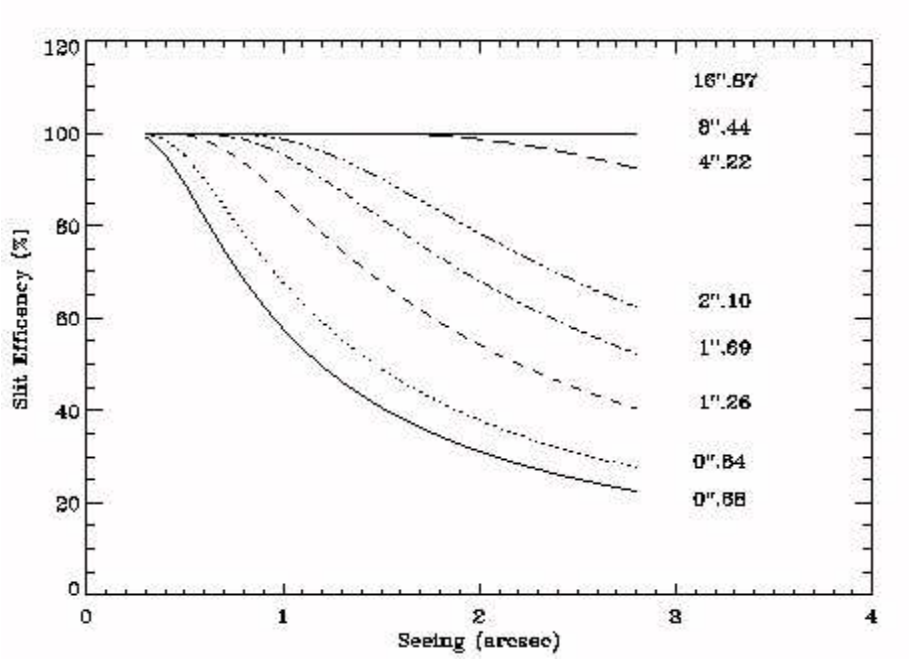

Figure 2.4: Efficiency of the AFOSC slits for different seeing conditions.

Slit	Slit position pixel	λ_c Gr #4 Å
0.68	512	
0.84		
1.26	514	5458
1.69	513	5452
2.10	505	5418
3.00	518	
4.22	509	5436
8.44	466	
MF	544	5616
EC25		
SP25	509	5437

Table 2.5: Position of the AFOSC slits on the CCD and the corresponding wavelength at the center of Gr #4.

2.5 Filters

Table 2.6 lists the AFOSC filters. Narrow band filters are currently not available. OS1 is an order separator filters for the Grism #13. ND1, ND2, ND3, ND4 and ND5 are neutral filters to be used of very bright sources that would otherwise saturate the detector.

The transmission of Bessel and *i* Gunn filters is shown in Fig. 2.5–2.6. The *i* Gunn filter is routinely used instead of I Bessel filter, since, when coupled with the AFOSC optical system, it gives a very good match of the standard Cousins photometric system.

When mounted on their holders, the filters are inclined by 6 deg with respect to the optical axis, to reduce spurious reflections. The insertion of the filters introduces a significant shift in position on the focal plane and of the focus of AFOSC camera (Table 2.7).

Filter	λ_c nm	FWHM nm	Peak Transm.	Remarks
U	363.95	34.54	0.53	Bessel
B	420.05	72.82	0.71	Bessel
V	547.44	89.90	0.94	Bessel
R	647.59	156.98	0.86	Bessel
I	870.97	236.26	0.97	Bessel
i	785	180	0.90	Gunn
OS1				Order Separator for Gr #13
ND1	–	–	0.1	neutral filter
ND2	–	–	0.01	neutral filter
ND3	–	–	0.001	neutral filter
ND4	–	–	0.0001	neutral filter
ND5	–	–	0.00001	neutral filter

Table 2.6: AFOSC filters.

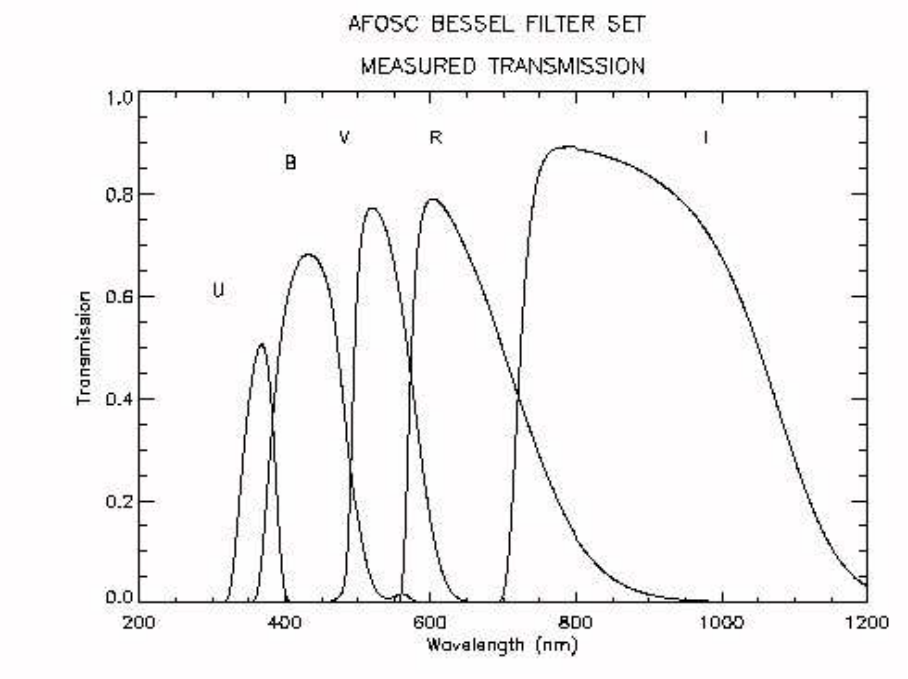

Figure 2.5: Transmission of UBVRI Bessel filters.

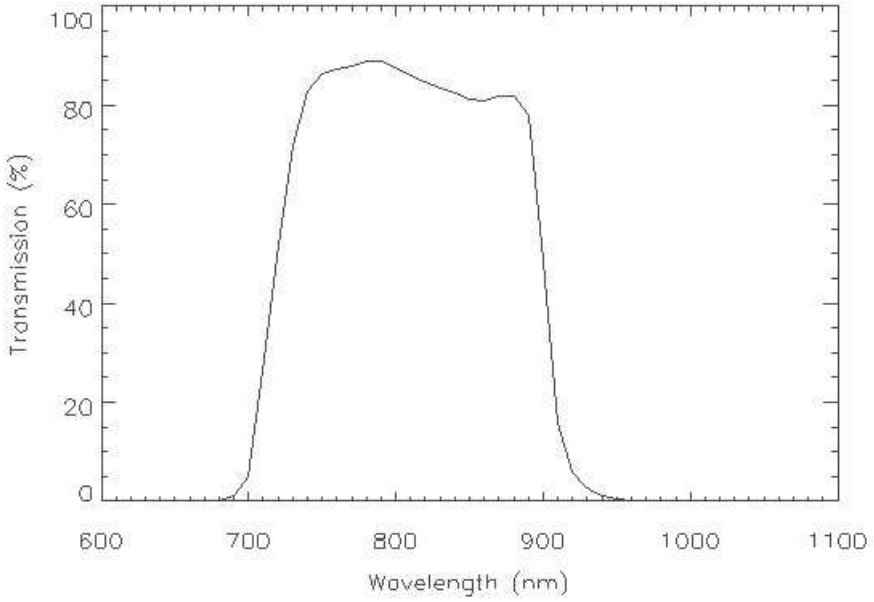

Figure 2.6: Transmission of i Gunn filter.

Parameter	Shift X pix	Shift Y pix	Shift Focus counts
U	5.4	0.8	–8700
B	–1.5	9.3	–5800
V	0.9	–2.9	–2500
R	–8.1	2.4	0
i	–2.1	0.5	8400
OS1	0.3	–0.6	
ND3	1.5	0.2	

Table 2.7: Shift in position and focus caused by the filters. The focus shift is expressed in encoder counts. See Sect. 2.13.1 for details.

2.6 Grisms

AFOSC is equipped with a large set of grisms. In resolving product RS[4] the orginal set of grism range from ≈ 200 to ≈ 3600 and in each resolution domain blue, visual, and red grisms are available. The recently installed five VPH grism reach RS=5000, in different wavelength ranges 500-900 Å long.

Fig. 2.7 shows the spectral range vs RS product for each grism. Tables 2.8–2.9 lists the basic parameters of the AFOSC orginal grisms. The Volume Phase Holographic (VPH) grism are described in Sect. 2.6.1.

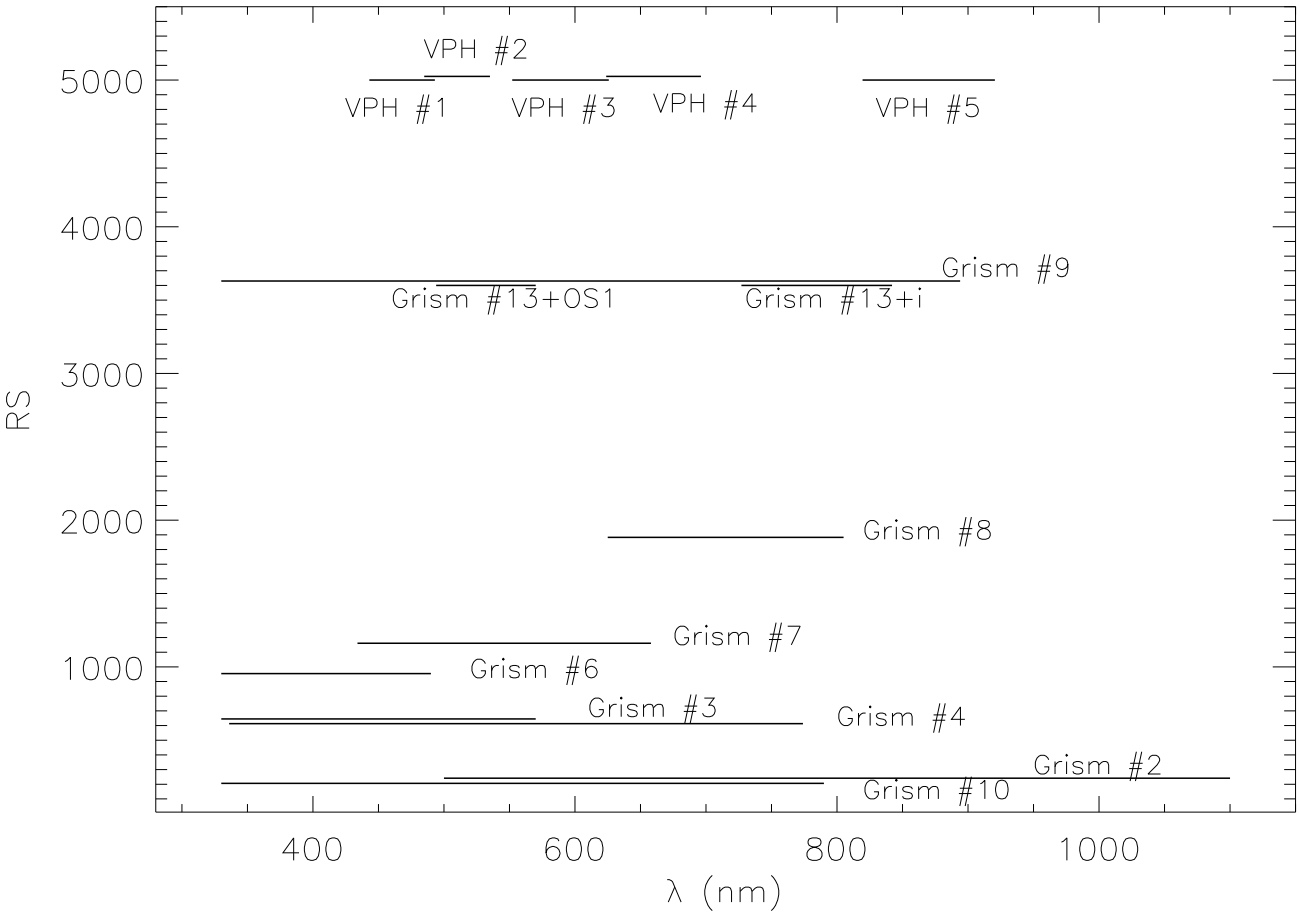

Figure 2.7: Wavelength range vs resolution for the AFOSC grisms.

The efficiency curves of the AFOSC grisms are reported in the Appendix B.

Grisms #2 and #10 are designed to be used as cross disperser for the echelle grisms (Grisms #9 and #13). However, they can be used also as normal grisms when a very low resolution spectrum with broad spectral coverage is required.

[4]The RS product is the resolution for a 1 arcsec slit.

Grism	gr/mm	Blaze Angle deg min	Prism Glass	Prism Angle deg min
#2	100	7 15	OG515	7 24
#3	400	15 00	LF5	16 36
#4	300	14 36	LF5	17 18
#6	600	22 00	LF5	23 12
#7	600	34 00	LaK8	25 34
#8	600	54 00	F8 + OG515	45 18
#9	79	63 30	LF5	65 48
#10	150	5 24	UBK7	6 18
#13	316	63 30	BaK2	65 48

Table 2.8: AFOSC grisms characteristics.

Grism	λ_{cen} Å	λ_{blaze} Å	Dispersion Å/mm	Dispersion Å/pixel	RS	Purity Å	Wavelength Range Å
#2	7200	7366	653	14.3	241	3.1	5000–11000
#3	4300	3916	146	3.2	645	6.1	3300–5700
#4	5800	5094	208	4.3	613	8.3	3360–7740
#6	4000	3806	93	2.0	954	4.0	3300–4900
#7	5250	5676	100	–2.2	1161	4.9	4340–6580
#8	7000	8161	84	–1.8	1883	4.3	6250–8050
#9			26		3615		see Table
#10	3900	3800	412	9.4	206	18.4	3300–7900
#13					3600		see Table

Table 2.9: AFOSC grisms characteristics. Gr #9 and #13 are echelle grisms. The wavelength range and dispersion (Å/pixel) are measured on the AFOSC spectra used for the preparation of the lamps atlas (App. C). The wavelength range may be slightly different for different slits (see Table 2.5). The blue limit of Grisms #2, #3, #6, and #10 and the the red limit of Grism #2 is set by the instrument efficiency; the other limits are fixed by detector size.

2.6.1 Volume Phase Holographic Grisms

AFOSC has been recently equipped with a set of VPH grisms. They allow to reach higher resolution than classical grisms, and with a rather high efficiency (typically about 80%). The basics of VPH technology are described in Giro et al. (2002). For the user, the VPH grisms behave very similar to normal grisms. Some line curvature is present and must be considered in the reduction.

Table 2.10 summarize the main properties of the AFOSC VPH grisms. Only VPH1, VPH4 and VPH5 are currently available.

Grism	λ_{cen} Å	Wavelength Range Å	Dispersion Å/mm	Dispersion Å/pixel	RS	Grooves mm^{-1}	Angle deg
VPH #1	4680	4430–4930	20	0.5	5000	2310	31.38
VPH #2	5100	4849–5351	20	0.5	5000	2310	34.60
VPH #3	5890	5521–6258	30	0.7	5000	1720	30.67
VPH #4	6600	6238–6961	29	0.7	5000	1720	34.60
VPH #5	8700	8195–9205	41	1.0	5000	1280	34.60

Table 2.10: Nominal characteristics of the AFOSC VPH grisms.

2.6.2 Echelle Spectroscopy

AFOSC offers the possibility to do intermediate-resolution spectroscopy (RS $\approx$ 3600) covering a large spectral range using one of the two echelle grisms (#9 and #13) and using one of the low-resolution grisms[5] as a cross-disperser (CD).

Echelle mode is obtained mounting the echelle grism in the grism wheel and the cross-disperser in the filter wheel, turned 90 deg with respect to the normal grisms.

The spectral format of Grisms #9 (+Grism #10 as cross disperser) includes 13 spectral orders, covering the whole wavelength range between 304 and 894 nm (Table 2.11)[6]. The minimum separation between the spectral orders with this instrument set–up is 8.3 arcsec (spectral orders 19-20).

Grism #13 has 4 spectral orders, not covering the full wavelength range as the individual orders are longer than the detector can accommodate. Grism #13 is intended mainly for use with an order sorter filter to give intermediate-resolution spectroscopy with a long slit but it can also be used with one of the cross disperser grisms. In these cases, the minimum inter–order separation is 62.8 arcsec (Gr #13 + Gr #2) and 61.5 arcsec (Gr #13 + Gr #10). This use is not recommended since spectra with similar spectral resolution and broader wavelength coverage can be obtained with Gr #9. Table 2.12 reports the spectral range covered with two different order separator filters.

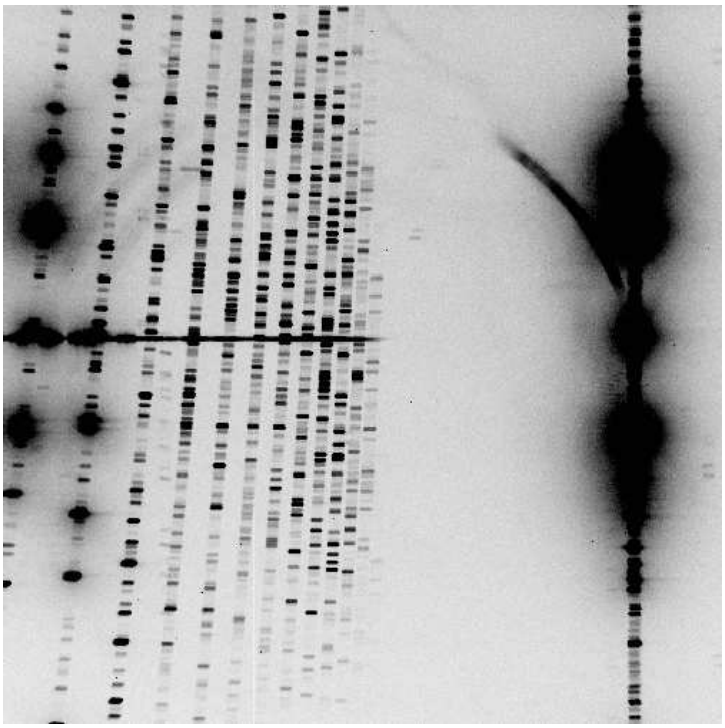

Figure 2.8: Thorium Lamp image taken with Grism #9 + Grism #10 using the echelle slit. The very bright contribution on the right of the image comes from the zero order of the cross disperser.

[5]Only Grism #10 can be used as cross disperser for Grism #9.

[6]Further spectral orders are present in the spectral format of Grism #9 at DFOSC, thanks to its larger detector size.

Order	λ_{start} Å	λ_{center} Å	λ_{end} Å	Dispersion (Å/pixel)	Separation pixel	Separation arcsec	Remarks
8	7787	8325	8942	1.13			
9	6959	7431	7974	0.99	100.0	47.3	
10	6299	6720	7205	0.88	74.1	35.0	
11	5763	6141	6578	0.80	60.4	28.6	
12	5318	5662	6059	0.72	50.3	23.8	
13	4946	5258	5621	0.66	42.2	20.1	
14	4629	4915	5248	0.60	36.1	17.1	
15	4357	4620	4927	0.56	31.6	14.9	
16	4121	4364	4648	0.51	27.3	12.9	
17	3915	4140	4403	0.48	24.1	11.4	
18	3735	3943	4188	0.44	21.8	10.3	
19	3575	3768	3998	0.41	19.1	9.0	
20					17.6	8.3	
21							very faint

Table 2.11: Spectral range covered by Grism #9 + Grism #10 as measured on AFOSC spectra. The separation between the spectral orders refers to the order center.

Filter	λ_{start} Å	λ_{end} Å	Dispersion Å/pixel	Remarks
OS1	4940	5700	–0.7	
i	7270	8420	–1.1	

Table 2.12: Spectral range covered by Grism #13 coupled with different order separator filters. The wavelength range and dispersion are measured on the AFOSC spectra used for the preparation of the lamps atlas (App. C). The wavelength range may be slightly different for different slits (see Table 2.5).

2.7 Wavelength Calibration

The following lamps are available for the wavelength calibration: Argon (Ar), Helium (He), Neon (Ne), Mercury-Cadmium (Hg-Cd), and Thorium (Th).

Only three holders are available for the lamps. Th lamp is permanently mounted, since its holder is different from the other ones. In the other two it is possible to choose between Ar and Ne lamps and between He and Hg-Cd lamps.

Table 2.13 reports the main properties of the lamps. The atlas for wavelength calibration and the suggested exposure times are reported in Appendix C. Due to lack of significant lines in some spectral regions, it could be useful to take spectra of two lamps and perform the wavelength calibration using the coadded spectrum[7]. See Sect. 3.3.4 for the lamps to be coupled to each grisms.

In addition, a quartz lamp (QHT) is available for internal flat field calibrations.

Lamp	Useful range (nm)	N_{lines}	Remarks
He	380–730	~ 10	
Ar	700–1000	~ 10	
Th	380–1000	many	line blending, Ar lines
Ne	570–880	~ 20	
Hg-Cd	360–1000	~ 20	Ar lines
QHT		–	continuum

Table 2.13: Calibration Lamps

[7]It is not possible to acquire simultaneously the spectra of two lamps. The spectra has to be taken separately and then coadded. The images have to be summed as float to avoid problems with long integers.

2.8 The AFOSC Polarimeter

A polarimetric device can be inserted in the grism or filter wheel. It consists of a simple combination of two Wollaston prisms and two wedges. This configuration allows simultaneous measurements of the polarized flux at angles 0, 45, 90 and 135 degrees without the need of $\lambda/2$ rotating plates or other moving elements.

Fig. 2.9 shows the optical layout of the instrument. Light incoming from the telescope intercepts a polarimetric mask on the telescope focal plane. After the collimator, light is splitted into four beams by the two Wollaston prisms and the camera refocuses the four images on the CCD. The two wedges avoid overlap between ordinary rays and between extraordinary rays incoming from the two Wollaston prisms. The double quartz polarimetric prism has been built by Bernhard-Halle.

The polarimetric mask mounted on the slit wheel consists in four apertures of 1.8 (PM18) or 2.0 (PM20) mm length (22.7 and 25.0 arcsec respectively). The separation between the apertures is set by the requirement of avoiding any superposition between the strips (four for each aperture) on the detector. The use of PM18 is recommended to avoid any superposition at the edges of the strips. For stellar objects a large slit (20 arcsec) could be used instead of the mask.

Mounting the polarimeter on the filter wheel and inserting a grism it is possible to obtain spectro–polarimetric observations. In this case, it is necessary to use a short slit (maximum length = 1.8 mm= 22.7 arcsec) to avoid superposition between the channels of the polarimeter. Recently, a slit with such length (and width 2.5 arcsec) has been realized. Four spectra corresponding to the four channels of the polarimeter are obtained.

The AFOSC polarimeter is described in detail in Pernechele & Giro (2002).

2.9 The Pyramid Focus

A pyramid focus device is permanently mounted on the grism wheel. It allows to determine the focus of the telescope with a single exposure. The beam of light is splitted in 4 images. From the analysis of the relative positions of the four images, the best focus of the telescope is evaluated.

The use of pyramid focus from the AFOSC GUI is described in detail in Sect. 4.14.

2.10 The Hartmann Masks

The Hartmann Masks are two special masks selecting one half of pupil each one, used for the determination of the AFOSC Camera focus. They are permanently installed on the grism wheel.

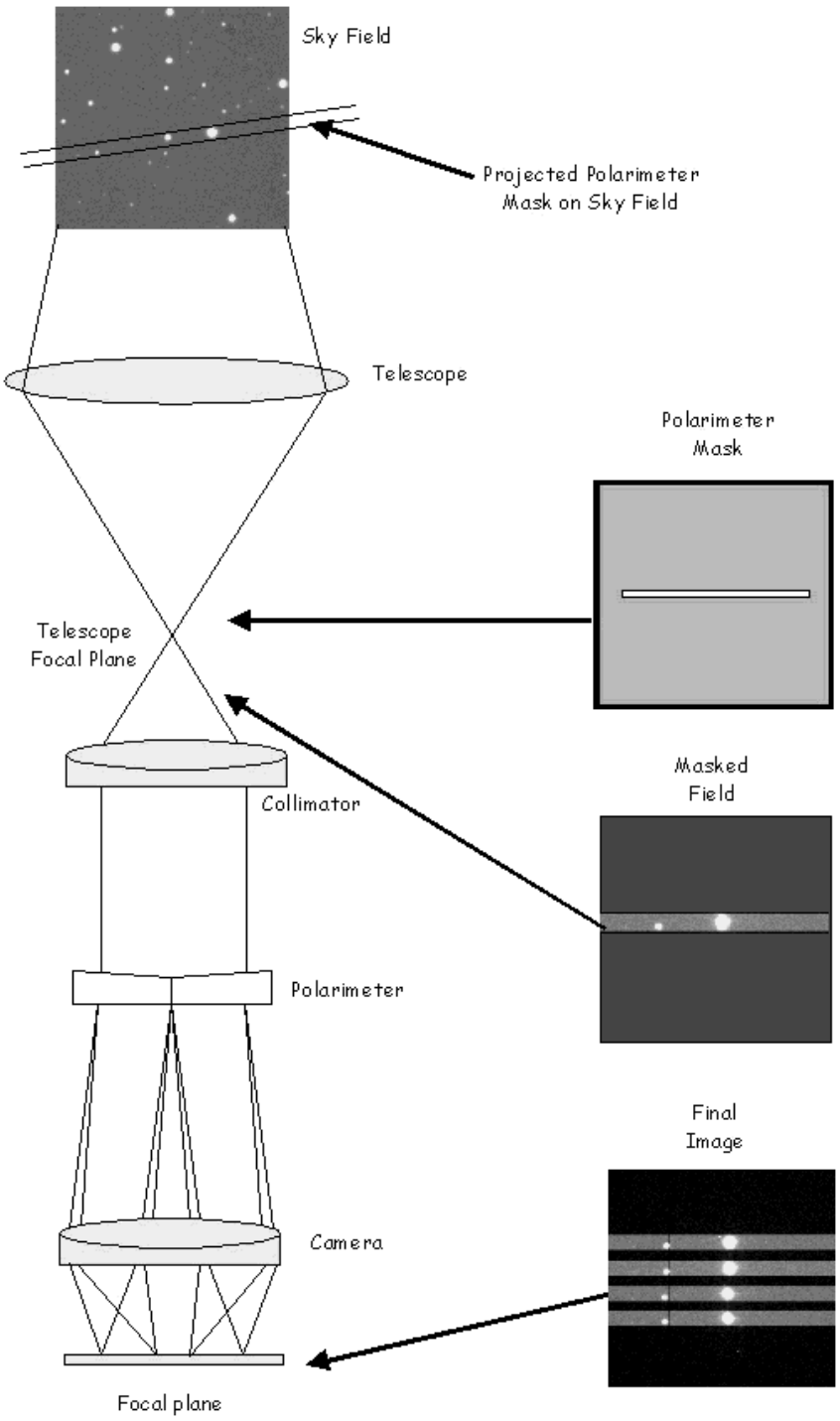

Figure 2.9: Optical layout of the AFOSC Polarimeter.

2.11 The Shack–Hartmann wavefront sensor

A Shack–Hartmann wavefront sensor can be inserted in the grism wheel[8], that is very close to the pupil plane. It allows to estimate misalignment between the primary and secondary mirrors and the amount of the residual optical aberrations.

This device consists on an array of microlenses (size 1.0 x 1.0 mm), that samples a 27.8 mm diameter pupil, followed by a negative lens to obtain a suitable image of the spots on the detector. Figure 2.10 shows the object image (a 5th magnitude star) and the reference image (obtained by illuminating the pinhole in the slit wheel with the dome flat lamp).

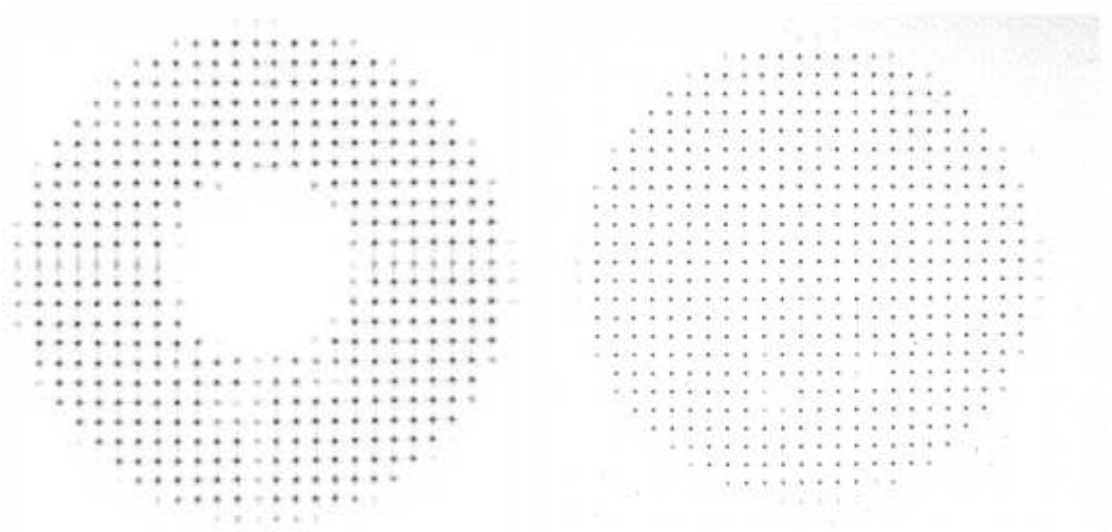

Figure 2.10: Images acquired with the AFOSC wavefront sensor: *a)*: object image; *b)*: reference image.

The wavefront sensor and the results based on its use are described in detail in Pernechele et al. (2000). A package to properly determine the aberration parameters from the analysis of the images was prepared.

2.12 The Shutter

The AFOSC shutter is of throttle type. This guarentees the same level of exposure over the whole CCD field. Timing errors at 0.1 sec level was measured (see Sect. 3.2.4).

[8]The Shack–Hartmann wavefront sensor can not be mounted in the filter wheel due to space constraints.

2.13 The Camera

2.13.1 Focus

The focus of the AFOSC is adjustable by moving the camera lens. The total range of the encoder is 140000 counts, corresponding to a physical range of ~ 2 mm.

The focus shows a mild dependence on temperature (-10.3 μm/C), as shown in Fig. 2.11 for the previous mechanical mounting of the detector (SITe). We do not expect a big difference of the trend for the current one (of course it will be checked), only the zero point of the focus position is shifted up ~ 65000 encoder counts .

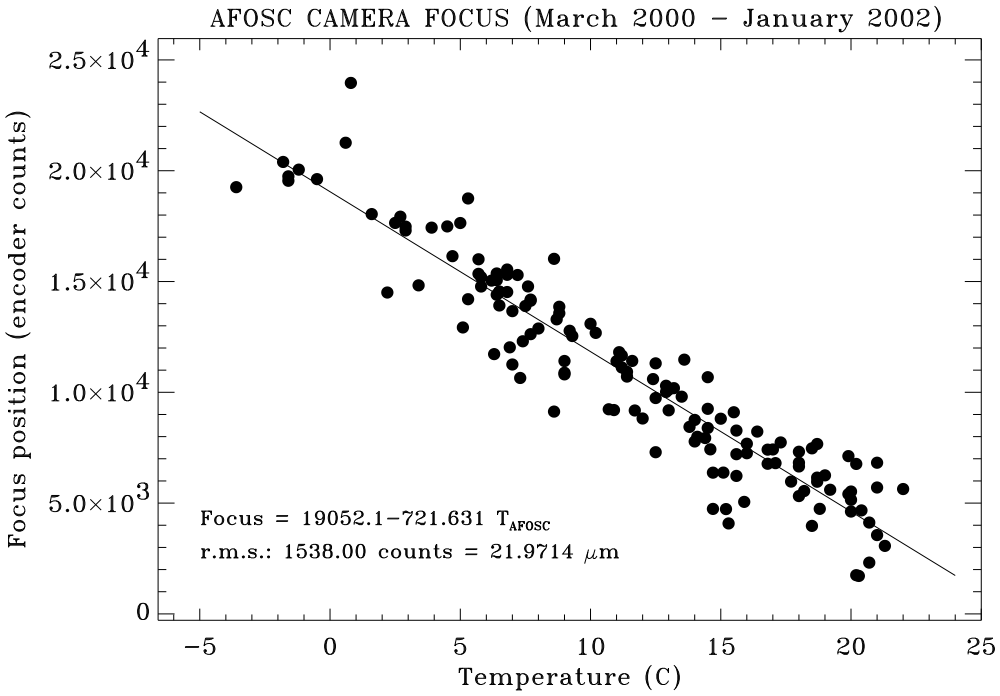

Figure 2.11: Focus of the AFOSC Camera as a function of temperature. Only measurements taken after March 2000, when the CCD adapter was modified, were considered.

Measurement of the focus shift caused by filters shows a clear zero point offset, different for each filter (see Tab. 2.7), while the slope of the relation focus – temperature is not significantly altered.

2.14 The Detector

2.14.1 General Characteristics

The CCD currently in use with AFOSC , which has been mounted on 1 June 2003, is a TK1024 CCD Imager, back illuminated, with 1024 x 1024 24μm pixels, which corresponds to 0."473/pxl on the AFOSC focal plane.

The architecture of the CCD controller follows the TNG standards (Bonanno et al. 2000).

Typical readout time is about 50 sec for the full frame. It is possible to select a window on the chip to reduce readout time. Binning the pixels is not currently available.

To exclude the overscan region, the AFOSC images can be trimmed (X axis: pixel 25 to 1048; Y axis: pixel 76 to 1100, see Fig 2.13).

CCD characteristics are reported in Table 2.14 and its quantum efficiency in Fig. 2.12.

The position of current CCD is shifted up about 50 pixel compare to the previous CCD, which makes an offset of slits positions and wavelength ranges of grisms (e.g. the offset for the grism #4 is about 20 nm).

Parameter	Value
Format	1024 x 1024 pix
Array size	24.6 x 24.6 mm^2
Pixel size	24 μm
Pixel scale (on AFOSC)	0.473 arcsec/pix
Technology	3PCCD
Type	Thin
Quantum efficiency	80% at 650 nm
Range	330–1100 nm
Gain	1.8
Readout noise	9 e- (rms)
Readout time	50 sec. (full frame)
Dark current	$6e^-$/pix/hr
Full well capacity	300000 e/pix (typical),
Fringes	2% at 800 nm
Features	a faint grid, observable only with flat field, is present

Table 2.14: CCD characteristics.

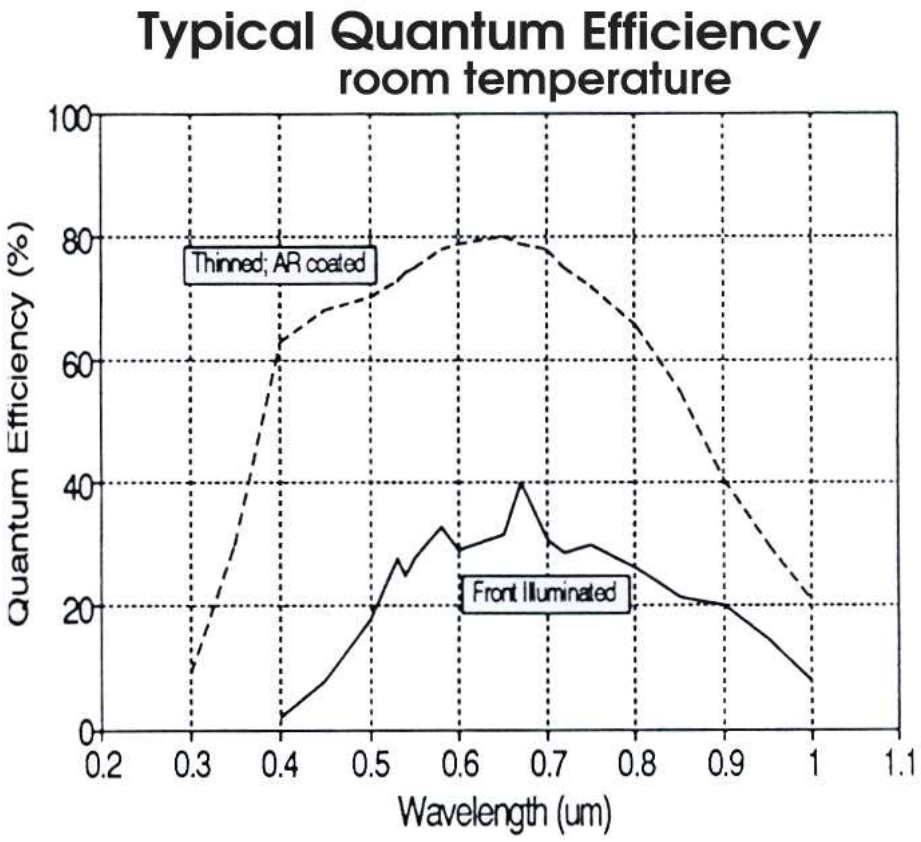

Figure 2.12: Top curve is the efficiency of the current AFOSC CCD.

2.14.2 Cosmetics

There are some pixels and pixel groups effected by the dust. The biggest groups are at (589,572)[9], (714,640) and (380,761) (see Fig 2.13). When placing the star in the slit it is better to avoid these pixels .

2.14.3 Bias and Dark Current

With the present set–up, the bias level is about -31800 (i.e. 967 ADU above -32767). The stability over a single night is typically within $\pm$20 ADU level on daily timescales. It is recommended to use overscan during data reduction.

The measured dark current is less than $6e^-$/pix/hr.

2.14.4 Field of view

With the instrument rotator in the default position, the image appears in the window of the AFOSC GUI that opens automatically at the end of every exposure with north up and

[9]The pixel numbers refer to an image without any trimming.

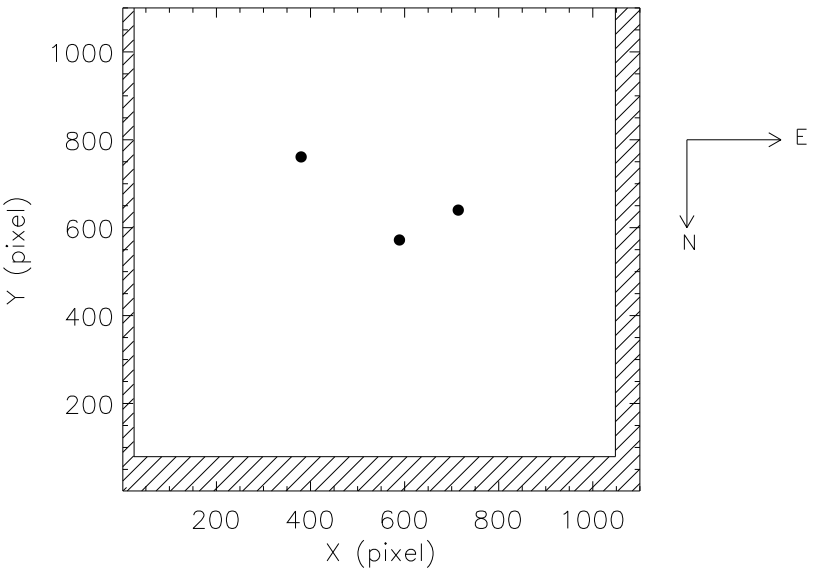

Figure 2.13: Bad pixels map of the AFOSC CCD. Dashed area is the overscan region. Note that the image appears in the display in the control room reversed in the Y direction.

east to the right. The image written on disk instead appears on IRAF with north down and east right, as shown in Fig. 2.13.

2.14.5 Windowing

It is possible to window the CCD to reduce readout time. The windowing boxes in the exposure definition window (Fig. 4.5) are defined according to the orientation of the image as it appears on the OFFSET window (Sect. 4.9).

When using windowing, it is recommended to take flats using the full frame format, because the residual charge in the pixels outside the selected box might introduce some contamination. This effect is usually much smaller on science frames, characterized by a much lower light flux.

Chapter 3

AFOSC Performances

3.1 Introduction

This chapter describes the instrument performances with the various observing modes, including some tests performed on the sky. Other observations and tests are in progress.

3.2 Imaging

3.2.1 Flat Fields

Dome Flats

Dome flats can be obtained using one of the two lamps (0.3 and 1.0 kW) projected on the white screen in the dome. Telescope must be positioned at $\delta \sim 0$ deg and HA ~ 0, with the azimuth of the dome of 311 deg. However, for R and i filters, saturation is achieved in 1 sec exposure time even for the 0.3 kW lamp. To obtain dome flats, it is possible to project the lamps opposite to the screen or to use daylight from the windows, obtaining a diffuse, lower level, illumination. In these cases, however illuminations gradients can introduce spurious gradients in the FF pattern (up to at 5% level). The comparison between sky and screen flats shows smaller differences ($\sim$ 2% peak to peak in the V band). The exposure times quoted in Table 3.1 for R and i are very indicative.

Sky Flats

Acquisition of sky flats is strongly recommended, in order to avoid the mentioned problems with dome flats, especially for R and i bands. As a practical rule, sky flats in U can be started when the light flux as measured by the Pyranometer of the meteo station is about 15 W/m^2. A list of empty fields useful for sky flats is reported in App. F.

Flat Fields Stability

Temporal stability of the FF is rather good. During a single run, typical differences between normalized FF are at 1% level (r.m.s. of differences of normalized flats), without large

Filter	Lamp	T_{exp} (sec.)	Counts	Remarks
U	1.0 kW	20	+11000	Dome screen
B	1.0 kW	1	+18000	Dome screen
V	0.3 kW	1	+13000	Dome screen
R	0.3 kW	7	+15000	Lamp opposite to the screen
i	0.3 kW	5	+15000	Lamp opposite to the screen

Table 3.1: Suggested exposure times for imaging dome flats.

scale patterns. Therefore, dome flats can be safely taken during daytime while skyflats obtained during one night can be used for the whole observing run.

Sky Concentration

As other focal reducers, AFOSC should be affected by sky concentration. This effect makes it difficult to produce good flat fields, since scattered light is preferentially directed toward the center of the field. This causes a underestimate of the counts in the central part of the flat field. This effect has not yet measured on AFOSC. For DFOSC, a twin instrument of AFOSC, it is at 2% level. A procedure to correct for such effect is described by Andersen et al. (1995).

3.2.2 Photometric calibration[1]

Calibration equation using photometric standard (Landolt, 1992) were obtained during the night June, 19, 2001, after mirrors aluminization. The equations, expressed in ADU, were computed for t_{exp}=1 sec, airmass=1.0. The standard extinction coefficients ($k_U = 0.58$, $k_B = 0.29$, $k_V = 0.16$, $k_R = 0.12$, $k_I = 0.08$) have been used for Asiago.

$$U - u = 20.59 + 0.12\ (U - B) \tag{3.1}$$

$$B - b = 23.24 - 0.04\ (B - V) \tag{3.2}$$

$$V - v = 23.95 + 0.06\ (B - V) \tag{3.3}$$

$$R - r = 23.92 + 0.06\ (V - R) \tag{3.4}$$

$$I - i = 23.34 - 0.01\ (V - I) \tag{3.5}$$

[1]The photometric calibration is done for the previous CCD

Filter	Count Rate ADU/s	Count Rate $e-/s$	I_c $ADU/s/pix$
U	170	340	64
B	1980	3960	740
V	3800	7600	1422
R	3700	7400	1384
I	2170	4340	811

Table 3.2: Expected count rates for a 15th magnitude star in 1 sec at airmass=1.0. The intensity of the central pixel is for a seeing of 2.0 arcsec. The contribution of the sky is not considered.

The Eq. 3.5 refers to the Gunn i filter, that gives a better match than Bessel I of the standard photometric system.

Equations 3.1–3.5 are indicative only. Zero point changes according to the transparency of the sky and mirrors reflectivity[2].

3.2.3 Efficiency

From Equations 3.1–3.5 the expected count rate for a star of magnitude $m*$ can be derived, using the following equation:

$$F_* = G \quad 10^{0.4(m_0 - m*)} \quad e-/s \tag{3.6}$$

where G is the CCD gain (2.0 for AFOSC); m_0 is the zero point of the calibration equation. For a 15th magnitude star and neglecting the color terms, the count rates reported in Table 3.2 are obtained. The sky contribution is not included.

The intensity I_c of the central pixel can be estimated using

$$I_c = \frac{0.188 \; F_{*(ADU)}}{FWHM^2_{seeing}} \quad ADU/s \tag{3.7}$$

where $F_{*(ADU)}$ is the count rate in ADU/s and $FWHM_{seeing}$ is the seeing in arcsec.

The maximum exposure time to avoid saturation for a star with flux $F_{*(ADU)}$ $e-/s$ is given by

$$t_{max} = 335000 \; \frac{FWHM^2_{seeing}}{F_{*(ADU)}} \quad s \tag{3.8}$$

The saturation magnitude for a star with 1 sec exposure time for various seeing conditions are listed in Table 3.3.

[2]Efficiency of the telescope after mirrors aluminazation improved by a factor of 2.1, 2.0, 1.8, 1.7, 1.6 in U, B, V, R and I band respectively.

Filter	Seeing 1.0	Seeing 2.0	Seeing 3.0
U	6.8	5.1	4.4
B	9.4	7.8	7.1
V	10.1	8.5	7.8
R	10.1	8.5	7.7
I	9.5	7.9	7.2

Table 3.3: Saturation magnitude for a star in 1 sec exposure time in different observing conditions.

3.2.4 Shutter timing

Shutter timing as measured from the light flux of standard stars taken with different exposure times shows differences at 0.1 s level for 1 sec exposure time. Therefore the exposures times has to be properly corrected to obtain accuracies in photometric calibration at 0.01 mag level, when exposures shorter than 10 sec are considered.

3.3 Spectroscopy

3.3.1 Flat Fields

Flat fields for spectroscopy can be obtained using the lamps projected on the white screen, as for imaging dome flats. The 1 kW quartz lamp helps to keep shorter exposure times. Saturation can occur for the 1 kW lamp only with Grisms #2 and #10. The resulting spectrum is free of lines, but a very strong gradient along the dispersion is present for the grisms with large wavelength coverage, since the lamp emission peaks in the red (Fig. 3.1). Obtaining flat field with high signal to noise in the blue region while avoiding saturation in the red can be achieved by acquiring several flats.

Table 3.4 reports the recommended exposure times using the 1kW lamp for the AFOSC grisms. They must be taken as indicative: some variations due to different illumination (orientation of the lamp toward the screen, collimation of the beam toward the screen, slightly different telescope position) as well as some possible intrinsic variation of the lamp itself (we measured variations up to 15 %, with an increasing in the lamp flux in the first hour likely due to the lamp heating) might change the effective light flux.

An alternative is to use the Quartz lamp in the calibration arm (QHT). However this choice is not recommended due to limited number of available positions for the lamps (only two would remain for wavelength calibration).

As for imaging, the stability of the FF is good, allowing to take flats during daytime. The lights in the dome has to be turned off to avoid the superposition of their emission lines.

Grism/Slit	0.70	0.85	1.26	1.69	2.10	3.00	4.22	8.44	ES	Lamp
#2	10		6		4		2	1	–	0.3 kW
#3					6				–	1.0 kW
#4	9		5	3	2	2	2	1	–	1.0 kW
#6	20		12	10	6	6	4	3	–	1.0 kW
#7	20		12	10	6	6	4	2	–	1.0 kW
#8	20		12	10	6	6	4	2	–	1.0 kW
#9 + #10	–	–	–	–	–	–	–	–	35	1.0 kW
#10	1		1	1	1	1	1	1	–	0.3 kW
#13 + OS1	120		70	60	40		25		–	1.0 kW
#13 + i	50		30	25	15		10		–	1.0 kW
VPH #1									–	1.0 kW
VPH #2									–	1.0 kW
VPH #3									–	1.0 kW
VPH #4					18				–	1.0 kW
VPH #5					10				–	1.0 kW

Table 3.4: Recommended exposure times for the available slits. Exposure times are fixed to obtain maximum counts of +10000 ÷ +20000 (i.e. 40000 ÷ 50000 counts overall). The 0.3 kW has to be used for Grism #2 and #10 to avoid saturation. The Zero Order of Grism #10 is saturated with 1 sec exposure time for all the slits but th 0.70 arcsec one. This fact does not compromise the quality of the flat in the part of the detector including the scientific spectrum.

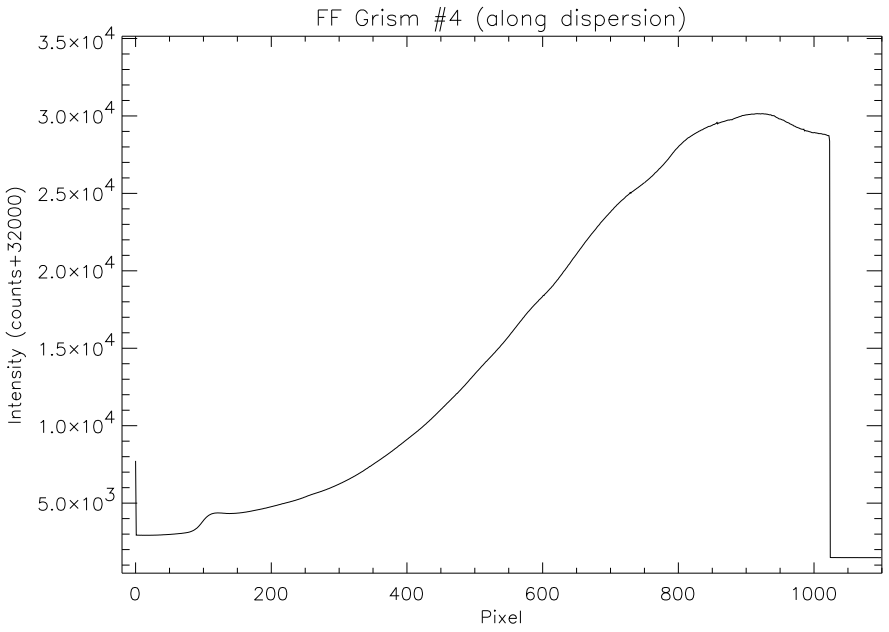

Figure 3.1: Dome flat of Grism #4 with the 2.1 arcsec slit.

3.3.2 Fringing

The fringing of the AFOSC CCD is rather low. From the analysis of a flat field spectrum taken with Grism #2, a fringing pattern at a few percent level red–ward 8000 Å is present (Fig. 3.2).

3.3.3 Background subtraction

Some grisms show more or less pronunced reflexes from zero order. They are highly variable both along and across dispersion, making their subtraction critical. The most affected grisms are Grisms #3, #4 and #6. In the case of Grism #4 (Fig. 3.3) the contamination is limited to the blue region, below $\sim$ 4200 Å. Such effect can be reduced by positioning the object in the slit at about 100 pixels from the chip center.

3.3.4 Wavelength Calibration

Since in most cases it is not possible to obtain a good wavelength coverage using a single lamp, it is recommended to sum together the spectra of two or three lamps (Table 3.7). Spectral atlas reported in Appendix C include both single lamp and combined spectra. The calibration exposures should be taken consecutively (without moving the telescope or changing the AFOSC set-up) to avoid the occurrence of instrumental shifts. In these conditions, the short term stability of AFOSC (within the accuracy of measurements on a timescale of a few minutes) allows to sum the spectra without any degradation of the resulting calibration. When summing the spectra, real values have to be used to avoid problems with long integers (e.g. to sum two images under IRAF use the option calctype=real in imarith).

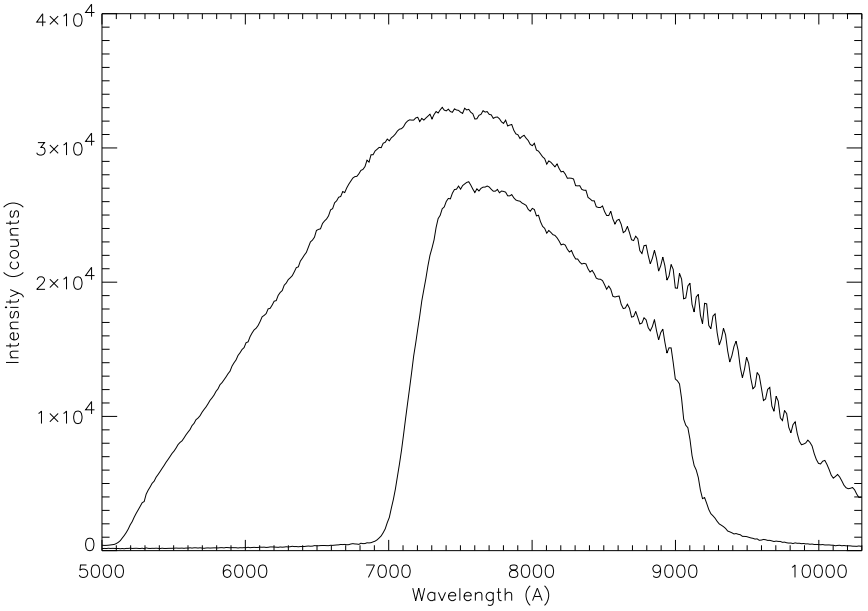

Figure 3.2: Flat field spectrum taken with Grism #2. Only a low level fringe pattern redward 750 nm is present, reaching ∼10% above 9000 Å. The lower line is the spectrum taken with the same set-up and inserting the i filter. It results that i band is only marginally affected by fringing.

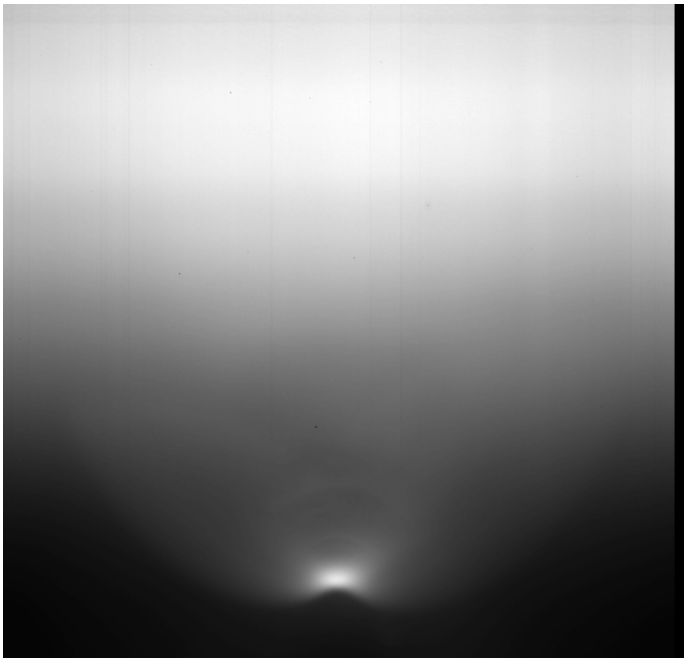

Figure 3.3: Dome Flat image taken with Grism #4 and the 2.10 arcsec slit. The reflex in the lower part make difficult to extract good quality spectra in the blue region.

Lamp/Grism	#2	#3	#4	#6	#7	#8	#9 + #10	#10	#13 + OS1	#13 + i
Ne	6	300	10	–	20	12	300	3	300	120
He	10		14	240	16	50	300	10	300	300
Ar		300	30	–	–	25	300	4	300	40
Hg-Cd	60	120	60	120	100	300	300	40	300	300
Th	3	240	8	240	240	10	300	1	300	20

Table 3.5: Recommended exposure times for the calibration lamps using the 2.1 arcsec slit. More detailed tables, including all the slits, are presented in App. C.

Lamp/Grism	VPH#1	VPH#2	VPH#3	VPH#4	VPH#5
Ne	–				120
He					
Ar					
Hg-Cd					300
Th					10

Table 3.6: Recommended exposure times for the calibration lamps of the VPH using the 2.1 arcsec slit. More detailed tables, including all the slits, are presented in App. C.

To obtain a good wavelength calibration, it is necessary to obtain the lamp spectra with the same slit used for science observations (or slits with same Y position, see Tab. 2.5), since calibration spectra taken with different slits show typically shifts of a few pixels.

To **save time** when obtaining a number of calibration spectra, it is useful to prepare the full sequence of lamp spectra in the exposure window of AFOSC GUI (see Sect. 4.6). This allows the calibration arm to remain inserted during the whole sequence, while at the end of every single exposure it would be moved outside position to insert the probe.

3.3.5 The AFOSC Stability

When moving the telescope, some flexures do occur. Test performed keeping fixed HA=0 and moving the telescope in declination and test performed keeping fixed $\delta = +46$ and moving the telescope in right ascension indicate that flexures amount to 0.1 pixel or less, with a small hysteresis effect (Claudi 1998).

Grism	Lamps combination
#2	Hg-Cd or He + Ar
#3	Hg-Cd or Th
#4	Ne + Hg-Cd or Ne + He or He + Ar
#6	Hg-Cd or Th
#7	Hg-Cd + Ne or He + Ne or Th
#8	Ne + Th
#9 + #10	Th
#10	Hg-Cd or He + Ar
#13 + OS1	Th
#13 + i	Ar or Th
VPH #1	Th
VPH #2	Th
VPH #3	Ne or Th
VPH #4	Ne + Th
VPH #5	Ne + Th

Table 3.7: Suggested calibration lamps to be used for various instrument set–ups.

3.3.6 Placing a Star in the Slit

Sect. 4.9 describes the procedure to put the target into the slit using the OFFSET window of the AFOSC GUI. Note that **the images used to perform the offset procedure have to be taken without filters**, due to the position shift they introduce (Table 2.7). When changing slit on the same object, the procedure has to be repeated, since some position shift between the slits is present (Tab. 2.5).

It is possible to rotate the rotator adapter, to change the slit orientation on the sky. This can be useful to align the slit along the parallactic angle (to avoid the effect of differential refraction), to place two objects simultaneously on the slit, or to observe an extended object along a given position angle.

An option in the AFOSC GUI (Sect. 4.11) allows one to calculate the angle between two objects and rotate the slit to put both objects into the slit.

The rotation angle of the adapter is defined as 0 for a E-W orientation of the slit (i.e. different from the usual definition of position angle, 0 for N-S orientation). The position error of the rotator adapter is about 1 arcmin.

3.4 Echelle spectroscopy

Echelle spectroscopy can be performed using the new echelle slit (width 2.5 arcsec, length 5.0 arcsec). The slit length was fixed to 5 arcsec to avoid order superposition in the blue region. However, with such small length sky subtraction cannot be easily performed, mak-

ing problematic the observations of faint objects. The subtraction of inter–order scattered light is also difficult in the blue region, where the spectral order are closely spaced. Some second order contamination can be present, especially when observing very blue objects.

The accuracy of the wavelength calibration using the Th lamp is limited by the line blending. The evaluation of the actual radial velocity precision achievable with the grism echelle is in progress. Some VPH grisms should yield better radial velocity performances in spite of the much shorter wavelength coverage, thanks to the higher spectral resolution and the much easier background subtraction and wavelength calibration.

3.5 Polarimetry

3.5.1 Flat Fields

Since the image is splitted in four channels, the exposure times for Flat Field has to be multiplied by a factor of four with respect to non polarimetric case (Table 3.1). Flat field calibration is critical for polarimetric observations, since flux differences from different CCD regions are considered for the polarization measurement. High signal to noise, achievable by adding several flats, is required. To avoid any systematic effect due to polarization of the light reflected from the white screen on the dome, is necessary to take flats at different rotation angles of the rotation adapter (0 and 90 deg). In this way the 0 and 90 deg beams (and similarly the 45 and 135 deg beams) are swapped on the detector and the dome polarization can be eliminated by summing the different images.

3.5.2 Instrumental polarization

To obtain reliable measurements of polarization on science targets a monitoring of the instrumental polarization is required. This can be done by acquiring polarimetric images of standard zero-polarization stars. Observations of stars of well known polarization may also help in checking instrument performances. In particular they are suitable to calibrate the possible discrepancies between the measured and known polarization angle. that could amount to 1 deg. A list of polarimetric standard is available in the control room.

Altought instrumental polarization as measured on zero–polarization standards is usually below 1%, the acquisition of polarimetric standard for every observing night is recommended.

3.5.3 Observing strategy

The observing procedure for polarimetric observations is rather simple. The target is places in a suitable position in the polarimetric mask using the same procedure used to place a star into the slit in spectroscopic mode (Sect. 4.9).

3.5.4 Data Analysis

A data analysis software, based on IDL scripts, for reduction of polarimetric observations of stellar objects can be downloaded from the AFOSC web page. It consists of an User

Interface, to load the four images requested for data reduction. The user simply displays the scientific image and select the object, following the instruction displayed at the bottom of the user interface. Two graphical windows allow to estimate the results, displaying polarization and flux. The polarization is calculated at three sigma from the center of the star. With a slide bar it is possible to change the range in which sky flux is selected.

3.6 Spectro–polarimetry

3.6.1 Instrument set-up

Spectropolarimetric observations are feasible mounting the polarimeter on the filter wheel and using a grism from the grism wheel. When polarimetric observation (with filters) are also required, the filters have to be moved into the grism wheel.

To avoid superposition of the four spectra produced on the detector, a special slit has been prepared. In this way, the spectra of 5 different regions, 22.7 arcsec long, are obtained.

3.6.2 Flat Fields

Similarly to polarimetric case, it is recommended to take several flats to achieve very high signal to noise, rotating the telescope rotator adapter at 0 and 90 deg to remove the effects of dome polarization.

Table 3.8 reports the suggested exposure times for the flat field calibration in spectropolarimetric mode.

Grism	t_{exp} (sec)	Remarks
#4	8	
#7	18	
#8	16	
VPH#4		

Table 3.8: Suggested exposure times for flat field calibration using the slit for spectropolarimetry, with telescope pointing the FF screen. The source is the 1.0 kW FF lamp.

3.6.3 Instrumental polarization

Spectropolarimetric observations of zero–polarization standards shows only a mild trend of instrument polarization as a function of wavelength.

3.6.4 Wavelength calibration

The four resulting spectra have different wavelength solutions due to lateral chromatism of the grims (see Fig. 3.4). This effect is larger for grisms with wide spectral coverage (e.g. Grism #4). The four spectra need therefore independent wavelength calibration.

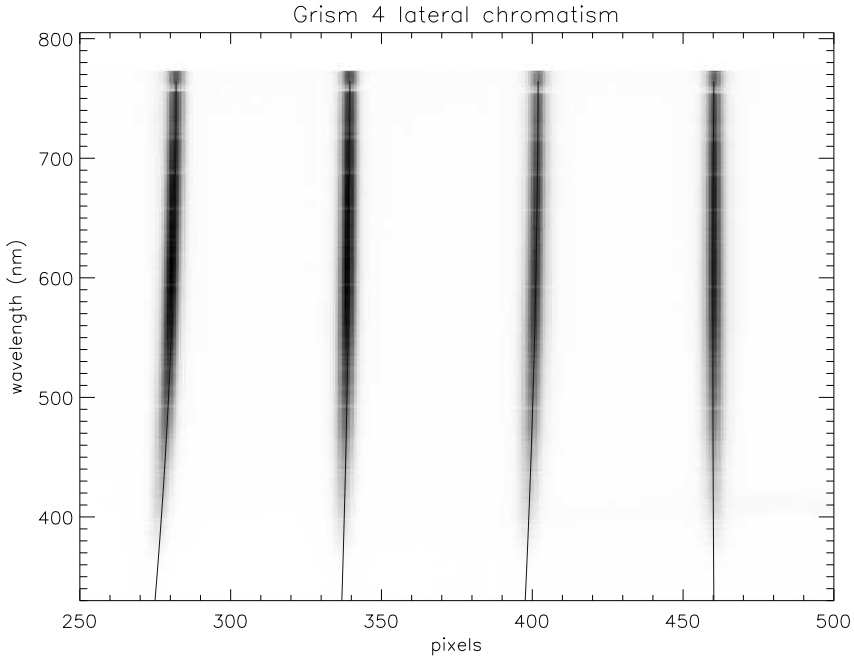

Figure 3.4: Lateral Chromatism.

3.6.5 Observing strategy

To properly take into account the changes in the line profile introduced by the polarimeter, it is strongly recommended to split each observation in two exposures, taken at 0 and 90 deg. In this way, channels exchange each other, allowing to remove this instruemental effect.

Chapter 4

The AFOSC Control System

4.1 Introduction

This chapter is a practical guide for an observing run with AFOSC. The Graphical User Interface (GUI) that controls AFOSC, the rotator/adapter and CCD is described.

The description of how to start and initialize the system and how to set the focus of the AFOSC Camera is also given (Sect. 4.2–4.5). Usually these operations are performed by the technical staff and the observer does not have to worry about them. The description of the part of the AFOSC Control Software involving the normal user starts at Sect. 4.6.

4.2 Starting the system

The system start–up follows these steps:

- switch on the electric power of the continuity group at the pedestal of the telescope,
- make sure that AFOSC, adapter and CCD electronics are switched on,
- switch on rotation electronics on the mount arm of the telescope,
- switch on the VME rack in the control room and wait until the boot is completed,
- log in the remoto account on alpha station wusche (ask the system manager for the password),
- Close any process that might affect the color palette (Netscape, IDL, IRAF, etc), to avoid problems with colors display in your AFOSC run,
- Click the *GO_AFOSC* icon on the left part of the desktop (over the clock),
- At this point the GATE environment starts-up on the VME and the console window of the GUI appears on the screen of the workstation (Fig. 4.1). The instrument is ready for the initialization.

Figure 4.1: The Consolle window of the AFOSC GUI.

4.3 Initializing the system

To initialize the system perform the following steps:

- Click the button UTILITIES on the console, another menu button appears (Fig. 4.11),
- Click the button INIT on this menu, the initialization window appears (Fig. 4.2),

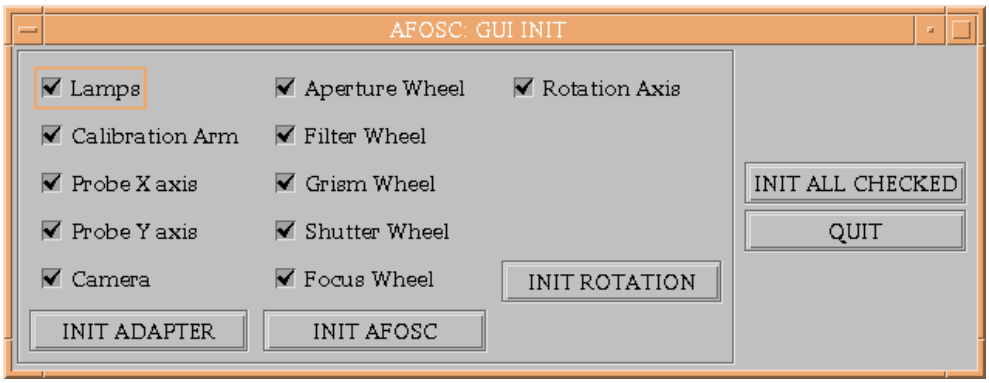

Figure 4.2: The initialization window.

The GUI INIT window is divided into three principal parts: adapter, AFOSC and rotation. You can choose which movements you want to initialize (mark the button to initialize). The three buttons permit to initialize the subsystem separately. Otherwise you can use the button INIT ALL CHECKED . During initialization the window is disabled, when initialization finishes the window is enabled again. During initialization the system can find some errors. See Chap. 6 to have a description of errors and how to solve them. Note that initialization is a reset of the system and so it must be performed ONLY WHEN STRICTLY NECESSARY.

When AFOSC remain switched on during the day while the telescope was switched off the rotation must be reinitialized.

After the change in the positioning of the guide camera (Febraury 2002), the Camera Axis initialization is no longer required.

4.4 Stopping the system

To stop the system, press DONE button in *GUI_CONSOLE* and wait until the console window is closed. This may take several seconds because the system parks probe axes before shutting-down. At this point you can switch off the VME, CCD, adapter, AFOSC and rotation controllers.

4.5 Focusing the AFOSC Camera

The FOCUS window (Fig. 4.3) allows to set the AFOSC camera focus positions. This is done by typing the desired position, pressing ENTER to confirm and clicking the GOTO button. When the position has been reached, the GOTO button is newly activated.

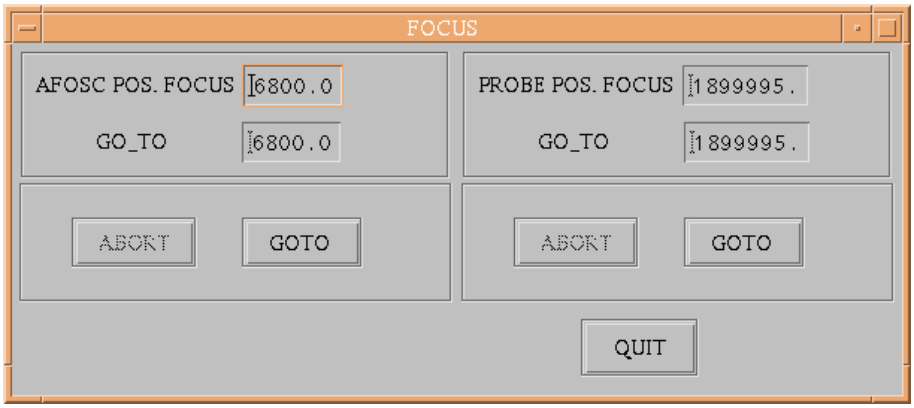

Figure 4.3: The Focus window.

Usually the AFOSC Camera Focus is determined in the morning, during the set–up operations; so that usually the previously measured focus is typed at beginning of the night. If the AFOSC temperature is very different with respect to the time of focus determination, it might be useful to re–determine the focus or to insert the value predicted by the equation in Fig. 2.11.

After the modification of the camera positioning, the positioning of the probe focus is no longer required.

4.6 Defining and executing exposures

Defining exposures is performed using the EXPOSURE window (Fig. 4.4), opened by clicking the EXPOSURE button on console. This panel consists of 10 rows defining 10 different exposures. The properties of the exposure that can be set are the following:

- Active/Not active: allows to activate and deactivate an exposure in the sequence[1],

[1]Only the activated exposures will be performed. This allows to keep an exposure definition in the window, with no need to prepare the exposure definition every time.

- Exposure type: allows to select image type[2]
- Repeat: sets how many times you want to repeat the exposure (9 times max),
- Identifier: allows to define object name,
- Time: sets exposure time (in seconds; minimum 1 sec),
- Slit: selects desired slit (only the slits currently mounted are included in the menu),
- Filter: selects desired filter,
- Grism: selects desired grism,
- Binning X (1 recommended, see Sect. 6.2)
- Binning Y (1 recommended, see Sect. 6.2)
- Left: set left column of the box of the image (box size)[3],
- Right: set right column of the box of the image (box size),
- Up: set up row of the box of the image (box size),
- Down: set down row of the box of the image (box size),
- Lamp: selects calibration lamp,
- Save/Not save: allows to choose if save or not save image.

Every text field must be confirmed typing ENTER from the keyboard.

When user does not choose to save the image, then it will be stored in *wusche* /tonight/scratch directory and this directory will be cleaned the morning after the observing night.

The user can also save to file (.exp) a sequence of exposures or load it from a file (.exp), use SAVE and LOAD button on the bottom of the window to use this facility.

To start the sequence use START button. A dialog window will appear (Fig. 4.5). From this window it is possible to stop, to pause, to change exposure time, and to stop and restart the auto-guide. Other information about the status of the system is also provided. **To stop an exposure the STOP button has to be used. The ABORT button implies a full logout of the system**.

The REPEAT EXP button is useful to repeat the last executed exposure, with the possibility to change only the exposure time (i.e. no changes in the wheels). In this case, the exposure starts immediately, allowing to save the time used to check for the wheels positions.

The resulting images can be visualized using the OFFSET window. The tools for a quick–look analysis of the images are described in Chapter 5.

[2]The following image types are possible: Bias, Dark, Flat, Calib (for calibration lamps), Science, Wipe (for wiping the CCD), Fast (fast readout mode). The exposure type is written in the file header.

[3]The box limits are defined according to the orientation of the images as it appears in the OFFSET window.

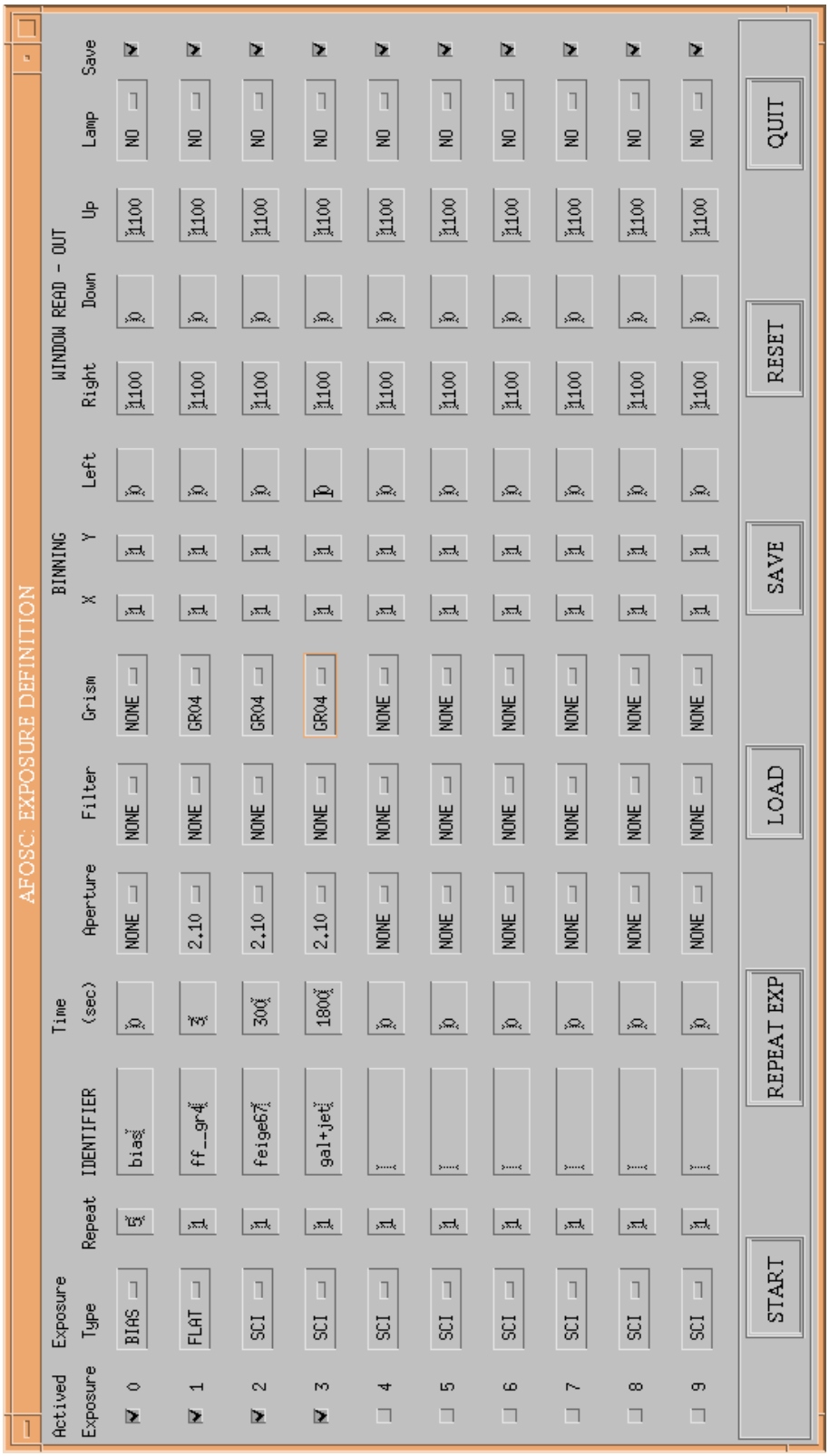

Figure 4.4: The exposure definition window.

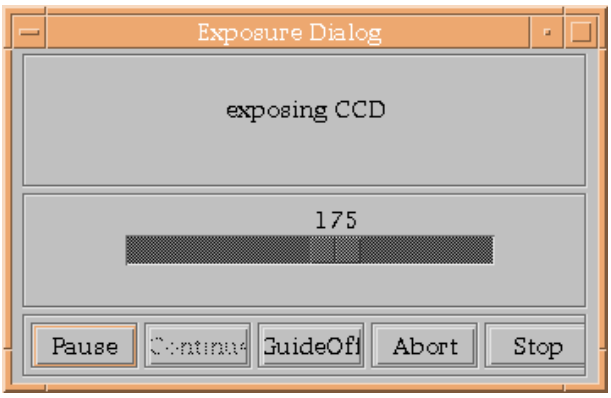

Figure 4.5: The dialog window that appears during an exposure.

4.7 Finding a Guide Star

Finding the guide star is achieved by moving the probe in the focal plane. The PROBE window allows to perform this task. Follow these instructions:

- Press PROBE button on console window. The window of Fig. 4.6 appears.
- Check the guide camera status (on/off, gain, focus) (This part is usually performed by the night assistant)
- (optional step)
  Display the GSC stars in the PROBE field. To use this utility simply click GO_GSC icon near GO_AFOSC icon. A GSC search window will appear (Fig. 4.7). Simply putting the desired coordinates, the limit magnitude and the radius field (default value 1800) in the corresponding fields, then click search button. If the PROBE window is open, at the end of the search found stars will be displayed on probe field. Now you can move the probe toward the selected star. Note that the probe field of view is about 60x90 arcsec so you must perform a set point (Sect. 4.12) before to use this utility.
- Click and release the left mouse button on the cross cursor and move the mouse toward desired position. Click the mouse to confirm the position. All the movements of probe will be disabled until the request position will be reached.
- When the probe is moving, check for the presence of stars in the guide camera. Note that the orientation of the field on the guide camera and on the probe window are opposite.
- To perform step movements you can use the arrows on the right part of the window combined with [micro, medium, large] selection. The direction of the movement is defined according the orientation of the field on the guide camera, i.e. clicking the UP arrow moves the probe up in the guide camera and down in the probe window. The stepsize of the movements with the arrows are 1, 6 and 61 arcsec for micro, medium, and large selection.

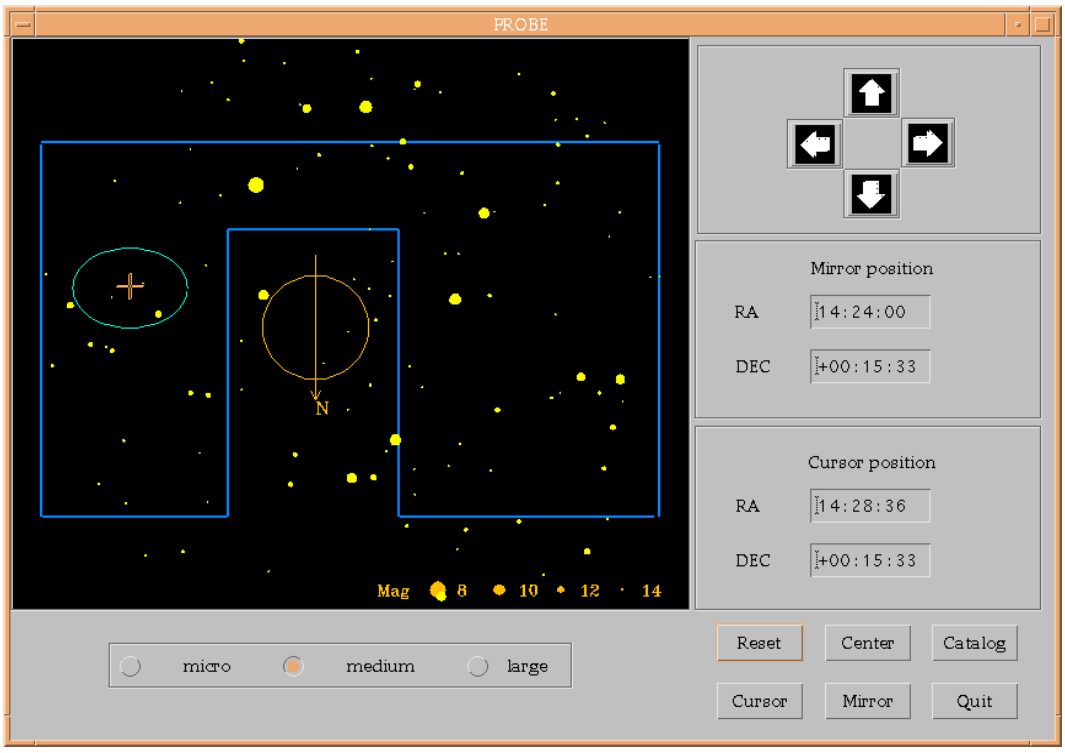

Figure 4.6: The PROBE window.

4.8 Using the Auto–Guider

AUTOGUIDE window (Fig. 4.8), allows to start and stop auto-guide and to select the box used with auto-guide. Follow these steps:

- Using PROBE find a good star for auto-guide (Sect. 4.7)
- Press GUIDE button on console, the AUTOGUIDE window will appears,
- Press GRAB button on the top left of the window. The image from auto-guide monitor will be grabbed and displayed on the window.
- Using left mouse button pick the position of the star selected to use for auto-guiding. A box will be displayed around the star. Use left button to move, central button to resize and right button to confirm it. After confirmation the box will be displayed on the monitor. The procedure can be iterated if the box is not satisfactory.
- Press GUIDE_STAR button if you want to start auto-guide moving the center of box on the star, or press GUIDE_BOX to start auto-guide moving the star in the center of the box.

N.B. If you have selected the box for auto-guide at least a time, and if the selected star is inside the (previously defined) autoguiding box, you can use GUIDE BOX without selecting the box again.

The GUIDE_OFF allows to stop auto-guide.

The use of differential guiding is described in Sect. 4.15.

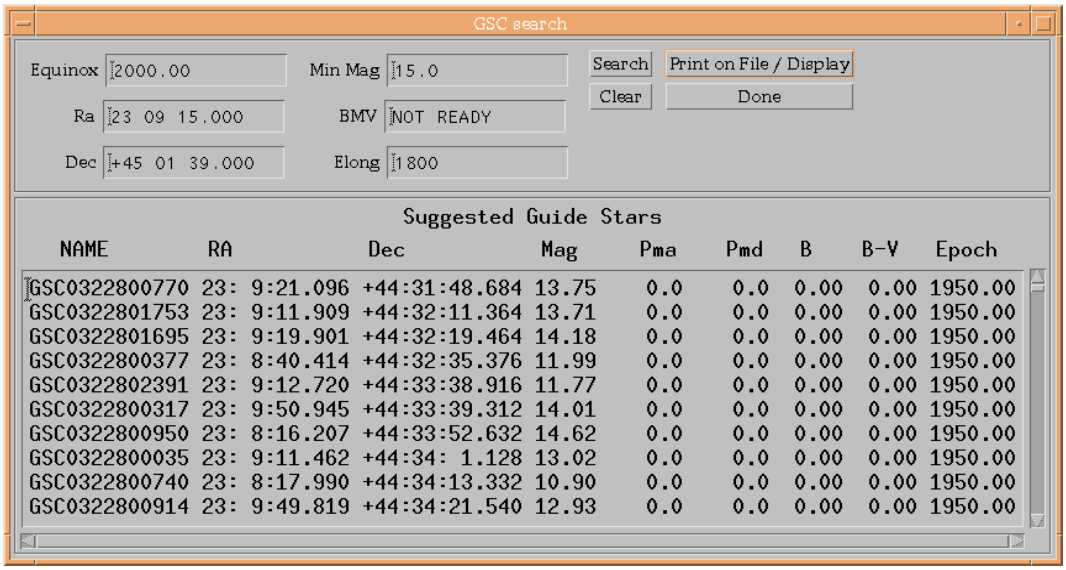

Figure 4.7: The GSC window.

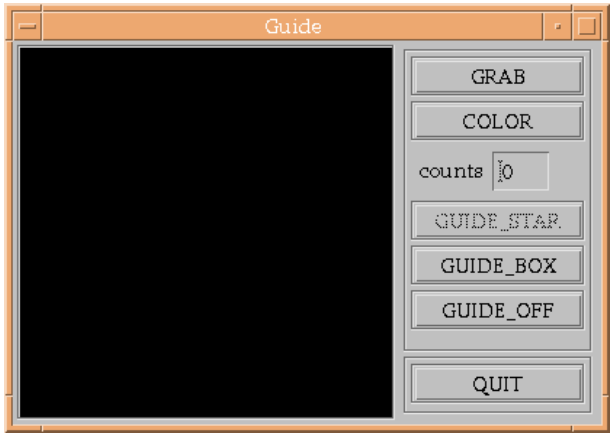

Figure 4.8: The guide window.

4.9 Performing Offset

The OFFSET window allows to calculate the distance between the actual position of the target and the desired position. Clicking the OFFSET button in the console, a window as Fig. 4.9 will appear with the last acquired image. We stress that the images used to perform offset have to be taken without any filter (because of the position shift they introduce) and with the auto-guider switched on. Using LOAD button is possible to load previous images. The window is divided into three parts:

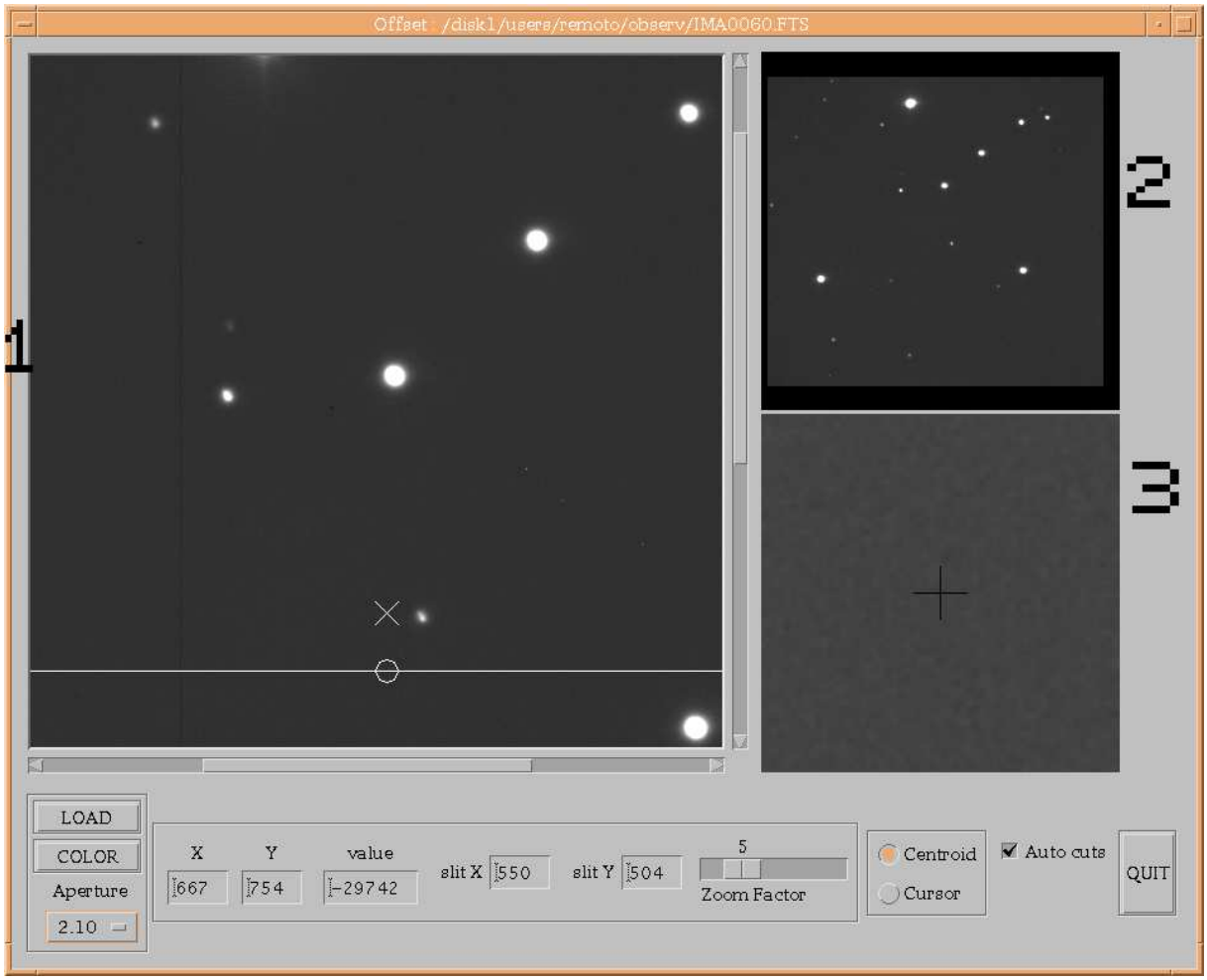

Figure 4.9: The offset window.

1. a main frame in which the central part of the image is displayed at full resolution,
2. a frame where the complete image is shown,
3. a frame in which a zoomed box (of variable enlargement) of the image is given.

Clicking the target in the complete frame, the object is displayed in the full resolution frame and in the zoomed frame. In the bottom left part of the window there is a menu with the slits. Selecting the slit the reference point for the offset is established. During

the instrument set–up an accurate measure of the center of all the slits is performed and registered in the system. In the bottom right part of the window there is an option menu to select how to calculate offset, if using centroid (stellar object non saturated) or cursor (galaxies and saturate object).

To calculate offset, after selection of the slit, simply click with the left button of the mouse on the target. The interface will ask to confirm the box of the centroid, if centroid option was selected with right mouse button in the zoomed frame. The box can be resized using the central mouse button at the corner of the box and moved with the left mouse button on the box and dragging it. After confirmation with the right mouse button, the TELESCOPE window will be opened (Fig. 4.10) and you are ready to put the star in the slit. Follow these steps:

- Mark the star position on the auto-guider monitor and press CMBO button. GUI will notice that the auto-guide will be switched off and will ask to confirm the movements of the probe.
- Click OK button. If a guide star too close to the edge of probe field is selected, the GUI notices that the offset cannot be performed, if the distance from the edge is not critical the star will appear on the auto-guide monitor to offset its position. In the telescope window the new coordinates for the telescope will be displayed.
- Point the telescope on the new coordinates. The guide star will appear on the guide camera monitor near the position marked before; you must approach the star to this point as much as possible. The GUI asks to restart auto-guide[4].
- Restart auto-guide.

Take another image and repeat offset calculations. If the star is not on the slit repeat combined offset. Typically no more than two iterations are necessary to put the star in the slit otherwise see Chapter 6.

4.10 Rotating the Slit

It is possible to obtain the spectrum of an extended object at the desired position angle. This can be performed

- Rotate the adapter (using the TELESCOPE window, Sect. 4.12) at the selected position angle
- Acquire an image after rotation has been performed
- Perform offset on the rotated image as described in Sect. 4.9 (except for the use of GSC, that is less precise in this case, see Sect. 6.2).

[4]When using the differential guiding, it is necessary to re-start the DG at this stage.

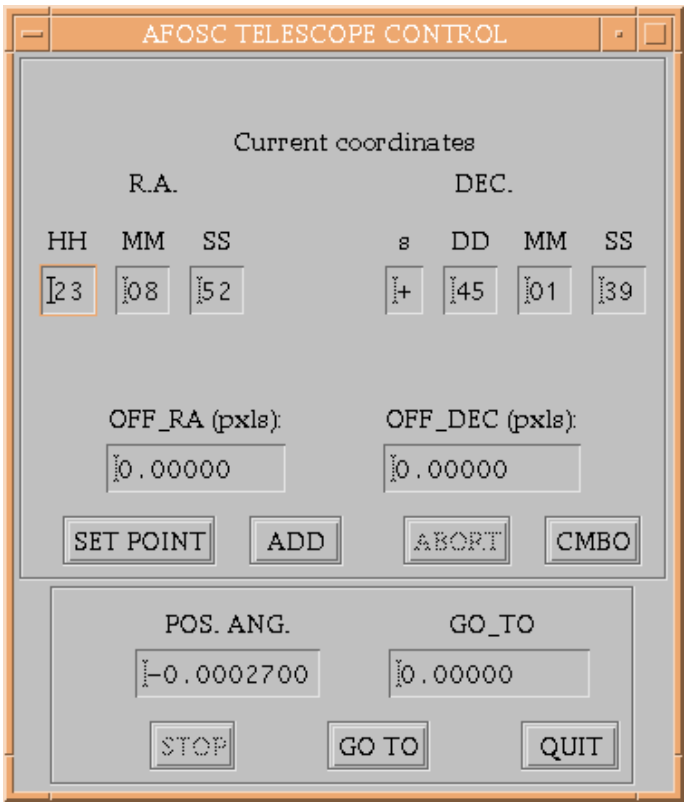

Figure 4.10: The telescope window

4.11 Positioning Two Objects into the Same Slit

The OFFSET window can be used also to compute automatically the position angle between two objects in the frame. This procedure allows to acquire spectra of two objects into the same slit. Follow these steps:

- Be sure the auto-guide is off;
- Select the centering mode (default=centroid);
- Click first object with the right button of the mouse;
- If in centroid mode, confirm the box in the ZOOM window;
- Repeat steps 3 and 4 for the second object;

  On the frame the straight line connecting objects and the position angle will appear. This angle is corrected for the adapter rotation. Automatically the TELESCOPE window will open with the position angle already set.
- Press GOTO to align the two objects relatively to the slit (sometimes two iterations are needed).

Continue with the Offset procedure.

4.12 TELESCOPE Window

In addition to the CMBO function, this window permits other functions:

- If you use OFFSET window, selecting NONE slit and clicking SET POINT button after the centroid (or cursor) calculation at the display of TELESCOPE window, you will have in the coordinates field the coordinates to put in the SET POINT field of the coordinate interface (PC near auto-guide monitor).
- Used in the same way of FOCUS window, the bottom part of TELESCOPE window permits the rotation of the adapter (angle expressed in degrees from north to east)
- Simply opening TELESCOPE window you have the actual position of the telescope in the coordinate field (the same data are displayed on the COORDINATE PC).

4.13 Utilities Window

This window presents several useful application: INIT for the AFOSC initialization, PYRAMID to determine the focus of the telescope using the pyramid focus, DF GUIDE to activate the differential guiding and NIGHT REPORT to fill in and submit the night report. The CLEAN SCREEN button refresh the monitor on which the images are displayed. The SETUP and SETUP REPORT application concern the instrument set–up while the COMMAND window allows to send commands directly to VME. This option could be useful in various cases of technical problems (see Chap. 6).

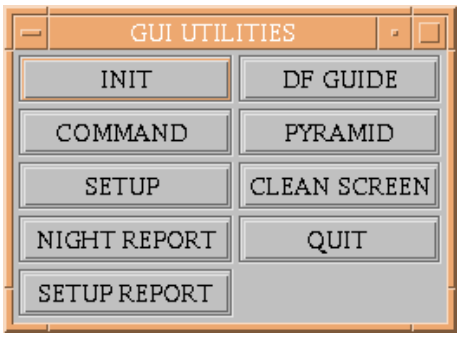

Figure 4.11: The GUI utilities menu.

4.14 Pyramid Focus

To determine the telescope focus using the pyramid focus take the following actions:

- Take an image of a stellar field using the pyramid focus (mounted on the grism wheel). The exposure times must be set taking into account that the beam is splitted in four, avoiding at the same time any tracking–induced image deformations.
- Open the PYRAMID window from the GUI UTILITIES menu (Fig. 4.12)

- Load the image
- Click with the left mouse button on the lower left image of some unblended stars
- Click with right button of the mouse when finished to calculate the focus correction (in mm)
- Adjust the telescope focus (this part is usually performed by the night assistant)

If the new focus is very different from the precedent one, it might be useful to repeat the procedure.

Figure 4.12: The Pyramid Focus window.

4.15 Differential Guiding

The differential guiding window is opened from the GUI UTILITIES menu. The required parameters are the velocities in right ascension and declination (in arcsec/hr) and the total time for which the DF guide is required. Such time must be longer than the planned exposure time to take into account overheads. When obtaining a sequence of images on the same object, it is recommended to select a time long enough to include the whole

sequence (including overheads) if allowed by the probe bounds. If the selected total time is longer than the maximum allowed by the probe bounds, an error massage is issued. A warning message is issued if the velocities exceedes 180 arcsec/hr, since in normal observing conditions the differential guiding at velocities larger than this limit introduces significant degradation of image (see Sect. 1.3.2).

The autoguide has to be on to activate differential guiding. To activate the differential guiding, press the DIFF ON button. Then the differential guiding continue for the selected time. Note that when such time is finished, no messages are provided (and the DF ON field remains unchanged). To stop the differential guiding before the whole time span has been elapsed, press the DIFF OFF button; to restart DG press the DIFF ON button (this restart the DG for the selected time).

The GUIDE OFF and GUIDE BOX buttons stop and start autoguide respectively (they can be used alternatively to the corresponding buttons on the GUIDE window).

The DF guiding is a fully independent system, so that it is recommended to keep the window permanently opened during observations using differential guiding.

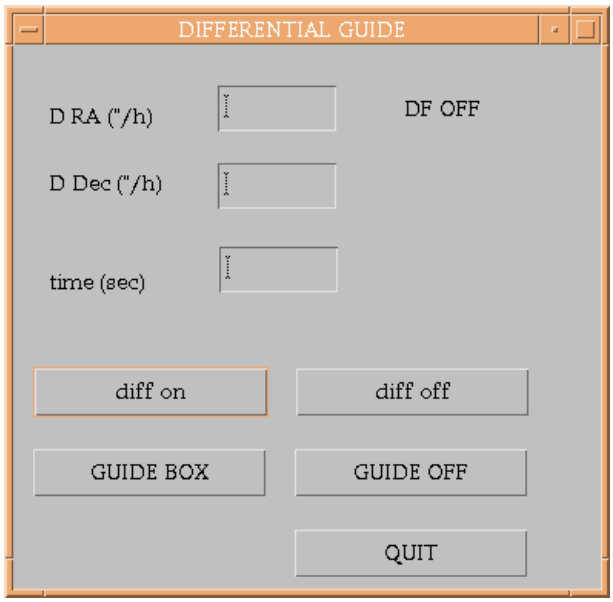

Figure 4.13: Differential Guiding window.

During the offset procedure to put the (moving) object in the slit, the autoguide is stopped. This causes also the differential guiding to be turned off. When the GUI ask to restart the auto-guide (see Sect. 4.9), the DG must be restarted too. If more than one offset is performed, this must be repeated every time. It must be noted that the telescope does not follow the movement of the moving object when performing the offset.

4.16 METEO window

Clicking METEO on main window menu opens the window with the currently meteorological data (Fig. 4.14). The data are displayed also at the web page http://alphek.pd.astro.it/meteo/index.php (Fig. 1.10).

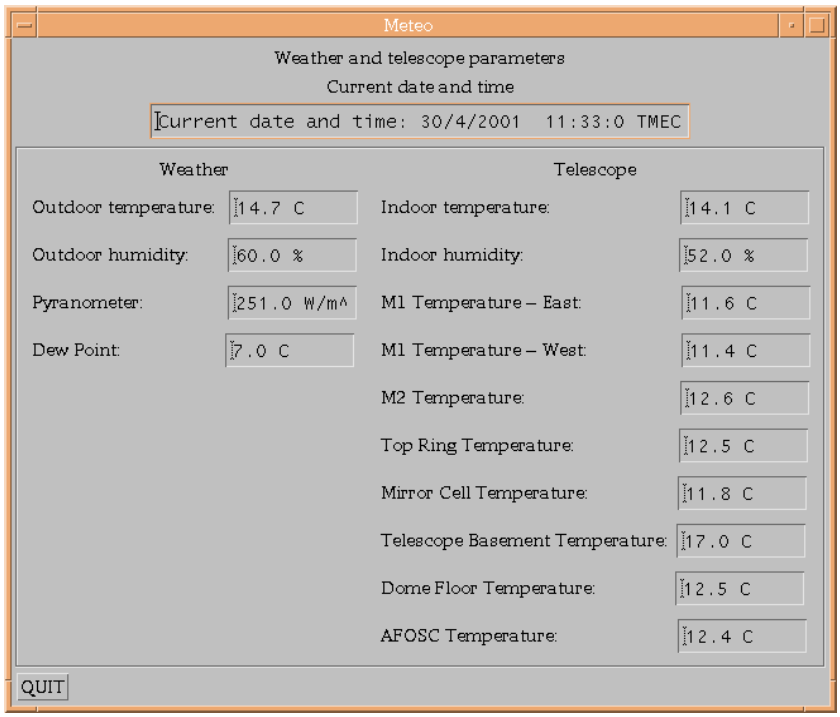

Figure 4.14: The meteo window.

4.17 Checking set–up

The SETUP window (Fig. 4.15) shows the instrument set–up.

4.18 STATUS window

This windows simply describes the status of the instrument (Fig. 4.16). No action can be taken from it. Among many other information, the STATUS windows reports the number of last image obtained. The telescope coordinates are also shown. If meaningless or wrong values are given, this mean that the serial connection between coordinate PC and VME is closed. It its not re–opened, no coordinates and UT are written in the file header.

4.19 End of Night

At the end of the night the visiting astronomer is required to fill the Night Report. This has to be performed using the form within the AFOSC GUI, opened by the NIGHT REPORT button of the GUI UTILITIES menu. The Night Report form is shown in Fig. 4.17.

When it has been filled, press SUBMIT: an e-mail report will be sent to the instrument staff.

Figure 4.15: The set–up window.

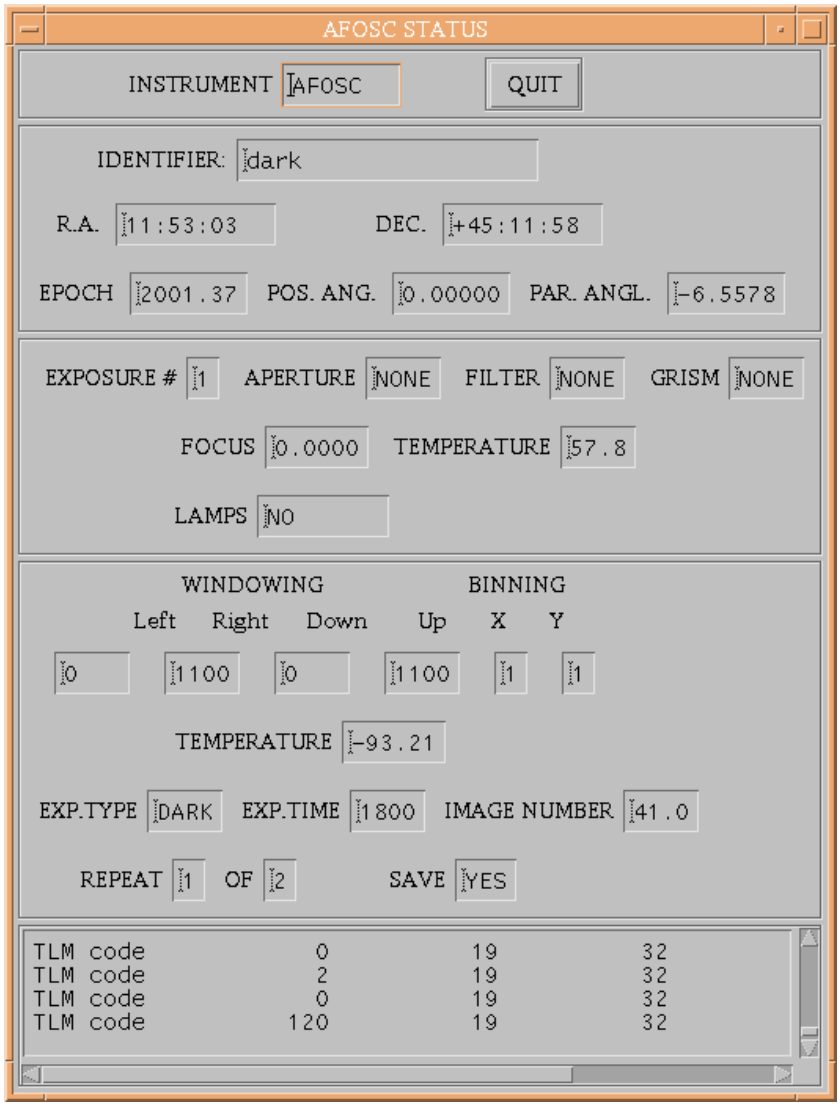

Figure 4.16: The status window.

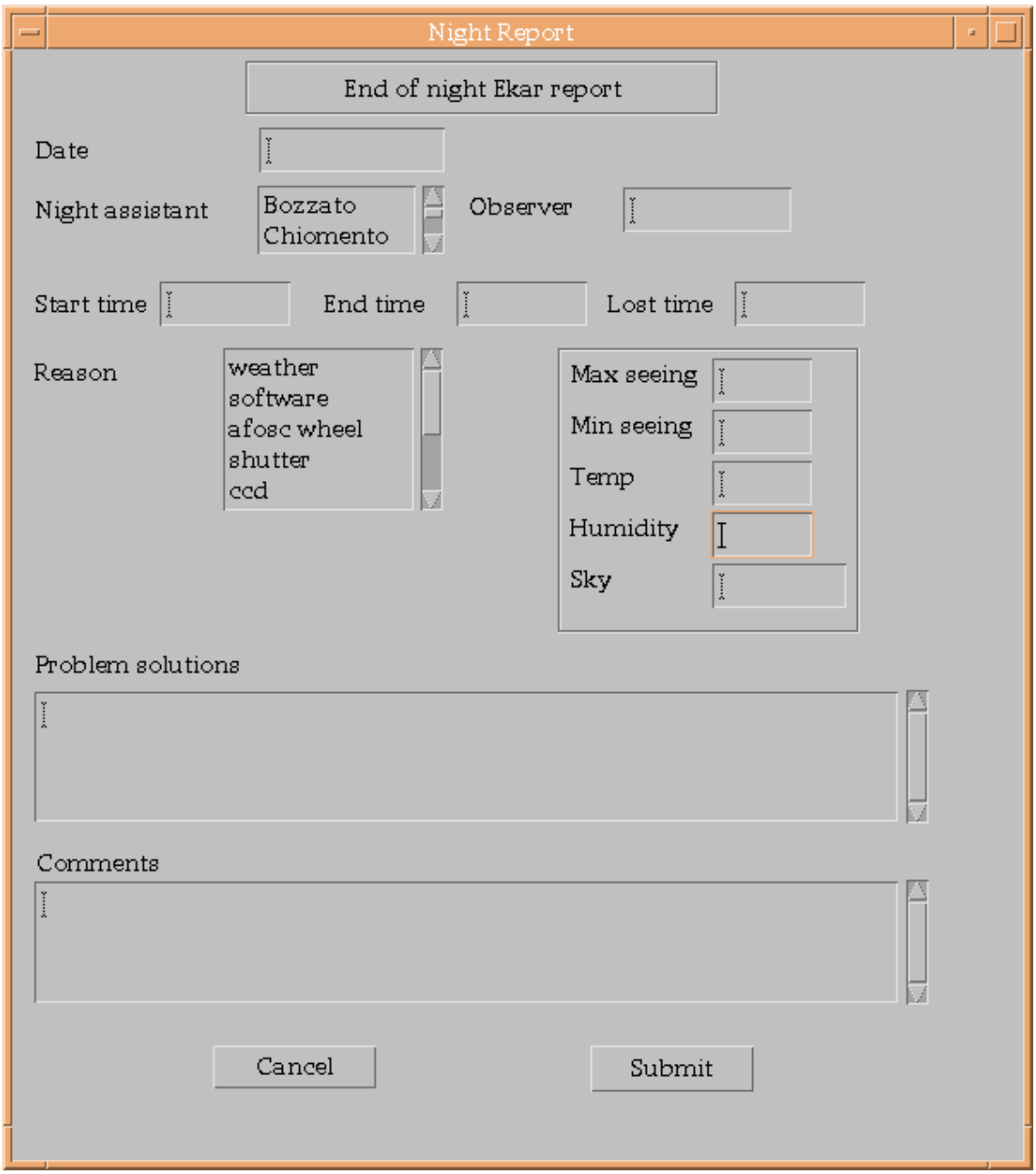

Figure 4.17: The End of Night report form.

Chapter 5

Quick Look Analysis

5.1 Quick look using AFOSC GUI

With the AFOSC Graphical User Interface it is possible to perform a preliminary examination of the images using the OFFSET window (see Sect. 4.9). The selected image (the last by default) is visualized. It is possible to check counts moving the cursor and to display enlarged the region of interest.

5.2 Quick look tools using IRAF

An additional workstation with IRAF, MIDAS and IDL packages is available in the control room for quick look analysis of the images. The images can be loaded on disk using the tool EKAR under IRAF.

To open IRAF click **cl+sao** on terminal menu, then type **ekar** at cl prompt to load ekar package. The following commands are available:

- **hekar**: list the commands available on EKAR package
- **lista**: list the images saved (remoto/tonight)
- **carica**: load and display the saved images of the current night (directory tonight)
- **carica1**: load and display the images of the precedent nights (directory observ)
- **carica2**: load and display the images that are NOT saved (directory scratch)
- **last**: load and display the last image
- **pyramfocus**: focus the telescope using the pyramid focus (superseded by the tool within AFOSC GUI)
- **slit**: overplot AFOSC slit on SAOIMAGE display (superseded by the tool within AFOSC GUI)
- **offset**: slit calculation (superseded by the tool within AFOSC GUI)

- **esamina**
  simple analysis of images

  Click on saoimage window and use the following commands: (they hold for the position of the cursor)

  - c : plot one column
  - l : plot one row
  - m : statistics on the selected area (default 20x20 pixels) (mean,
  - e : contour plot of the selected area
  - s : 3–dimensional plot of the selected area
  - r : show the average radial profile of the selected object
  - a : measure the magnitudine of the selected object
  - q : quit

  The results can be saved in disk as file *esamina.dat*

- **cesamina**
  change default parameters for **esamina**

  - Number of pixels for statistics (default 10)
  - Number of rows/columns to be averaged (default 5)
  - Radius for aperture photometry (default 9)

- **seeing**: measurement of seeing on the selected image

  Click on saoimage window and use the following commands:

  - **,** : measure the parameters of the selected star (FWHM, ellipticity, angle) (the cursor must be pointed near the center of the star)
  - **q** : exit

  The measured quantities are stored in the files *cursor.dat*, *mark.dat* and *seeing.dat*. They can be saved on disk. The mean of seeing, ellipticity and position angle are printed on the terminal and plotted

- **magnitudine**: it measures aperture photometry

- **spettro**: automatic extraction of the spectrum for B&C

Chapter 6

Troubleshooting and Pending Problems

6.1 Introduction

This chapter presents:

- A list of the AFOSC problems still pending. The instrumentation staff is aware of them and work aimed to find the proper solution is in progress. When planning the observations, be careful in not including any of the sequences described here.
- A guide to react to possible problems to the instrument that may occur during an observing run. They has to be reported in the End of Night Report.

6.2 Pending problems

6.2.1 Rotation

- When AFOSC remain switched on during the day while the telescope was switched off the rotation must be reinitialized.

6.2.2 AFOSC shutter

- When AFOSC temperature is below 0 C, the shutter does not open rather frequently. In this case it might be necessary to re–initialize it

6.2.3 CCD

- The system crashes if the first exposure after initialization is of WIPE type
- For BIAS exposures the wiping of the CCD is not performed. Therefore the first two or three bias of consecutive sequence usually show an higher (and progressively decresing) level. The first bias just after initialization is saturated.
- Binning 2x2 the CCD is allowed by the GUI but produces at present low quality images.

6.2.4 GSC catalog

- When the rotator is not in default position (0 deg), it is not possible to use GSC to find the guide star, due to a misalignment bewteen mechanical and optical axis

6.2.5 Differential Guiding

- When the differential guiding starts, there is no feedback. For example, no messages are returned when DG stops.

6.2.6 Graphical User Interface

- Before to perform offset, the probe window must have been opened (without need to leave it opened)

6.2.7 File header

- The airmass keyword in the file header is not reliable

6.3 Troubleshooting

Important Information

The control system of the instrument is distributed on three subsystems:

- *Work Station WUSCHE for the Graphic User Interface (GUI);*
- *VME AFOSC for the real time control of instrument and adapter;*
- *transputer network for CCD handling.*

In case of troubleshooting it is important to act ONLY on the proper subsystem avoiding to reset the entire system uselessly.

6.3.1 Initialization

I.1. On a dialog window the message *AFOSC is not connected* appears. Take the following actions :

- Check the power of AFOSC controller is switched on;
- Check the RS232 cable between VME and AFOSC controller is connected;
- Init AFOSC again.

I.2. If the problem persists:

- Check the fiber optic connection between VME and CCD controller;
- Exit from GUI and from GATE;
- Enter the command ISPY from VME console in order to check the transputer network.

  A message like

  # Part rate Link# [Link0 Link1 Link2 Link3] by TNG!

  0 T805g-24 19k 2 [... 1:0 HOST ...]

  1 T16 -20 1.2M 0 [0:1 ... 2:3 2:0]

  2 T16 -20 1.7M 3 [1:3 ... ... 1:2]

  means transputers are OK.
- Start again GUI.

I.3. On a dialog window the message *ADAPTER is not connected* appears.

- Check the power of ADAPTER controller is switched on;
- Check the RS232 cable between VME and ADAPTER controller is connected and push the red button on the ADAPTER controller.
- Init adapter again.

I.4. On a dialog window the message *ROTATION is not connected* appears.

- Check the power of ROTATION controller is switched on;
- Check the RS232 cable between VME and ROTATION controller is connected.
- Init rotation again.

I.5. On a dialog window the message *Timeout on drive nn* appears.

- Init the drive nn again.
- If the timeout is referred to drive 1 (filter wheel) a whistle should come from AFOSC; in this situation:
- Switch off and switch on again the AFOSC controller (this operation must be executed as fast as possible);
- Init again ONLY drive 1 (filter wheel);
- If initialisation of drive 1 is successfully completed, init again the other drives, otherwise repeat the sequence starting from switching off the controller.

I.6. On a dialog window the message *Rotation timeout error* appears.

- Init the rotation again.

I.7. On a dialog window the message *AFOSC timeout error* appears.

- Init AFOSC again.

6.3.2 Image acquisition

A.1. A bias image appears instead of a scientific image:

- Init the shutter drive again; if the problem persists, act directly on the shutter mechanism (move it from the frozen position).

A.2. An unexpected strange image appears (the spectrum is tilted, only half image is visible only two channels of the polarimeter are present, etc.):

- Init AFOSC again.

6.3.3 User Interface

G.1. Mouse is not responding:

- Use keyboard to move foreground the IDL window and press Enter.

G.2. Calibration lamps don't turn on:

- Verify correspondence between GUI set up and lamps actually mounted;
- Verify the link between the power cable and the correspondent socket.

G.3. Pyramid focus produce useless values:

- This procedure has not been verified in the entire range of M2.

G.4. How to save images after acquisition:
An image not saved is stored in "∼/tonight/scratch" directory; to save it after acquisition:

- Find out its name from the title bar of the offset window (IMAnnnn.FTS);
- Copy it in "∼/tonight" directory using the following command from the prompt:
  Afosc> cp ∼/tonight/scratch/IMAnnnn.FTS ∼/tonight

G.5. After the combined offset operation (performed two times) the star is not on the slit:

- Take an image of the slit (without filters and grisms);
  compare it with its set-up position by clicking the slit identification in the OFFSET window;
  if the registered position of the slit does not correspond to the actual one, retrieve the current vertical slit position using the mouse;
- Click the UTILITY button and then the SETUP button in the UTILITY window in order to open AFOSC: SETUP DEFINITION window (Fig. 6.1)
- Click the EDIT CONFIGURATION button: the table shown in Fig. 6.2 is displayed:
  Finding out the hole number related to the selected slit in AFOSC: SETUP DEFINITION window, edit the corresponding slit positions on the last two columns of the table. Click the ACCEPT and SAVE buttons.
- Open OFFSET window and check slit position again.

G.6. The message *Operation 0* continuously appears on the terminal:

- Logout the system using the ABORT button on the dialog exposure window
- Restart the system

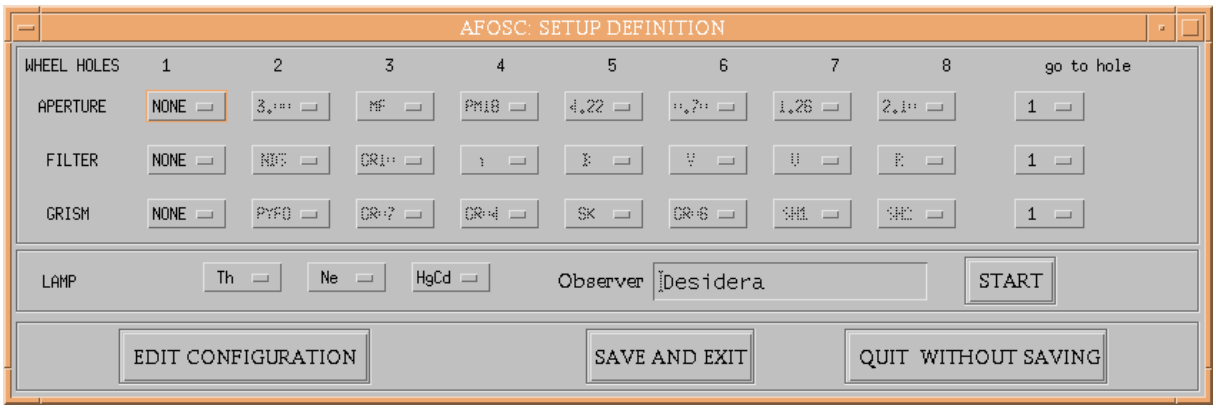

Figure 6.1: The set–up definition window.

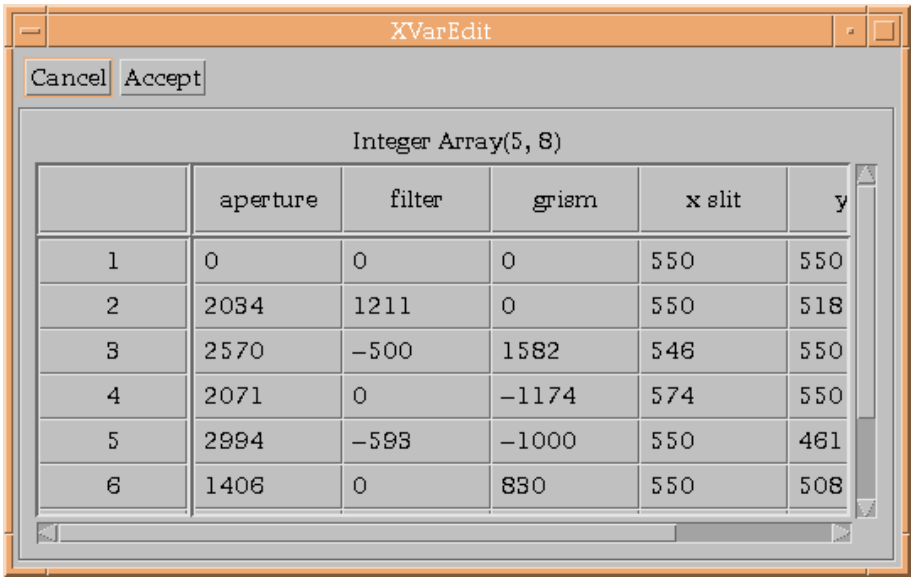

	aperture	filter	grism	x slit	y
1	0	0	0	550	550
2	2034	1211	0	550	518
3	2570	−500	1582	546	550
4	2071	0	−1174	574	550
5	2994	−593	−1000	550	461
6	1406	0	830	550	508

Figure 6.2: The set–up configuration window.

6.3.4 VME

V.1. On VME monitor the message *Destination task never in wait* appears:

- Exit from GUI and from gate, enter the command ISPY from VME console in order to check the transputer network is properly connected;
- Restart the system.

V.2. The guide camera signal is too feeble in the monitor connected to the digitalising board:

- Adjust the sensibility acting on offset and gain trimmers.

6.3.5 Coordinate PC

C.1. On the VME monitor the message *Coordinate PC is not responding* appears:

- Close the serial connection from the Coordinate PC dialog window and then open it again.

C.2. Meaningless or no coordinate values were given by the TELESCOPE, STATUS, and PROBE windows:

- Close the serial connection from the Coordinate PC dialog window and then open it again.

6.3.6 Ethernet connection

E.1. The VME system doesn't receive commands (on the VME monitor the message *Sending verification* doesn't appears):

- Start again GUI.

E.2. The system freezes during image transfer:

- Click ABORT from GUI, reset VME, start again GUI;
- The image is not lost: one can transfer it using ftp:
  Enter following commands from a *wusche* session (ask for the password to the night assistant); enter

  > ftp vmeacq

  > cd 15

  > bin

  > get tempima.img

  > quit

6.3.7 Meteo station

M.1. The web page Meteo Ekar and the Meteo window of the AFOSC GUI are continuously refreshed, but the meteorological data do not.

- Disconnect serial port from *alphek* and resume the SILIMET system (ask to the night assistant)

6.3.8 Final remarks

Every time a problem is found, it has to be described in the end-of-night report, pointing out the error code together with the sequence of operations performed to solve it (if it differs from the suggested one).

If a problem is not described in the present paragraph, it has to be signaled in the end-of-night report, marking it with the N code (New problem).

If a problem is related to an image, this MUST be saved in any case (see User Interface paragraph about how to save an image) and the image number has to be indicated in the report; if the problem is related to the system, indicate the time (UT) the problem arose.

Appendix A

Preparation of the instrument set–up

Each AFOSC wheel (slit, filter, grism) has 8 positions. Most of them are available for the choice of the instrument set–up. They are

- Slit wheel: 6 positions (2 are permanently busy for the hole (imaging mode) and for the pinhole (MF)
- Filter wheel: 7 positions (1 has to be left free for imaging mode)
- Grism wheel: 4 positions (hole for imaging mode, pyramid focus, and the two Hartmann slides are permanently included)

Grisms and filters can be hosted in both the grism and the filter wheel (excluding GR #8, #9, #13 and the VPH grisms, that can be placed only in the grism wheel due to space constrain); cross disperser grisms for echelle mode must be positioned in the filter wheel; the Shack-Harmann sensor must be positioned in the grism wheel due to space constrain. When observing in standard polarimetric mode, the polarimeter should be positioned in the grism wheel. For spectropolarimetric observations it must be placed in the filter wheel, with the grisms left in the grism wheel. If both polarimetric and spectropolarimetric observations are scheduled, the filters to be used in polarimetry must to be moved to the grism wheel. When planning polarimetric and spectropolarimetric observations, include the polarimetric mask (PM18) and the special slit for spectropolarimetry (SP25) respectively in the instrument set–up.

It is necessary to include in the instrument set–up the tools used more frequently in Target of Opportunity (ToO) observations: broadband filters B, V, R, i, Grism #4, 2.10 arcsec slit.

The AFOSC set–up has to be required in advance (at least one day before the observations) to the Asiago telescope staff[1].

[1]The e-mail addresses for set-up communications are: chiomento@pd.astro.it, contri@pd.astro.it, traverso@pd.astro.it, frigo@pd.astro.it.

Appendix B

Efficiency of AFOSC Grisms

This Appendix reports the laboratory measurements of the efficiency of the grisms. The efficiency of Grisms #8, #9, #10 was measured on DFOSC grisms (see www.ls.eso.org/lasilla/Telescopes/2p2T/D1p5M/#Dover). The measurement for Grism #2 is missing.

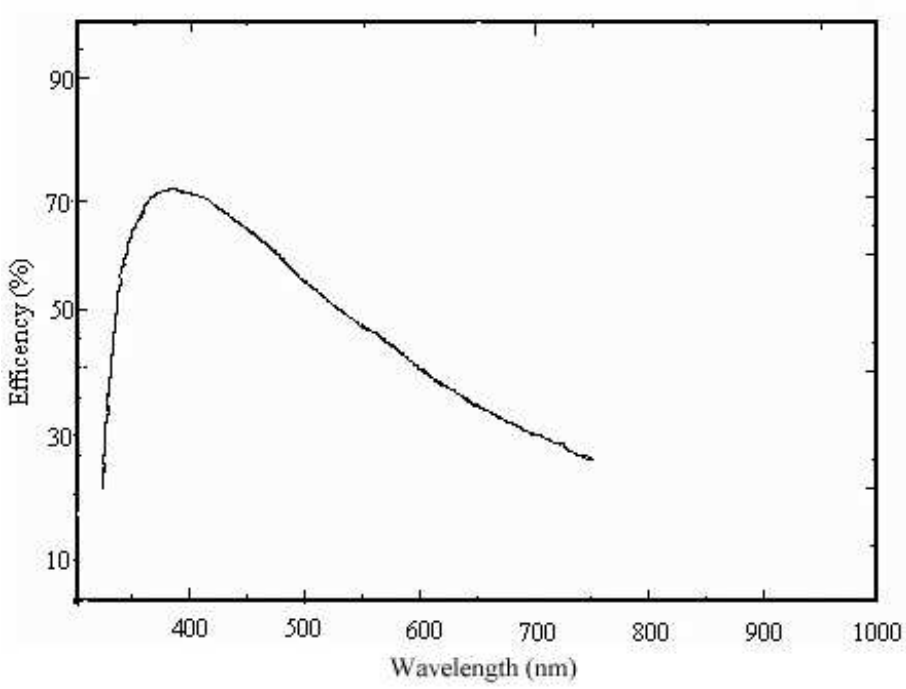

Figure B.1: Efficiency of Grism #3.

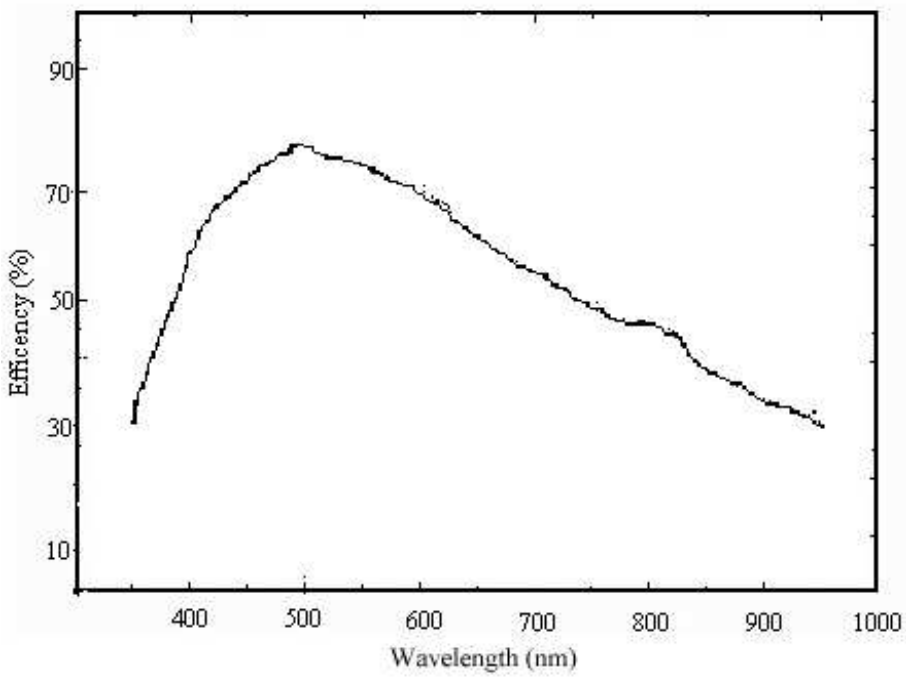

Figure B.2: Efficiency of Grism #4.

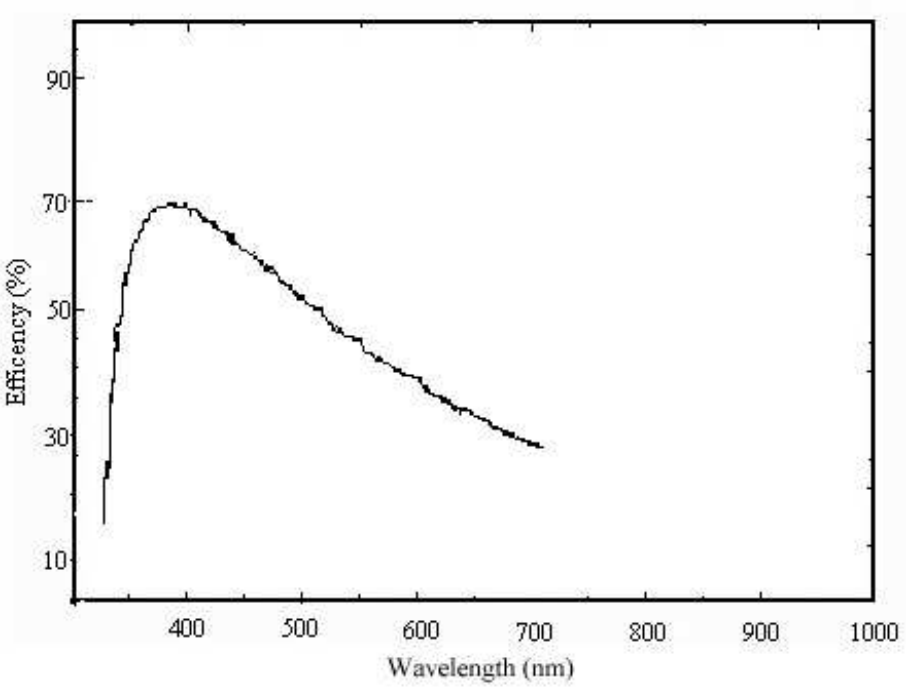

Figure B.3: Efficiency of Grism #6.

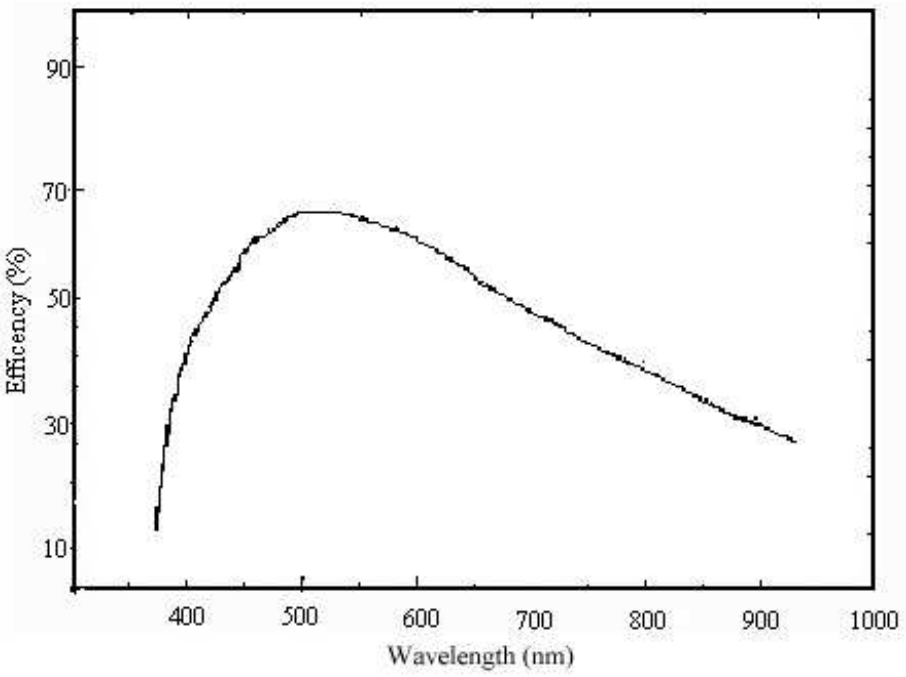

Figure B.4: Efficiency of Grism #7.

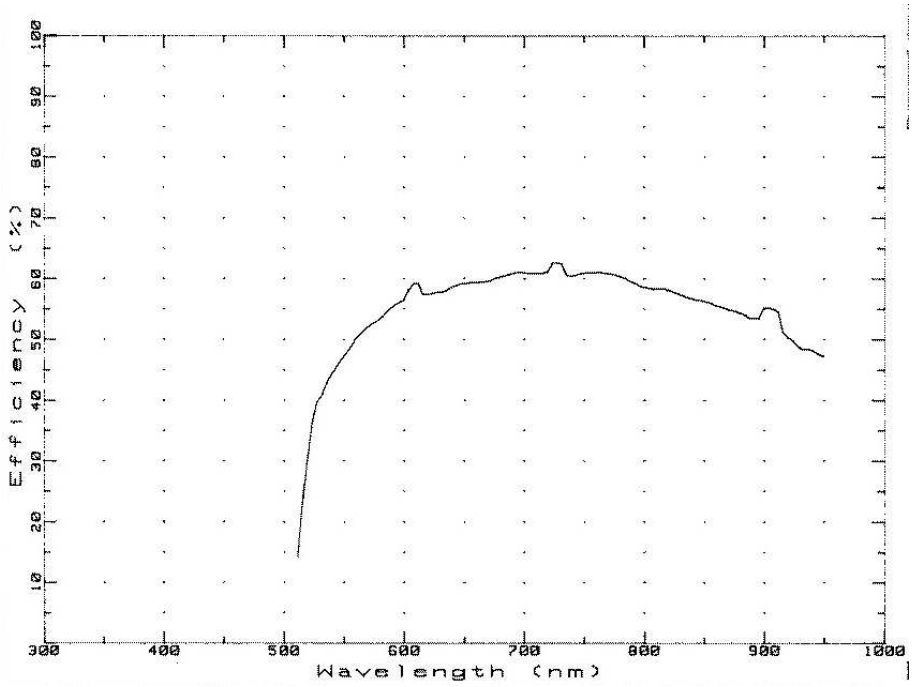

Figure B.5: Efficiency of Grism #8.

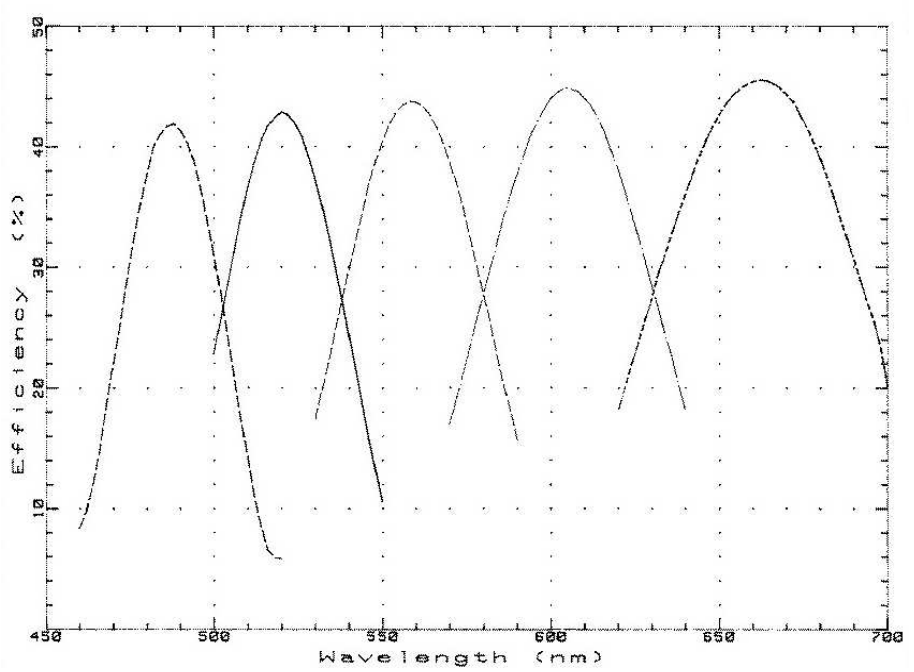

Figure B.6: Efficiency of Grism #9.

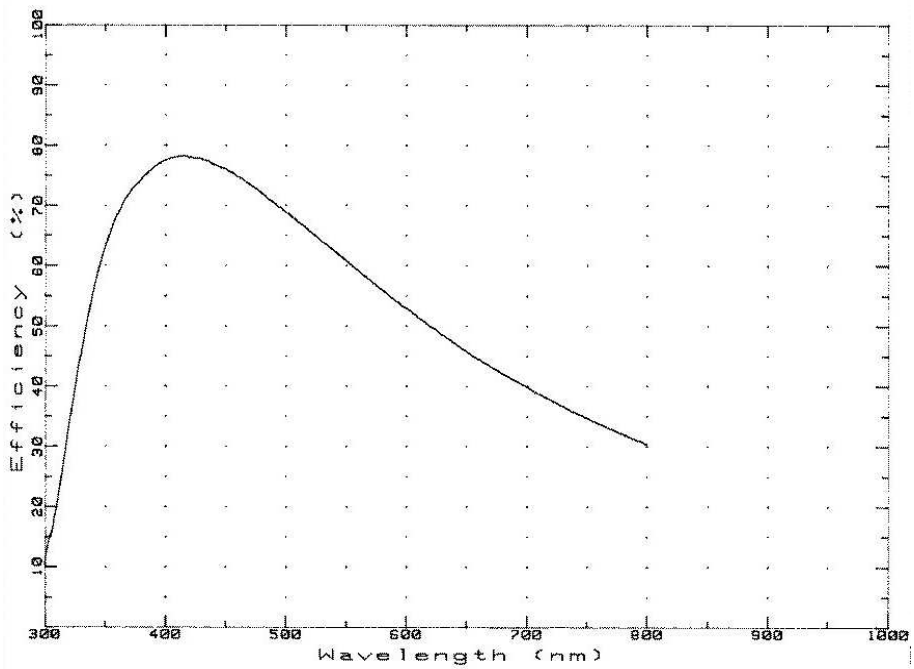

Figure B.7: Efficiency of Grism #10.

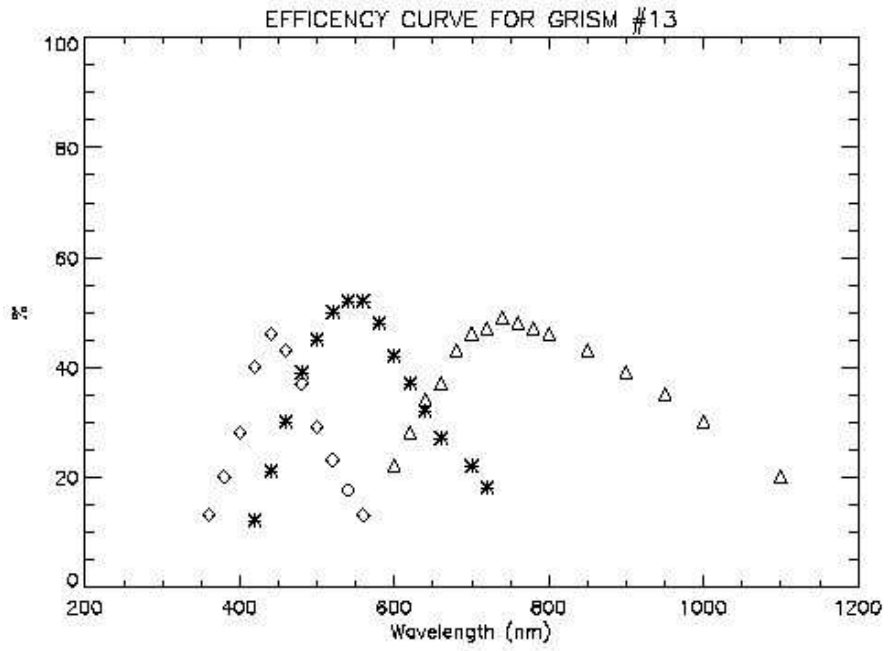

Figure B.8: Efficiency of Grism #13.

Appendix C

Atlas of comparison spectra

C.1 Introduction

This Appendix presents the atlas of comparison spectra useful for wavelength calibration of the AFOSC spectra and the tables with the recommended exposure times. The atlas is made using the mechanical mounting of the previous detector. The lines of comparision spectra are shifted ~ 50 pixels for the actual mounting. Exposure times are calculated to obtain 40000–50000 counts for the brightest line in the spectrum (except when indicated). They have to be considered indicative, since they are subjected to intrinsic intensity variations, lamp substutitions, different positionig of the lamps in their holders, etc.

As described in Sect. 3.3.4, a single lamp spectrum usually does not allow a good calibration due to the incomplete wavelength coverage and/or insufficient number of lines. For this reason we present the atlases of single lamp as well as coadded spectra of two lamps. All the spectra shown in this Appendix were taken with the 0.7 arcsec slit. This made easier the evaluation of possible blends when calibrating spectra taken with a wider slit.

The spectral range might show some changes, since shifts up to 50 pixels could be present between spectra taken with different slits. Run to run difference of spectra taken with the same slit are instead much smaller, typically within 2-3 pixels, if a given slit was permanently mounted on the instrument.

Tables C.1–C.3 report the list of lines of He, Ne, Ar and Hg-Cd lamps. They were taken from the FORS User Manual (left column) and IRAF linelist (right column). Some minor discrepancies are present between the two linelists. The Th lamp atlas was prepared by comparing the AFOSC spectra with the atlas of high resolution spectrographs like SARG and UVES. Only the lines that are relatively unblended are included in the AFOSC atlas.

The Neon lamp used for the preparation of the atlas presented here failed in July 2001. Exposure times and spectral lines intensities of the new lamp are similar to the older one.

Wavelength (Å)	Element	Wavelength (Å)	Element
		3187.743	He I
		3464.14	Ar II
		3520.472	Ne I blend with Ar 3520.0
		3545.58	Ar II
		3559.51	Ar II
3610.5000	Cd		
3650.1440	Hg		
3663.2739	Hg		
		3718.21	Ar II blend with Ar II 3724.51
		3780.84	Ar II
		3850.57	Ar II
3888.6460	He I	3888.646	He I
		3928.62	Ar II
		3964.727	He I
		4026.189	He I
		4044.418	Ar I
4046.5569	Hg		
		4072.2	Ar I blend 4072.01 4072.40
4077.8313	Hg		
		4131.73	Ar II
		4158.590	Ar II
		4259.361	Ar II
		4277.55	Ar II blend with Ar I 4272.168
		4300.4	Ar II blend
4358.3428	Hg		
		4426.01	Ar II
4471.4790	He I	4471.477	He I
		4510.733	Ar I
		4545.08	Ar II
		4579.39	Ar II
		4657.94	Ar II
4678.1602	Cd		
		4713.143	He I
		4764.89	Ar II
4799.9199	Cd		
		4806.07	Ar II
		4879.90	Ar II
4921.9292	He I	4921.929	He I
		4965.12	Ar II
5015.6748	He I	5015.675	He I
5085.8242	Cd		
		5187.746	Ar I
		5221.270	Ar I
5400.5620	Ne I	5400.562	Ne I
5460.7422	Hg		
		5495.872	Ar I
		5572.548	Ar I
		5606.732	Ar I
		5650.703	Ar I
		5748.299	Ne I
5764.4189	Ne I	5764.418	Ne I
5769.5981	Hg		
5790.6558	Hg		
		5852.4878	Ne I
5875.6201	He I	5875.618	He I
5944.8301	Ne I	5944.8342	Ne I
5975.5342	Ne I		

Table C.1: Wavelength of the lines of He, Ne, Ar and Hg-Cd lines.

Wavelength (Å)	Element		Wavelength (Å)	Element
6029.9971	Ne I		6029.9971	Ne I
6074.3379	Ne I		6074.3377	Ne I
6096.1602	Ne I		6096.1630	Ne I
6143.0625	Ne I		6143.0623	Ne I
6163.5938	Ne I		6163.5939	Ne I
6217.2812	Ne I		6217.2813	Ne I
6266.4951	Ne I		6266.4950	Ne I
6304.7900	Ne I		6304.7892	Ne I
6334.4277	Ne I		6334.4279	Ne I
6382.9912	Ne I		6382.9914	Ne I
6402.2456	Ne I		6402.246	Ne I
6438.4697	Cd			
6506.5278	Ne I		6506.5279	Ne I
6532.8799	Ne I		6532.8824	Ne I
6598.9531	Ne I		6598.9529	Ne I
6678.1489	He I		6678.149	He I
			6678.2764	Ne I
6717.0400	Ne I		6717.0428	Ne I
			6752.832	Ar I
			6871.290	Ar I
6907.1602	Hg			
6929.4678	Ne I		6929.430	Ne I
6965.4307	Ar I		6965.430	Ar I
7032.4126	Ne I		7032.4127	Ne I
			7065.188	He I
7081.8799	Hg			
7091.9902	Hg			
			7107.496	Ar I
			7125.80	Ar I
7147.0405	Ar I		7147.041	Ar I
7173.9390	Ne I		7173.939	Ne I
			7206.986	Ar I
7245.1670	Ne I		7245.167	Ne I
7272.9302	Ar I		7272.936	Ar I
7281.3491	He I		7281.349	He I
			7311.71	Ar I
7346.2002	Cd			
			7353.316	Ar I
			7372.118	Ar I
7383.8999	Cd			
7383.9805	Ar I		7383.980	Ar I
7385.2998	Cd			
7438.8999	Ne I		7438.899	Ne I
7488.8701	Ne I		7488.872	Ne I
7503.8677	Ar I		7503.867	Ar I
7514.6519	Ar I		7514.651	Ar I
			7535.775	Ne I
			7544.046	Ne I
7635.1060	Ar I		7635.105	Ar I
			7670.04	Ar I
7723.9844	Ar I		7723.8	blend 7723.760 - 7724.206
			7891.075	Ar I
7948.1763	Ar I		7948.175	Ar I

Table C.2: Wavelength of the lines of He, Ne, Ar and Hg-Cd lines.

Wavelength (Å)	Element		Wavelength (Å)	Element
8006.1567	Ar I		8006.156	Ar I
8014.7856	Ar I		8014.786	Ar I
			8053.307	Ar I
			8082.458	Ne I
8103.6929	Ar I		8103.692	Ar I
8115.3110	Ar I		8115.311	Ar I
8264.5225	Ar I		8264.521	Ar I
8300.3262	Ne I		8300.326	Ne I
8377.3672	Ne I		8377.607	Ne I
8408.2100	Ar I			
8424.6475	Ar I		8424.647	Ar I
			8495.360	Ar I
8521.4424	Ar I		8521.441	Ar I
8591.2588	Ne I			
			8605.78	Ar I
			8620.47	Ar I
8634.6484	Ne I		8634.648	Ne I
8654.3838	Ne I		8654.383	Ne I
8667.9443	Ar I		8667.943	Ar I
8704.1504	Ne I			
			8761.72	Ar I
			8780.1872	Ne I
			8783.755	Ne I
8853.8672	Ne I		8853.866	Ne I
8919.5000	Ne I			
			9075.42	Ar I
9122.9678	Ar I		9122.966	Ar I
			9194.68	Ar I
9224.4990	Ar I		9224.998	Ar I
			9291.58	Ar I
9300.8496	Ne I			
9354.2178	Ar I		9354.218	Ar I
9425.3799	Ne I		9425.38	Ne I
			9534.167	Ne I
9657.7842	Ar I		9657.874	Ar I
9784.5010	Ar I		9784.501	Ar I
10140.0000	Hg			
10394.5996	Cd			
10830.1709	He I			

Table C.3: Wavelength of the lines of He, Ne, Ar and Hg-Cd lines.

C.2 Grism #2

Lamp/Slit	0.70	0.85	1.26	1.69	2.10	3.00	4.22	8.44	Remarks
Ne	9				6				
Ar									
He	15								
Hg-Cd	90				60			20	
Th	5				3			1	only bright Ar lines

Table C.4: Exposure times (in seconds) of the calibration lamps using the Grism #2 for the available slits.

Remarks

- Zero order not shown in the atlas

Suggested lamps combinations

- Hg-Cd lamp
- He lamp

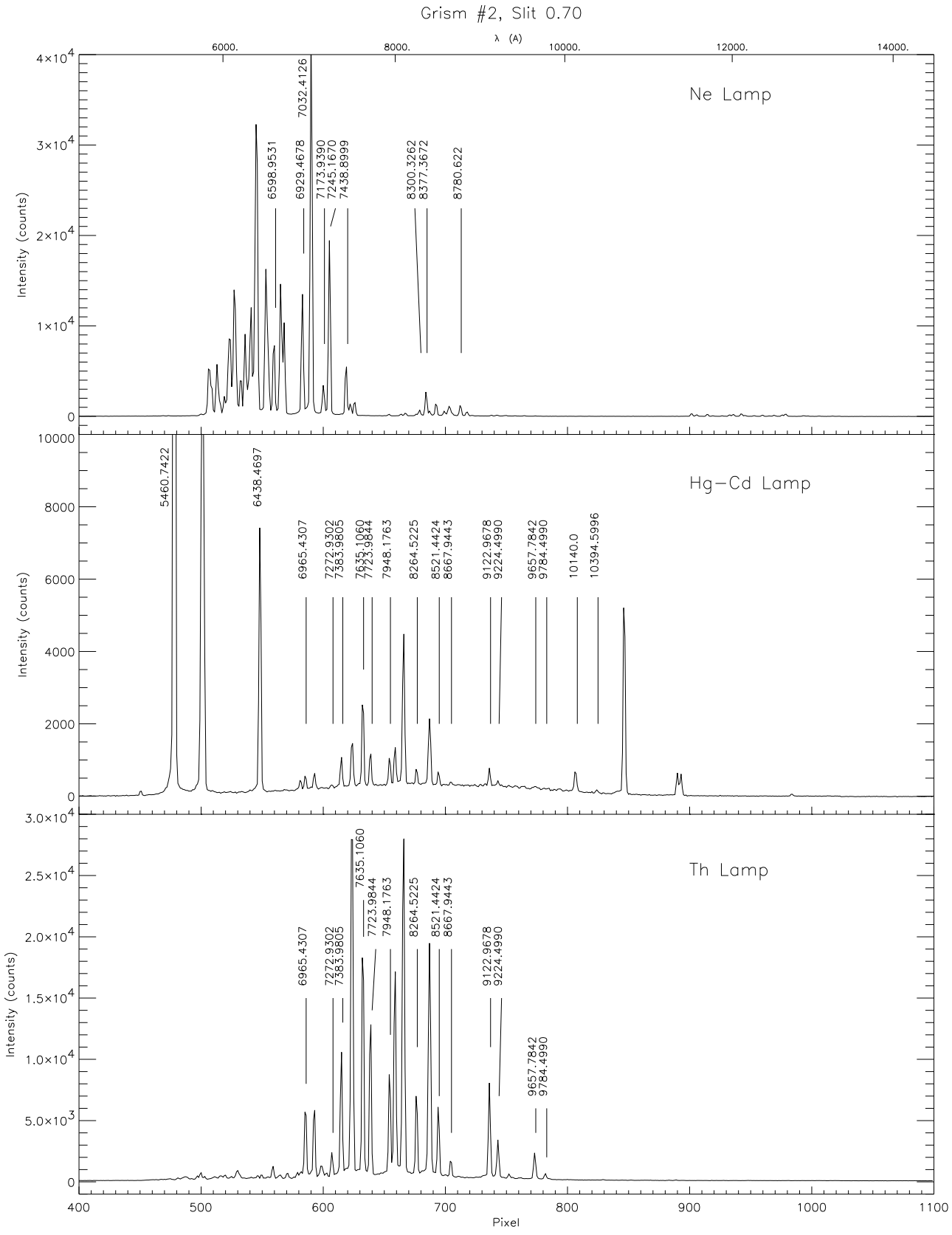

Figure C.1: Calibration spectra of Grism #2: Ne, Hg-Cd, and Th lamps

C.3 Grism #3

Lamp/Slit	0.70	0.85	1.26	1.69	2.10	3.00	4.22	8.44	Remarks
Ne	300				300				one faint line
Ar	300				300				very faint lines
He									
Hg-Cd	180				120				
Th	300				240				

Table C.5: Exposure times (in seconds) of the calibration lamps using the Grism #3 for the available slits.

Remarks

- Atlas of Ar and Ne lamps not included due to the lack of lines

Suggested lamps combinations

- Hg-Cd lamp
- He lamp
- Th lamp (when using narrow slits)

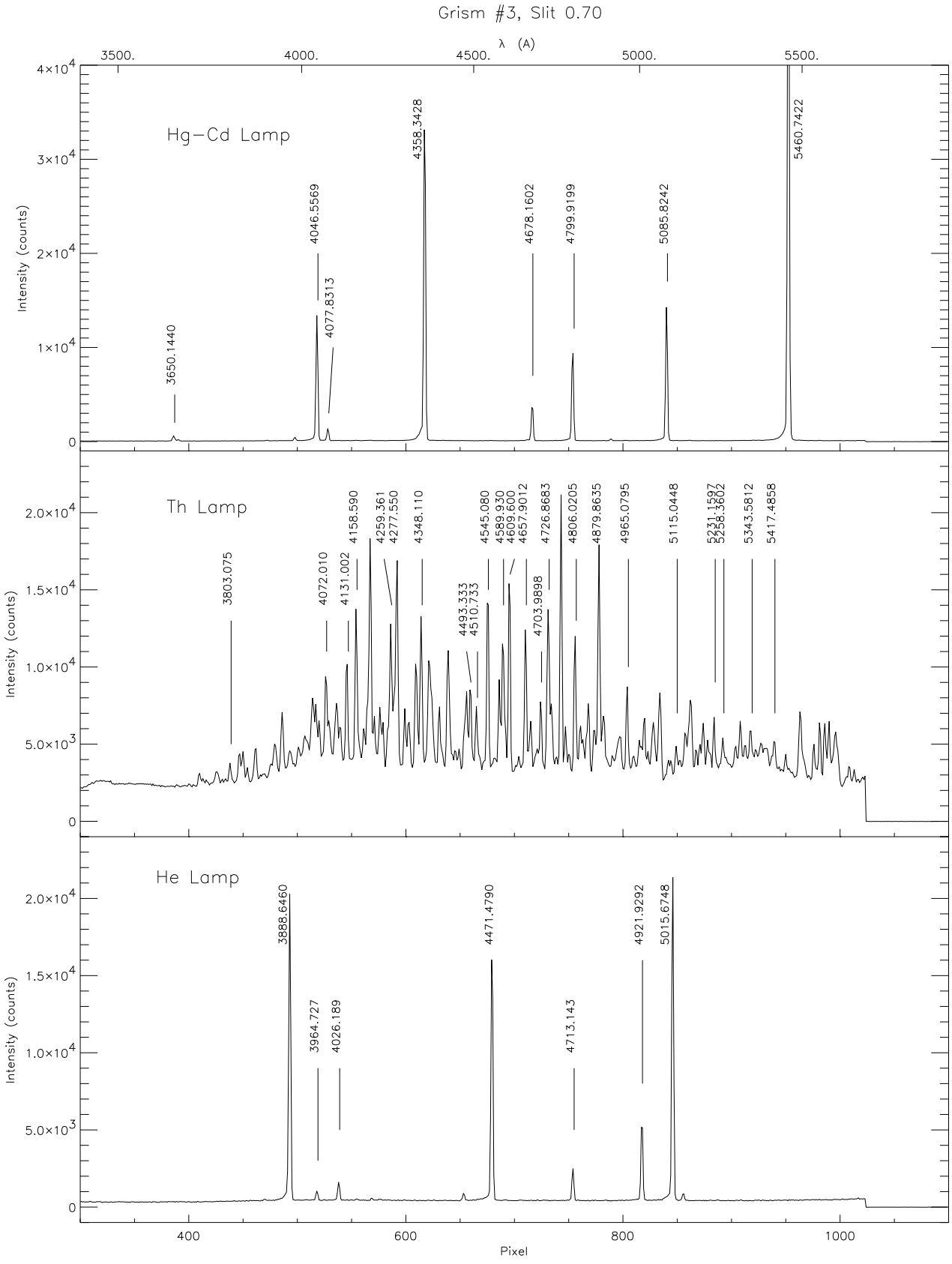

Figure C.2: Calibration spectra of Grism #3: Hg-Cd, Th and He lamps

C.4 Grism #4

Lamp/Slit	0.70	0.85	1.26	1.69	2.10	3.00	4.22	8.44	Remarks
Ne	15		12	10	10		8		
Ar	40		35	30	30				
He	20		18	16	14				
Hg-Cd	100		75	60	60	50			
Th	15		10	8	8		6		only bright Ar lines

Table C.6: Exposure times (in seconds) of the calibration lamps using the Grism #4 for the available slits.

Remarks

- Severe line blending with Th lamp

Suggested lamps combinations

- Ne + Hg-Cd lamps
- He + Ne lamps
- He + Ar lamps

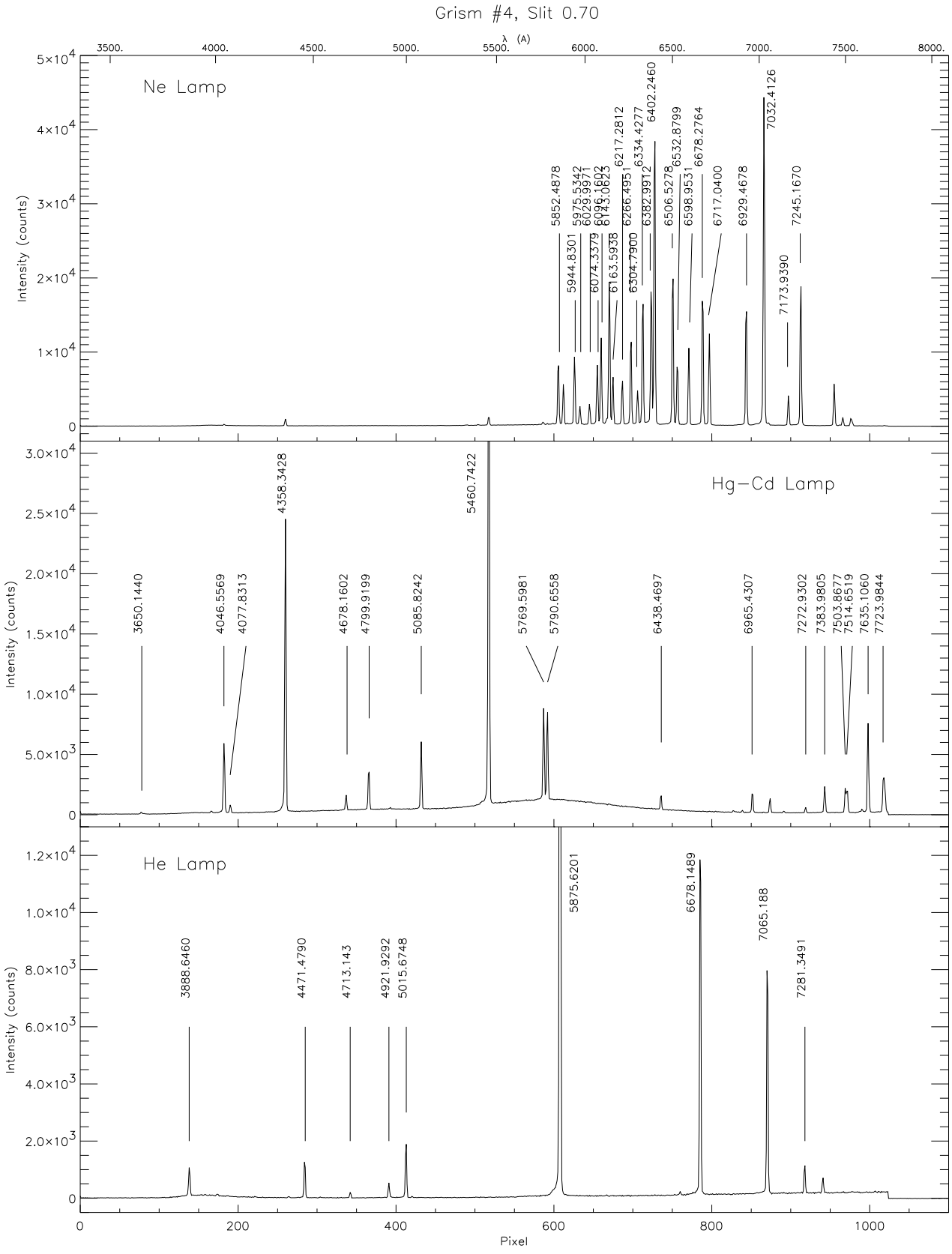

Figure C.3: Calibration spectra of Grism #4: Ne, Hg-Cd, and He lamps

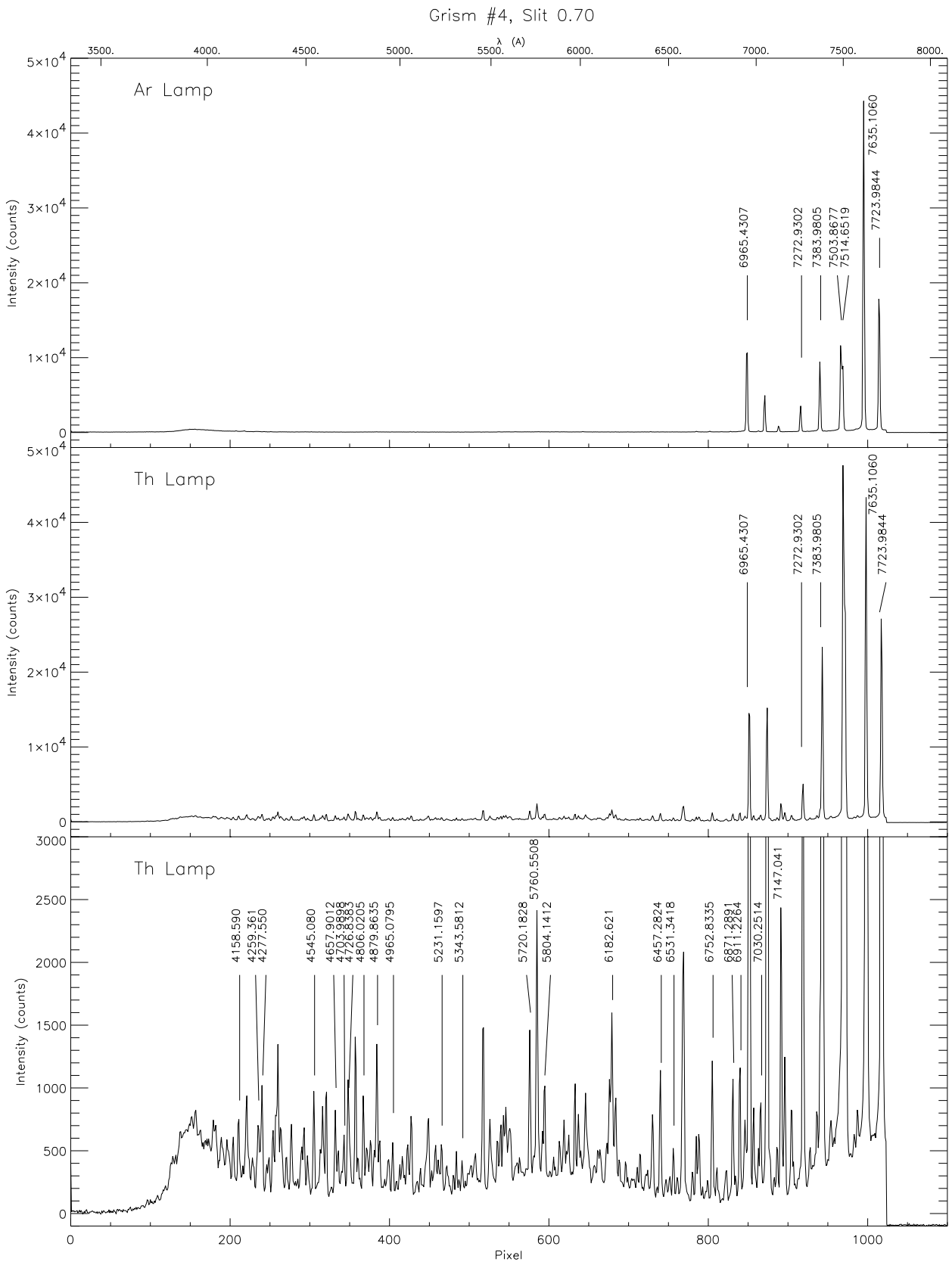

Figure C.4: Calibration spectra of Grism #4: Ar and Th lamps

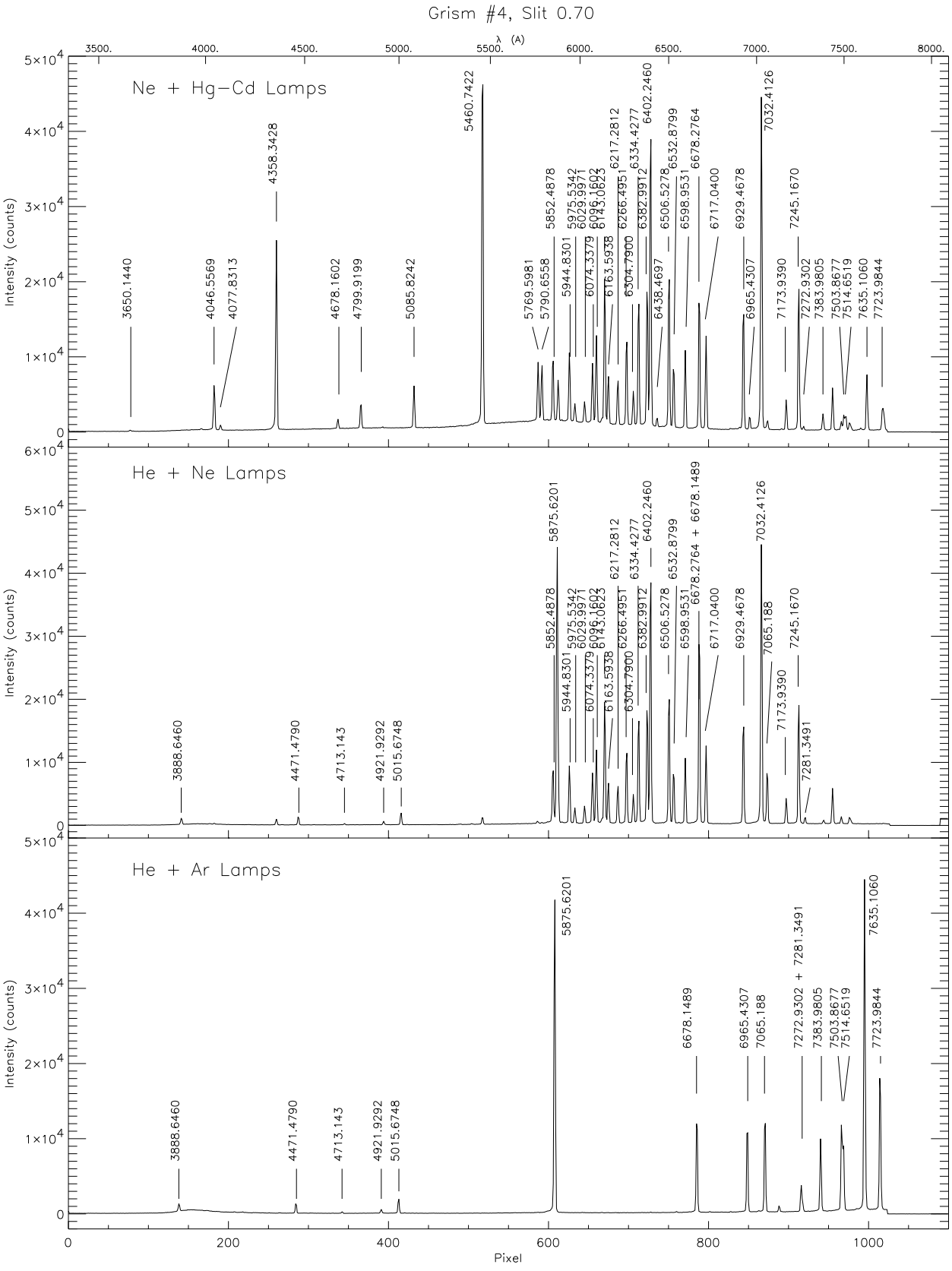

Figure C.5: Calibration spectra of Grism #4: combined spectra Ne+Hg-Cd, He+Ne and He+Ar lamps.

C.5 Grism #6

Lamp/Slit	0.70	0.85	1.26	1.69	2.10	3.00	4.22	8.44	Remarks
Ne	–	–	–	–	–	–	–	–	no lines
Ar	–	–	–	–	–	–	–	–	no lines
He	300								
Hg-Cd	150				120	120	120	80	
Th	300				240				

Table C.7: Exposure times (in seconds) of the calibration lamps using the Grism #6 for the available slits.

Remarks

- Atlas of Ar and Ne lamps not included due to the lack of lines

Suggested lamps combinations

- Hg-Cd lamp
- He lamp
- Th lamp (when using narrow slits)

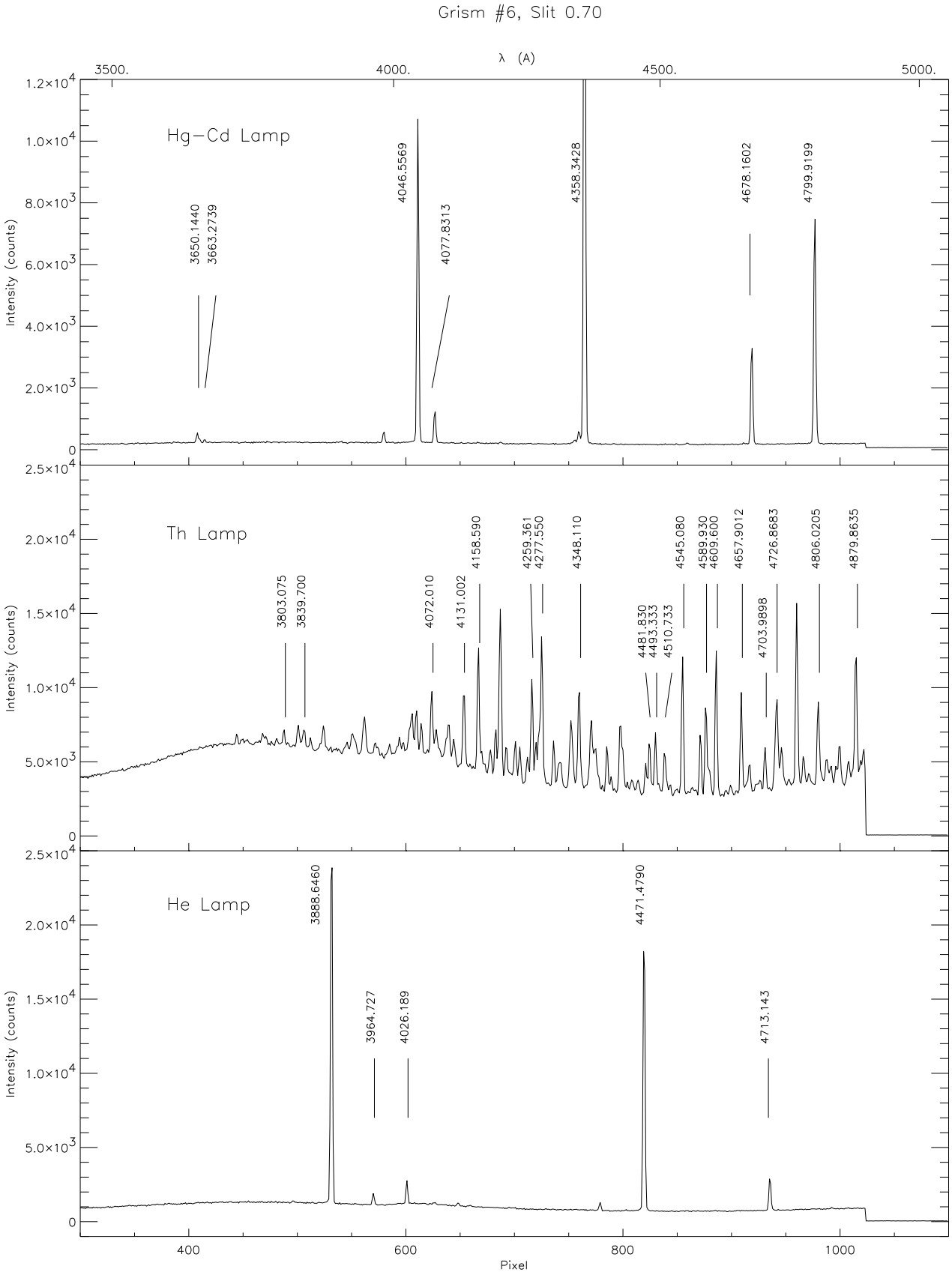

Figure C.6: Calibration spectra of Grism #6: Hg-Cd, Th and He lamps

C.6 Grism #7

Lamp/Slit	0.70	0.85	1.26	1.69	2.10	3.00	4.22	8.44	Remarks
Ne	30		25	25	20		20		
Ar	–	–	–	–	–	–	–	–	no lines
He	22		20	18	16				
Hg-Cd	150		120	120	100		90		
Th	240		300	240	240		180		

Table C.8: Exposure times (in seconds) of the calibration lamps using the Grism #7 for the available slits.

Remarks

- Atlas of Ar lamp not included due to the lack of lines

Suggested lamps combinations

- Ne + Hg-Cd lamp
- Ne + He lamp
- Th lamp (when using narrow slits)

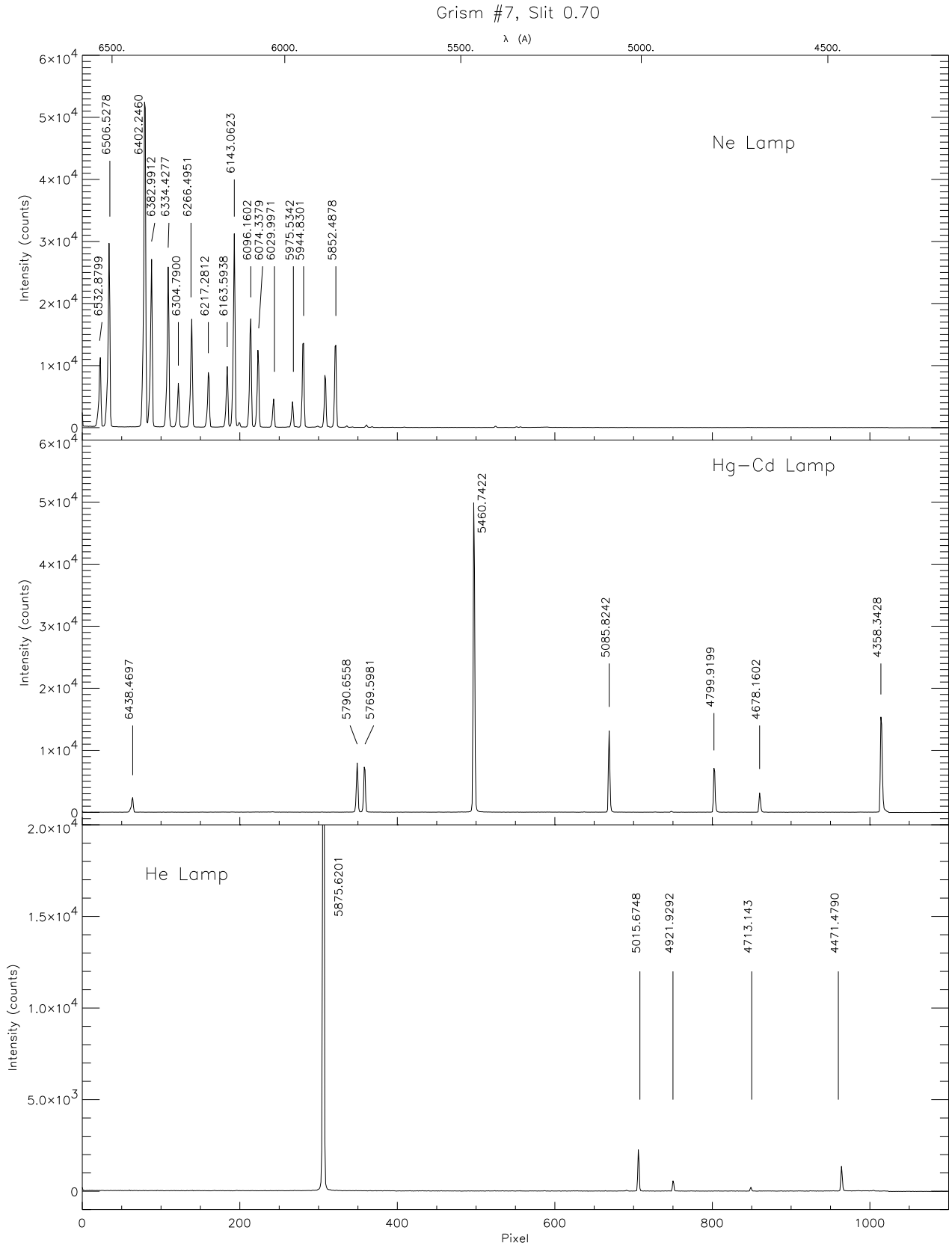

Figure C.7: Calibration spectra of Grism #7: Ne, Hg-Cd, and He lamps

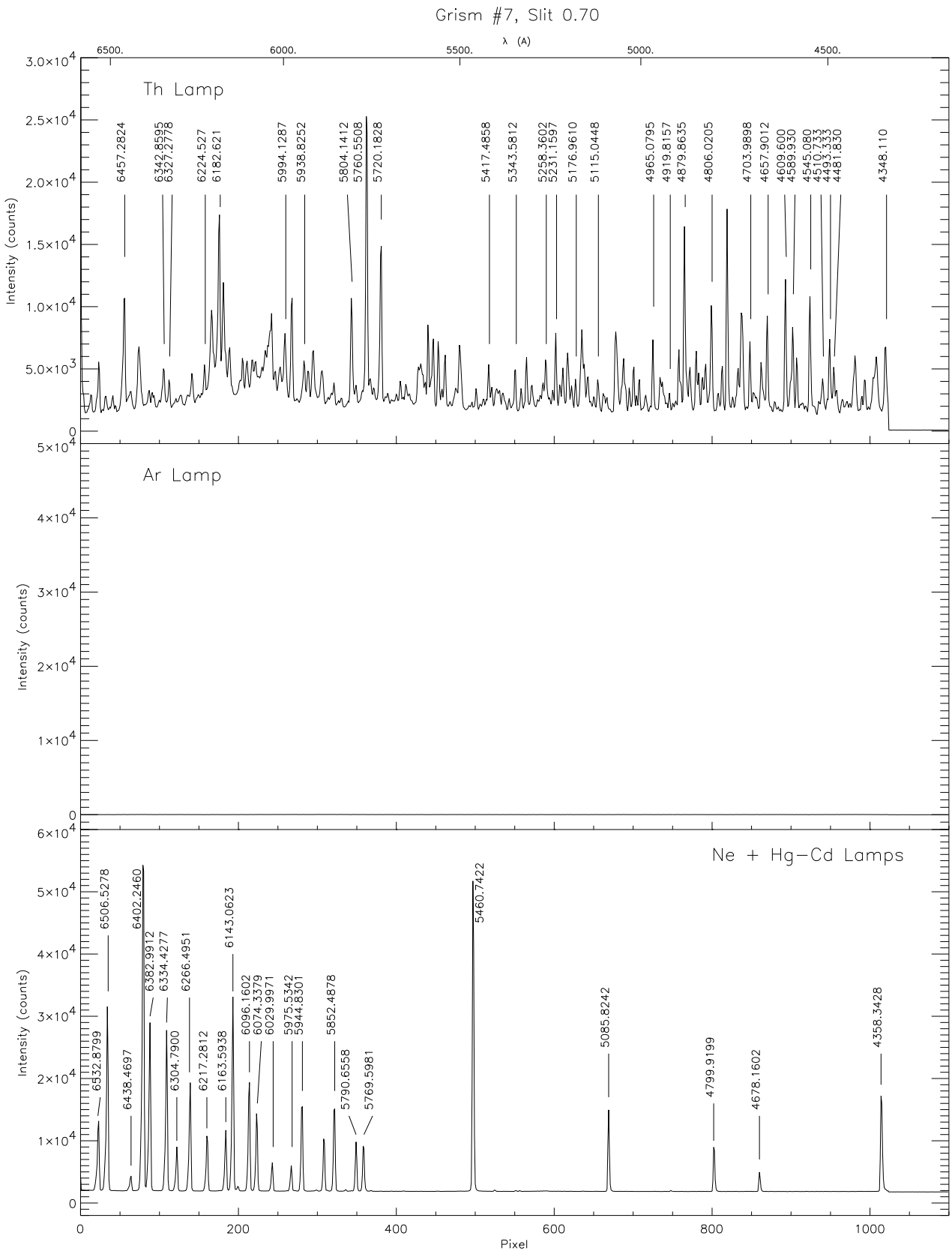

Figure C.8: Calibration spectra of Grism #7: Th, Ar and Ne+HgCd lamps

C.7 Grism #8

Lamp/Slit	0.70	0.85	1.26	1.69	2.10	3.00	4.22	8.44	Remarks
Ne	15		14	12	12		10		
Ar	35		30	25	25				
He	80	70	60	50					
Hg-Cd	300	300	300	300	300	300	300		Ar lines + 1 Hg line
Th	14		12	10	10				only bright Ar lines

Table C.9: Exposure times (in seconds) of the calibration lamps using the Grism #8 for the available slits.

Remarks

- Ar lines included in Ar, Th, and Hg-Cd lamps. Only one Cd line with the the Hg-Cd lamp

Suggested lamps combinations

- Ne + Th lamps

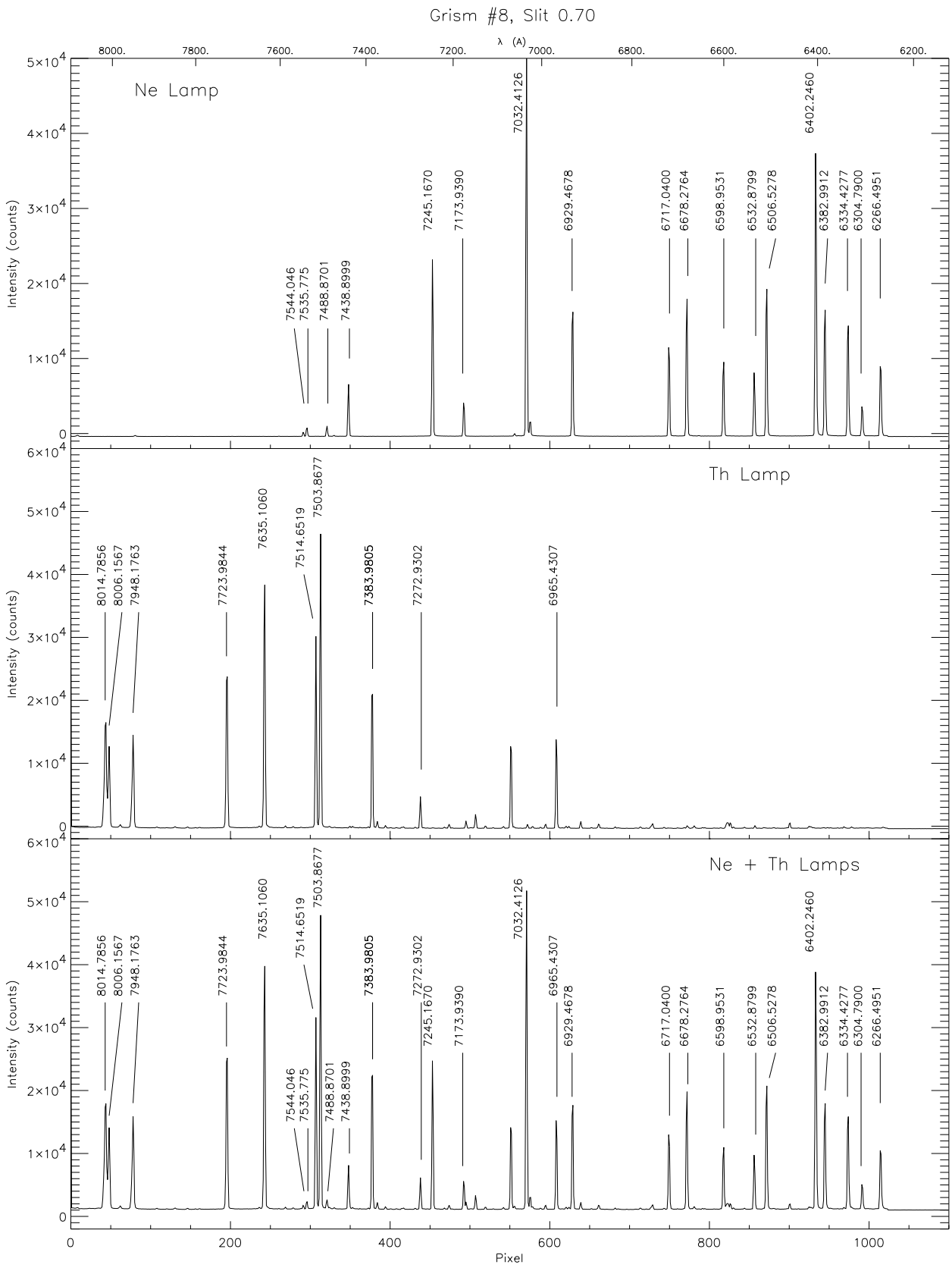

Figure C.9: Calibration spectra of Grism #8: Ne and Th lamps

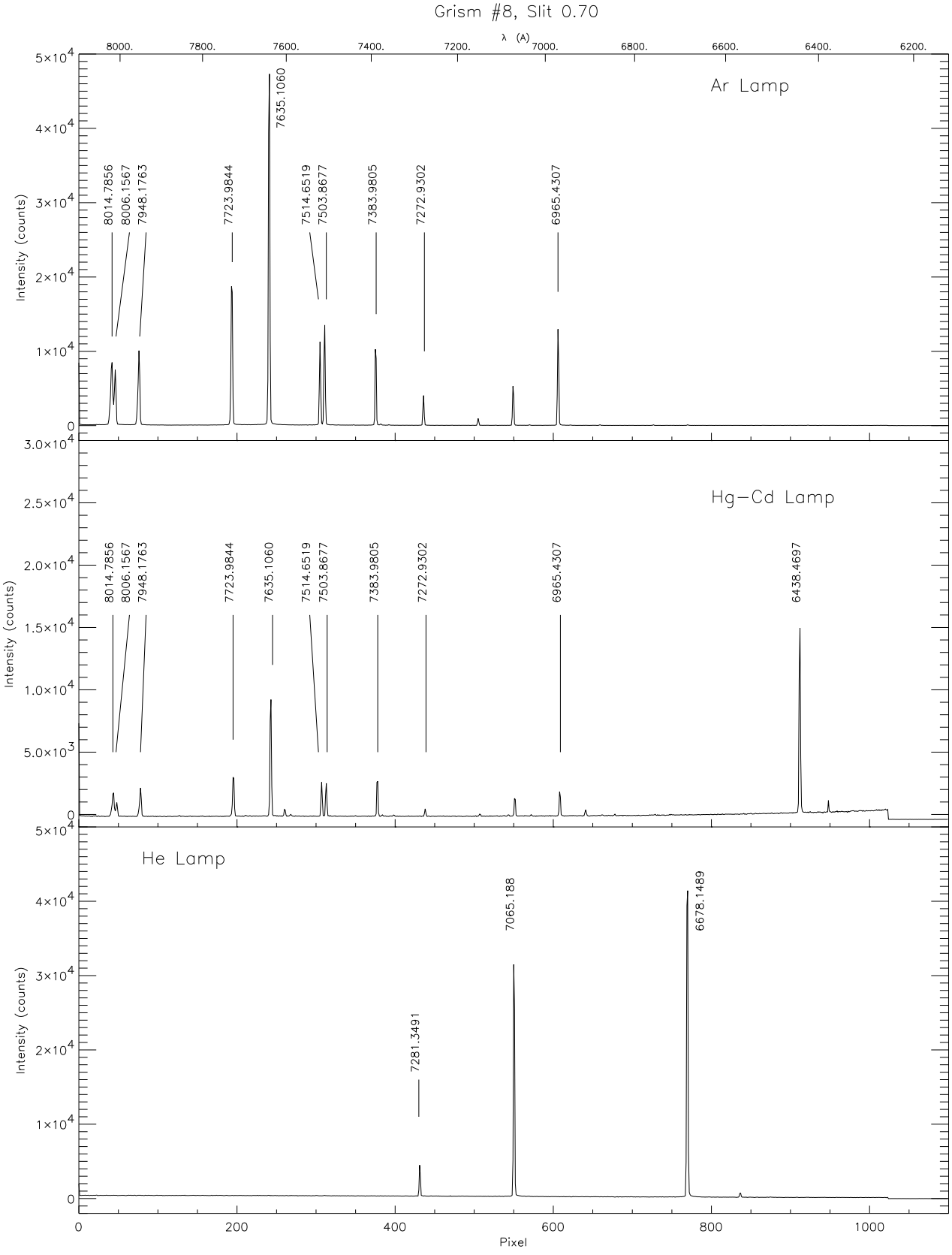

Figure C.10: Calibration spectra of Grism #8: Ar, Hg-Cd and He lamps

C.8 Grism #10

Lamp/Slit	0.70	0.85	1.26	1.69	2.10	3.00	4.22	8.44	Remarks
Ne	6		4	3	3				
Ar	8		6	5	4				
He	15		12	11	10				
Hg-Cd	70		60	50	40				
Th	2		1	1	1				only bright Ar lines

Table C.10: Exposure times (in seconds) of the calibration lamps using the Grism #10 for the available slits.

Remarks

- Zero order not shown in the atlas
- Exposure times fixed to avoid saturation of the zero order.

Suggested lamps combinations

- Hg-Cd lamp
- He lamp

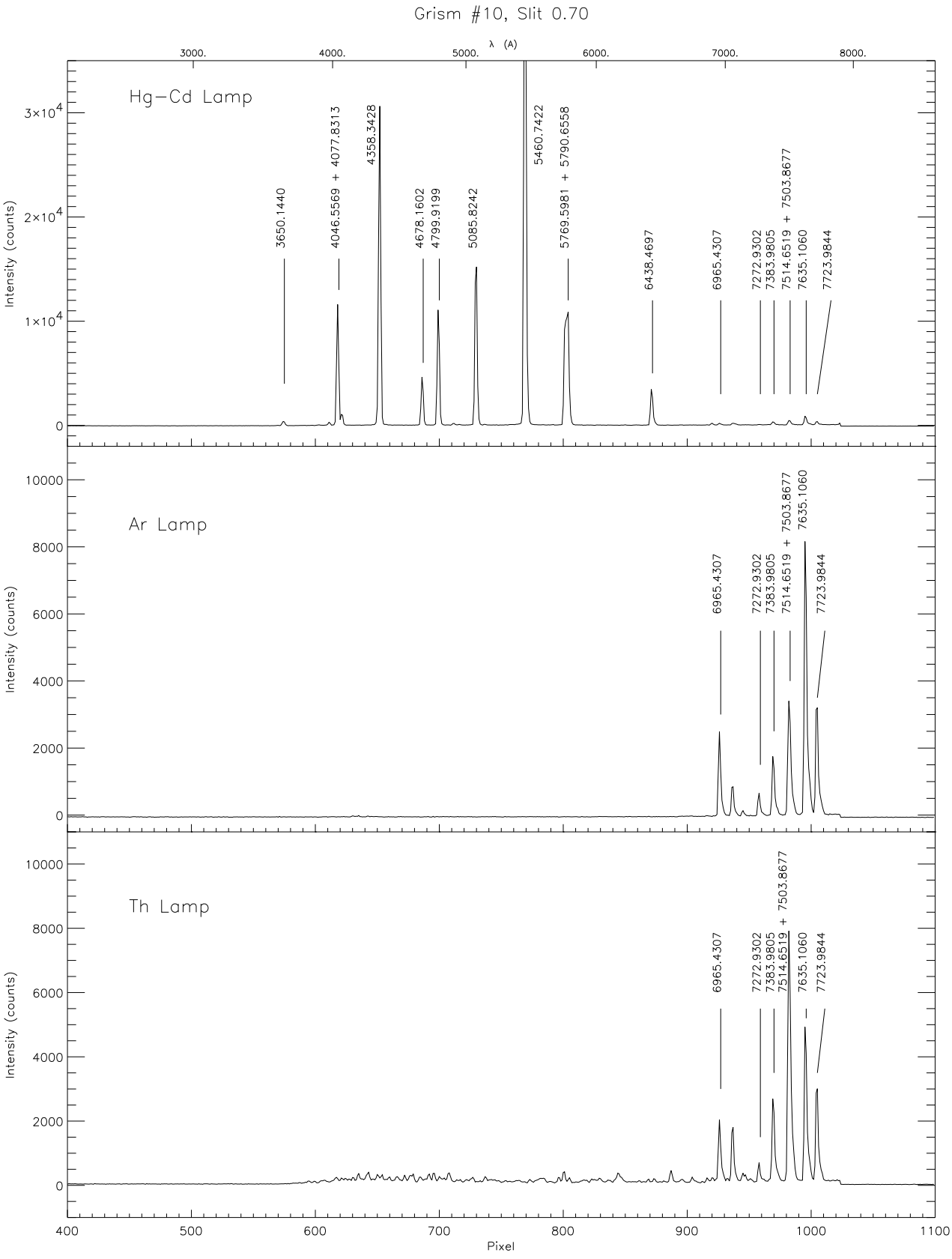

Figure C.11: Calibration spectra of Grism #10: Hg-Cd, Ar and Th lamps

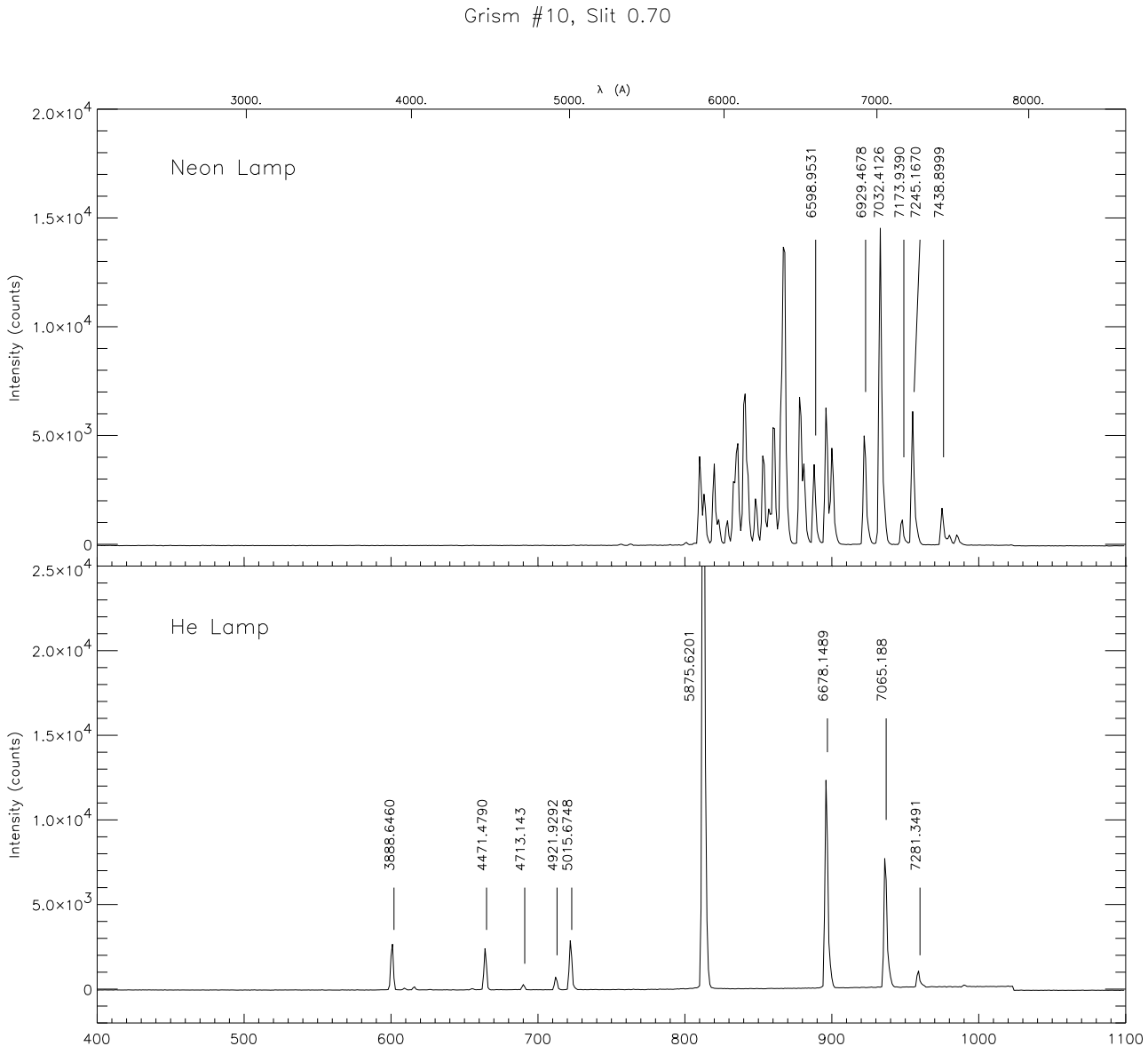

Figure C.12: Calibration spectra of Grism #10: Ne and He lamps

C.9 Grism #13

Lamp/Slit	0.70	0.85	1.26	1.69	2.10	3.00	4.22	8.44	Remarks
Ne	300	300	300	300	300	300	300	300	1 line
Ar	300	300	300	300	300	300	300	300	very faint lines
He	300								1 line
Hg-Cd	300				180				2 lines
Th	300	300	300	300	300				

Table C.11: Exposure times (in seconds) of the calibration lamps using the Grism #13 + OS1 for the available slits.

Lamp/Slit	0.70	0.85	1.26	1.69	2.10	3.00	4.22	8.44	Remarks
Ne	180				120				
Ar	60								
He	300								1 line
Hg-Cd	300	300	300	300	300	300	300	300	2 lines
Th	30				20				

Table C.12: Exposure times (in seconds) of the calibration lamps using the Grism #13 + i filter for the available slits.

Remarks

- The echelle configuration (Grism #13 + Grism #2 or #10 as cross disperser) is not considered due to its limited uselfulness

Suggested lamps combinations: Gr #13 + OS1

- Th lamp

Suggested lamps combinations: Gr #13 + i

- Ar lamp
- Th lamp

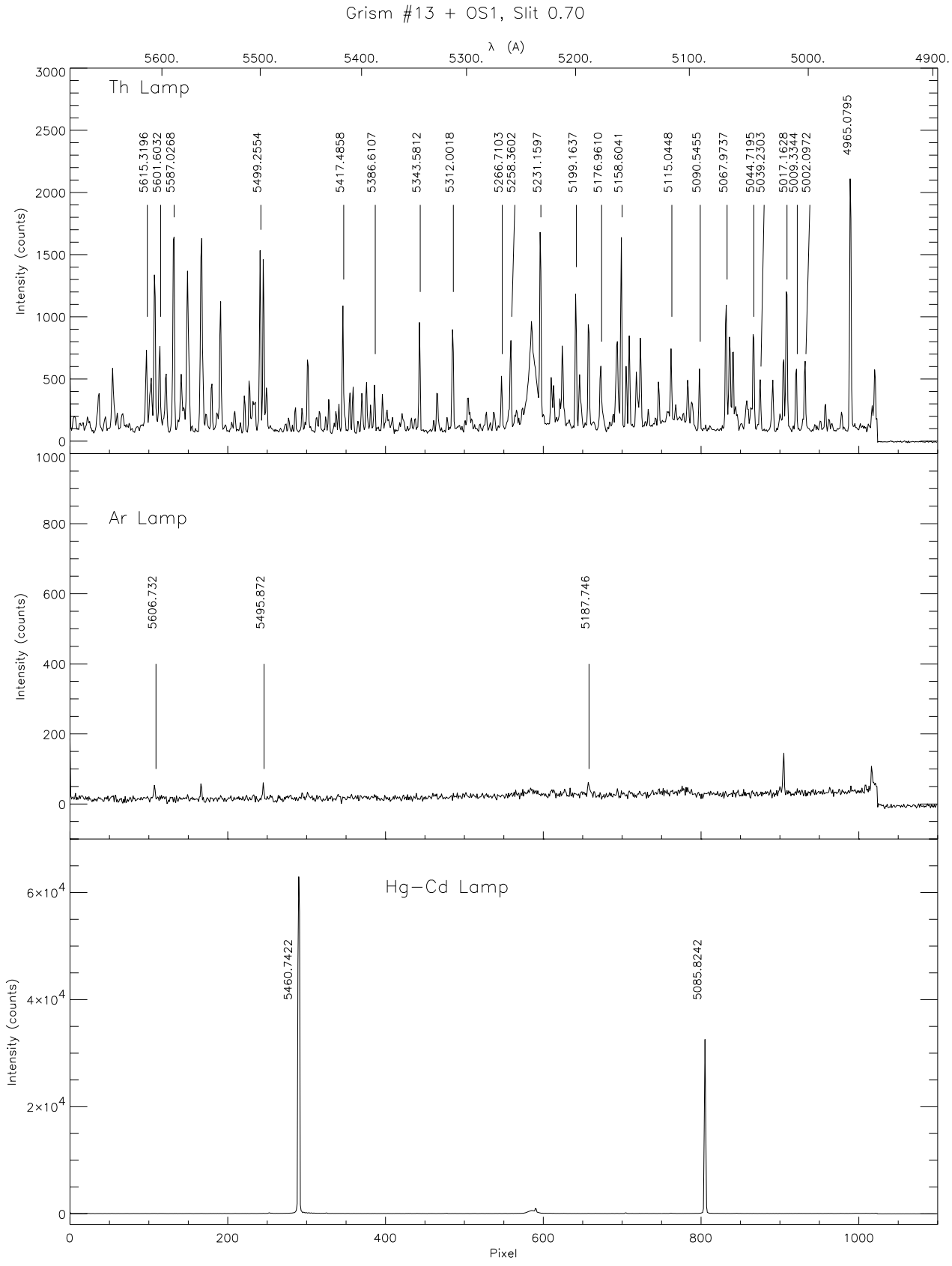

Figure C.13: Calibration spectra of Grism #13 + OS1: Th, Ar and Hg-Cd lamps

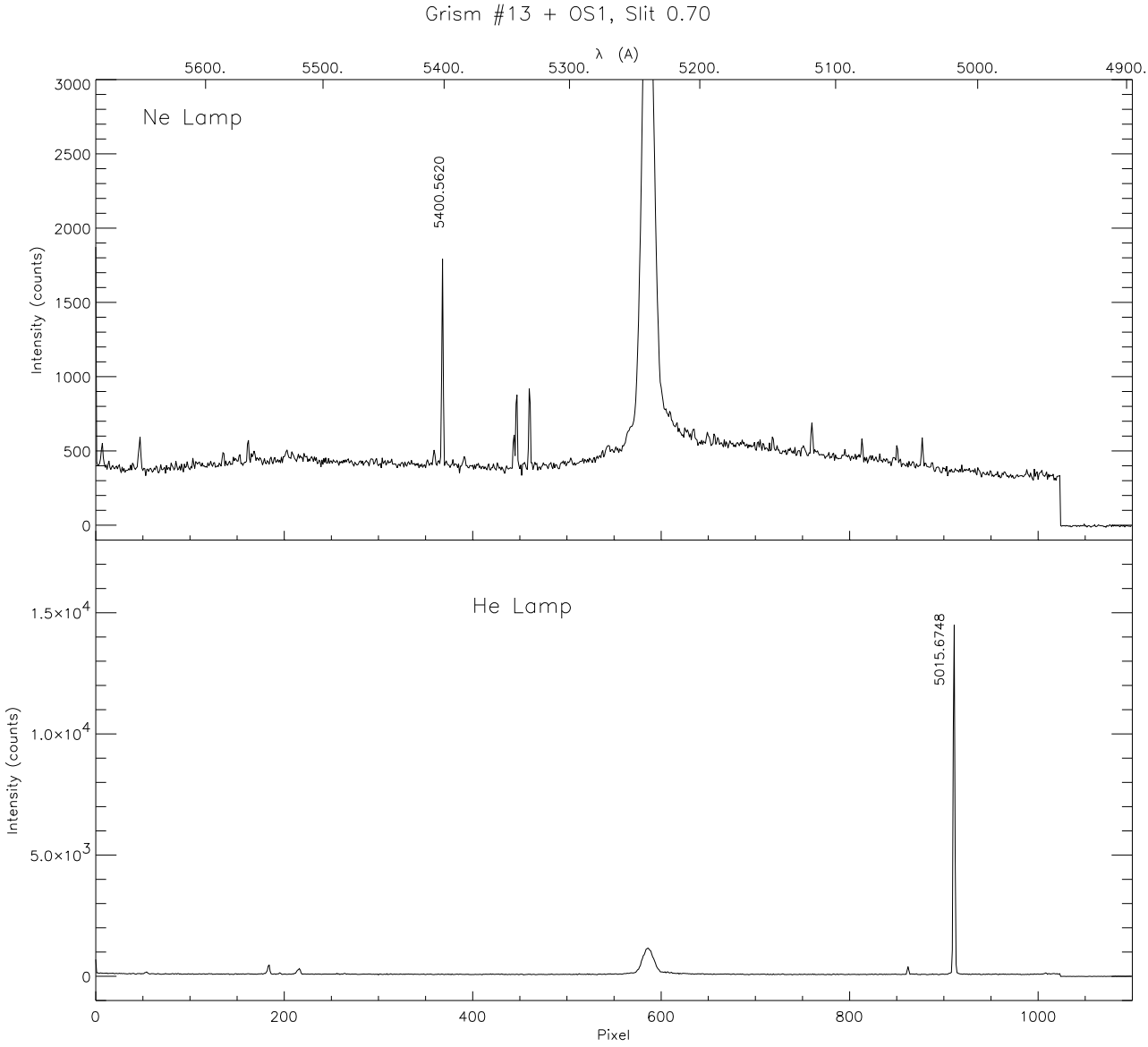

Figure C.14: Calibration spectra of Grism #13 + OS1: Ne and He lamps

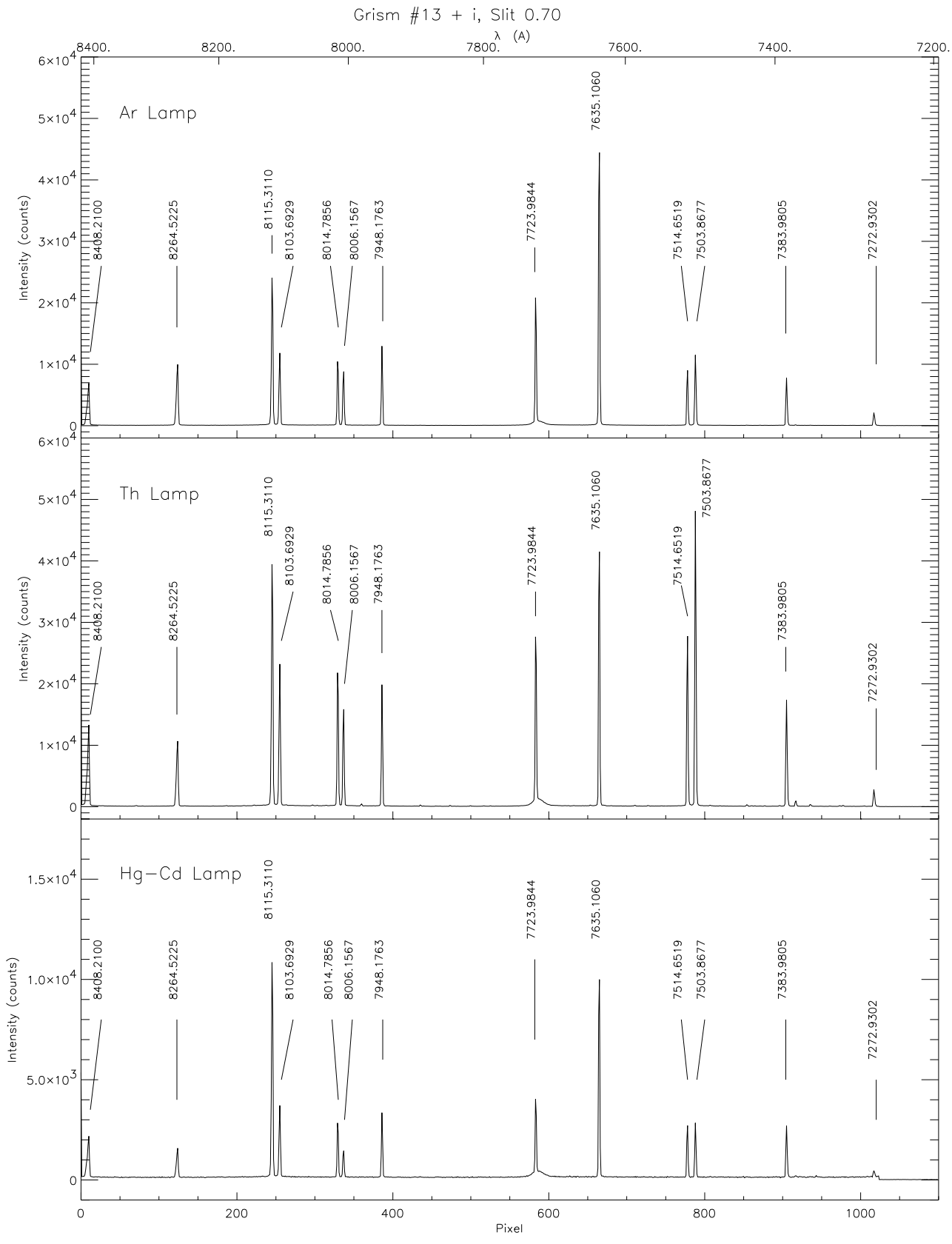

Figure C.15: Calibration spectra of Grism #13 + i: Th, Ar and Hg-Cd lamps

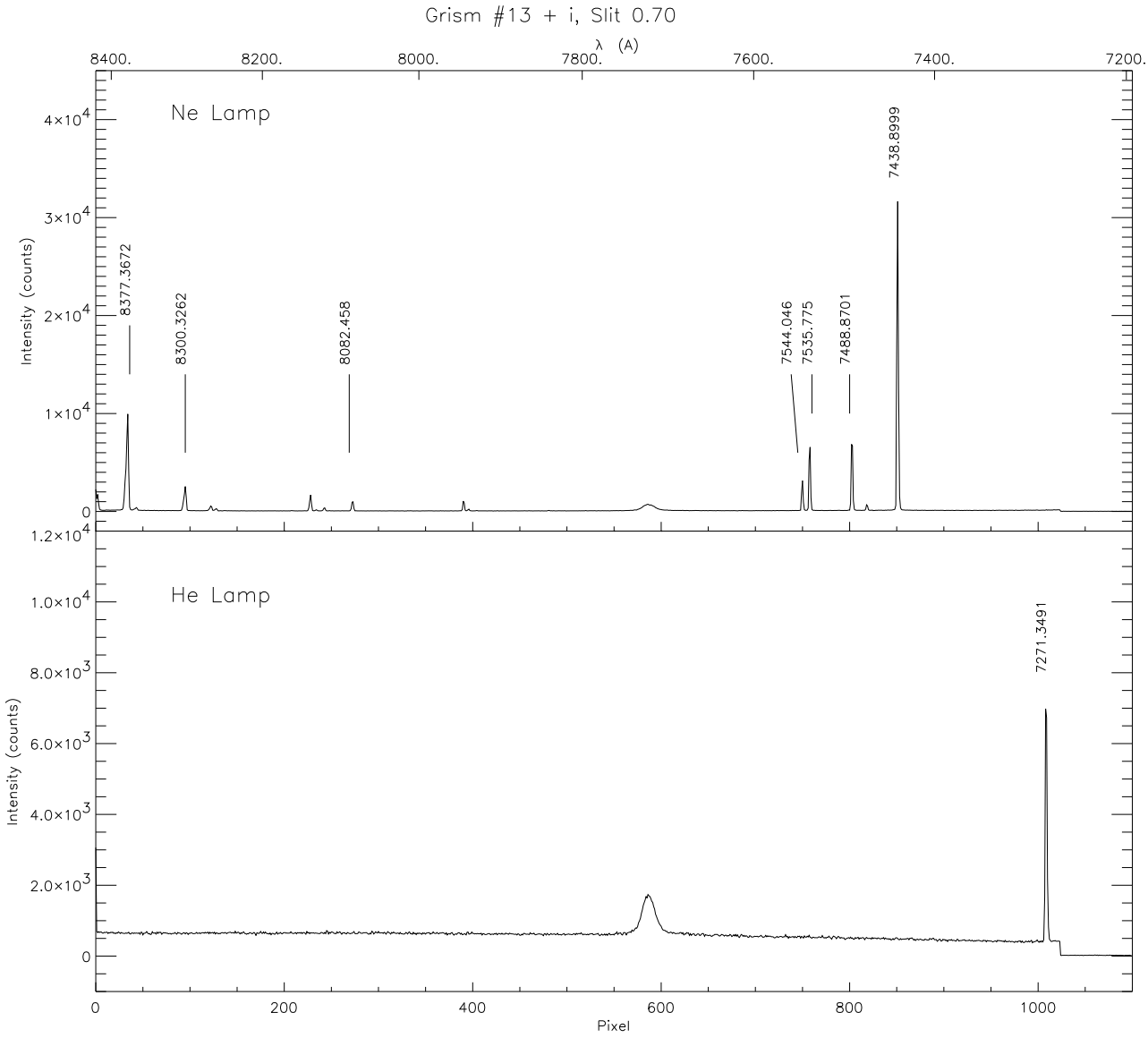

Figure C.16: Calibration spectra of Grism #13 + i: Ne and He lamps

C.10 VPH #1

Lamp/Slit	0.70	0.85	1.26	1.69	2.10	3.00	4.22	8.44	Remarks
Ne Ar He Hg-Cd Th	–	–	–	–	–	–	–	–	

Table C.13: Exposure times (in seconds) of the calibration lamps using the VPH1 #1 for the available slits.

Remarks

- Neon Lamp: no lines

Suggested lamps combinations

- Th lamp

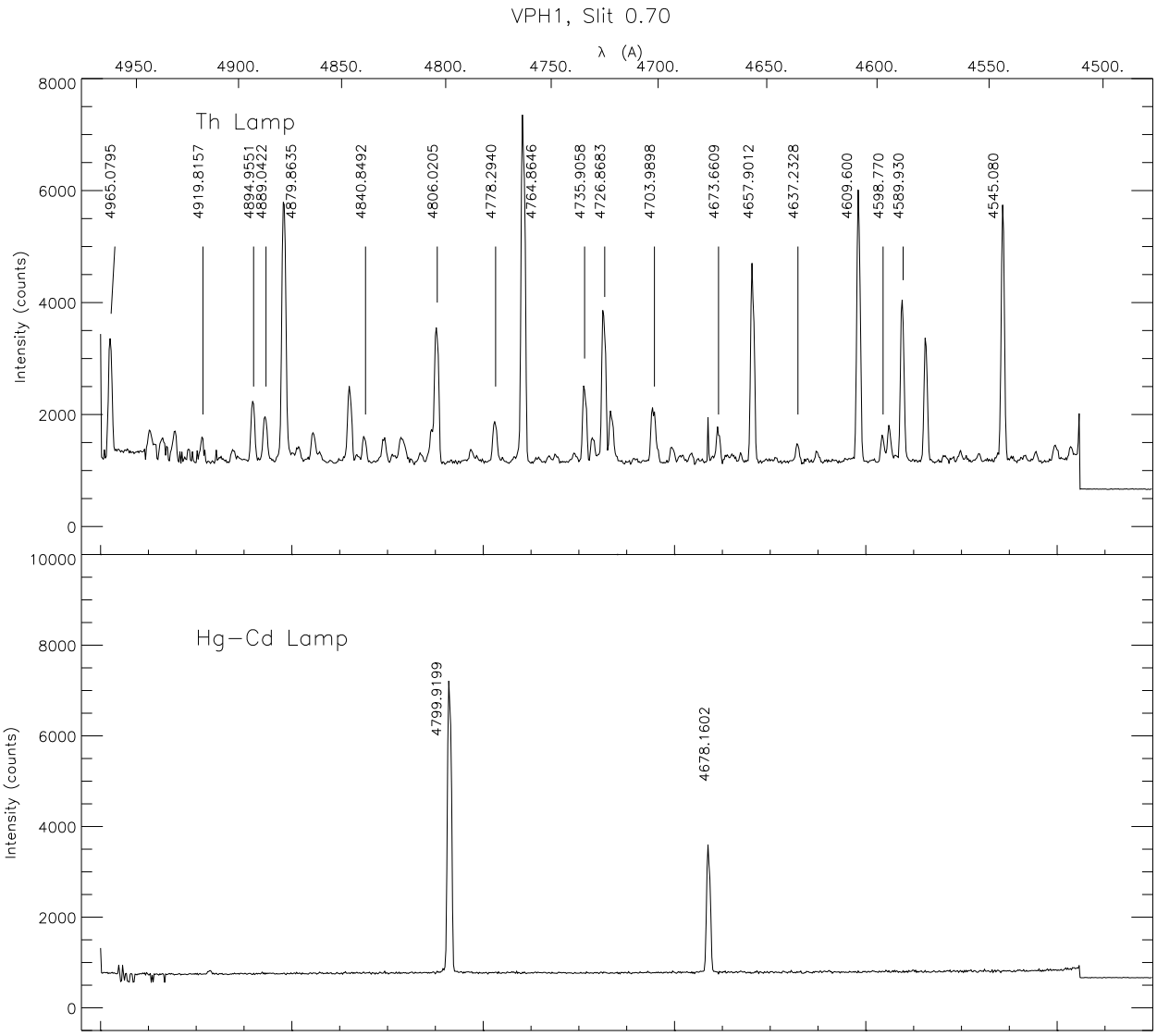

Figure C.17: Calibration spectra of VPH1 #1: Th, and Hg-Cd lamps

C.11 VPH #4

Lamp/Slit	0.70	0.85	1.26	1.69	2.10	3.00	4.22	8.44	Remarks
Ne			40						
Ar									
He									
Hg-Cd			300						
Th			30						

Table C.14: Exposure times (in seconds) of the calibration lamps using the VPH1 #4 for the available slits.

Suggested lamps combinations

- Ne + Th lamps

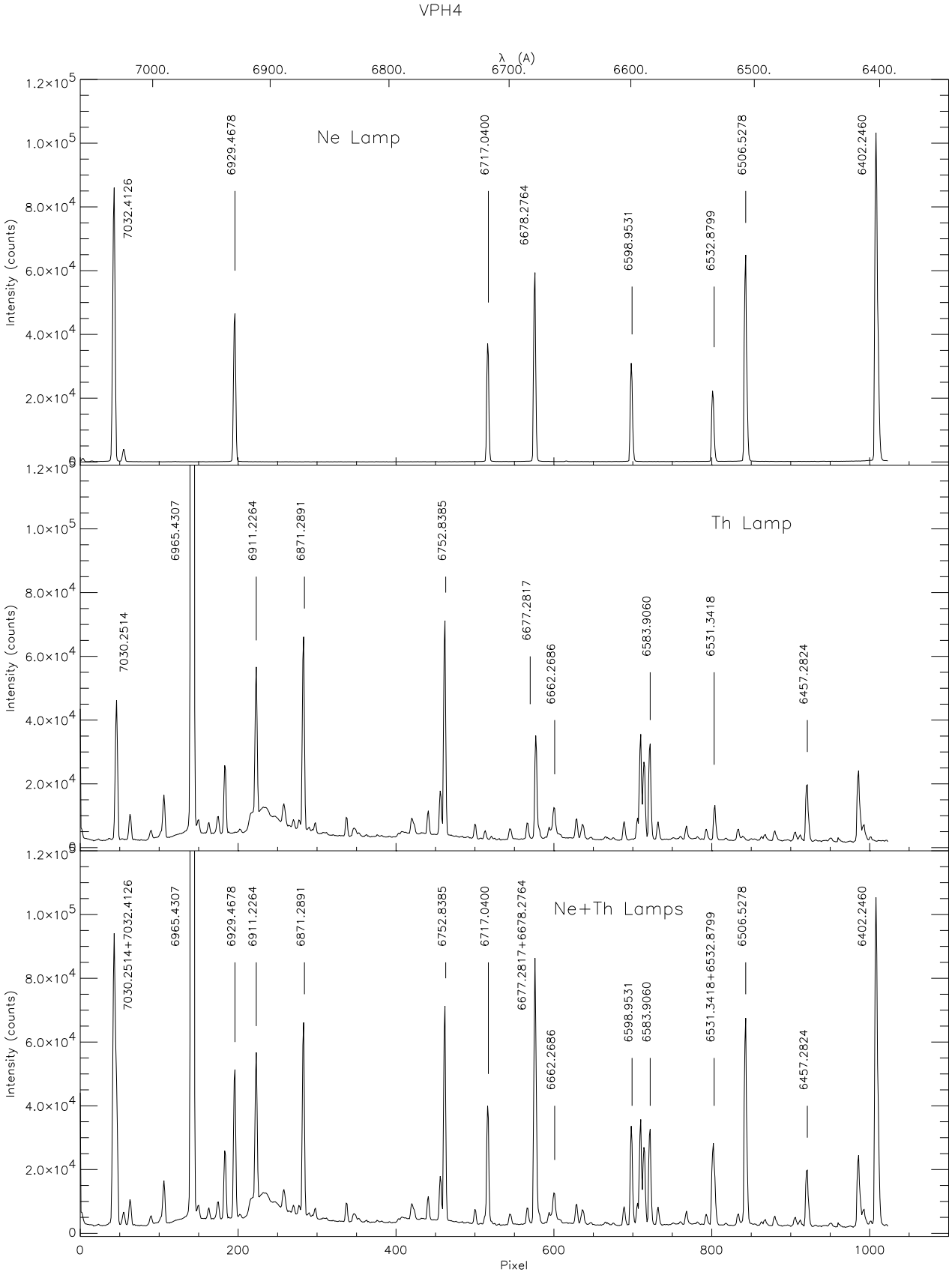

Figure C.18: Calibration spectra of VPH4 #1: Ne, Th, and Ne+Th lamps

C.12 VPH #5

Lamp/Slit	0.70	0.85	1.26	1.69	2.10	3.00	4.22	8.44	Remarks
Ne	180		150		120				
Ar									
He									
Hg-Cd	300		300		300				
Th	20		15		10				

Table C.15: Exposure times (in seconds) of the calibration lamps using the VPH1 #5 for the available slits.

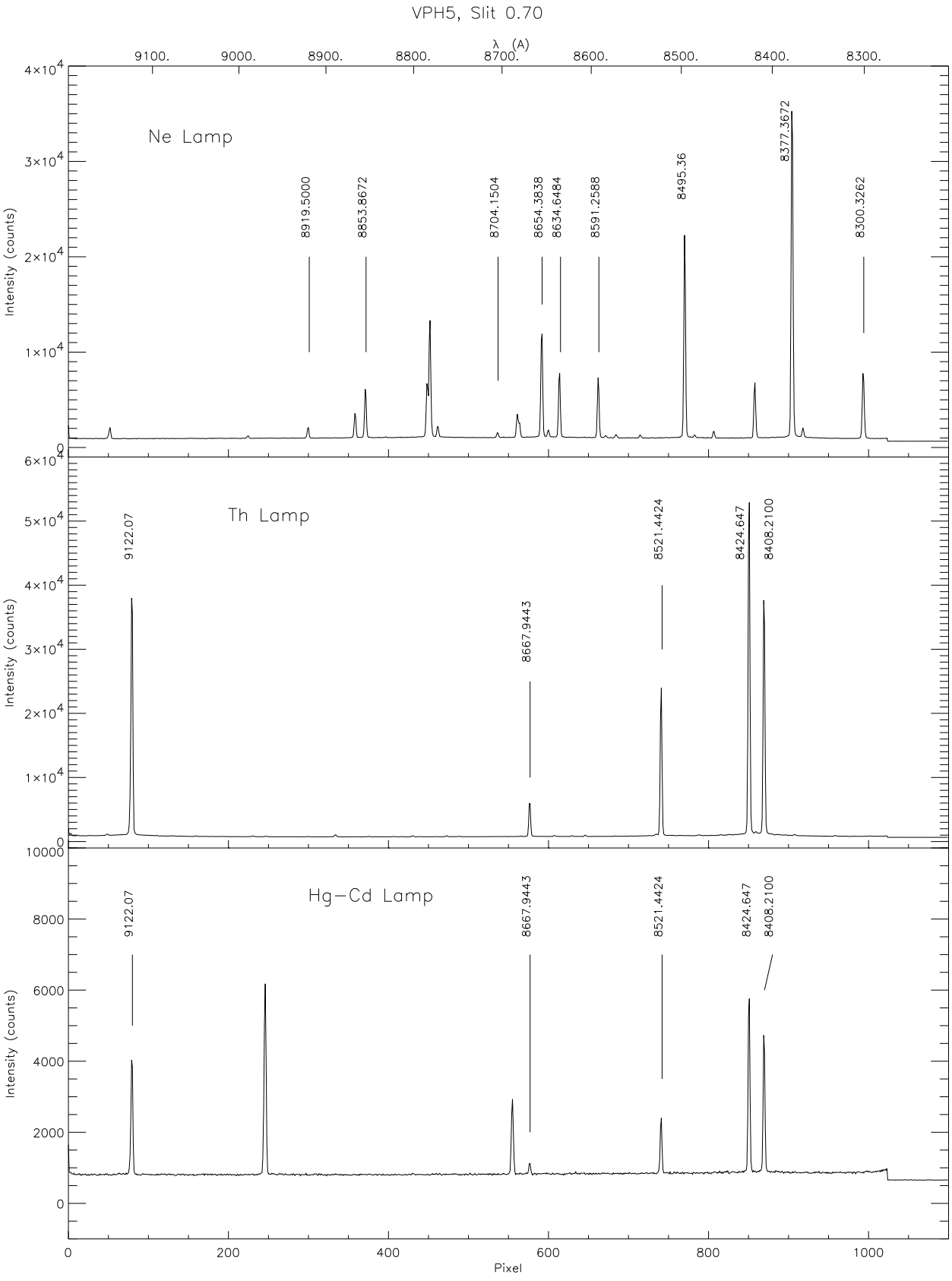

Figure C.19: Calibration spectra of VPH5 #1: Ne, Th and Hg-Cd lamps

C.13 Grism #9 + #10 (Echelle Mode)

Lamp/Slit	Echelle Slit	MF	Remarks
Ne		300	
Ar		300	
He		300	
Hg-Cd		300	
Th		300	

Table C.16: Exposure times (in seconds) of the calibration lamps using the Grism #9 + #10 with the echelle slit.

Remarks

- Atlas of Th lamp includes only relatively unblended lines
- Only Th lamp have a sufficient number of lines for the whole spectral range. Other lamps may be a useful addition in some spectral ranges
- Atlas of 2 very faint orders at blue extreme missing

Suggested lamps combinations

- Th lamp

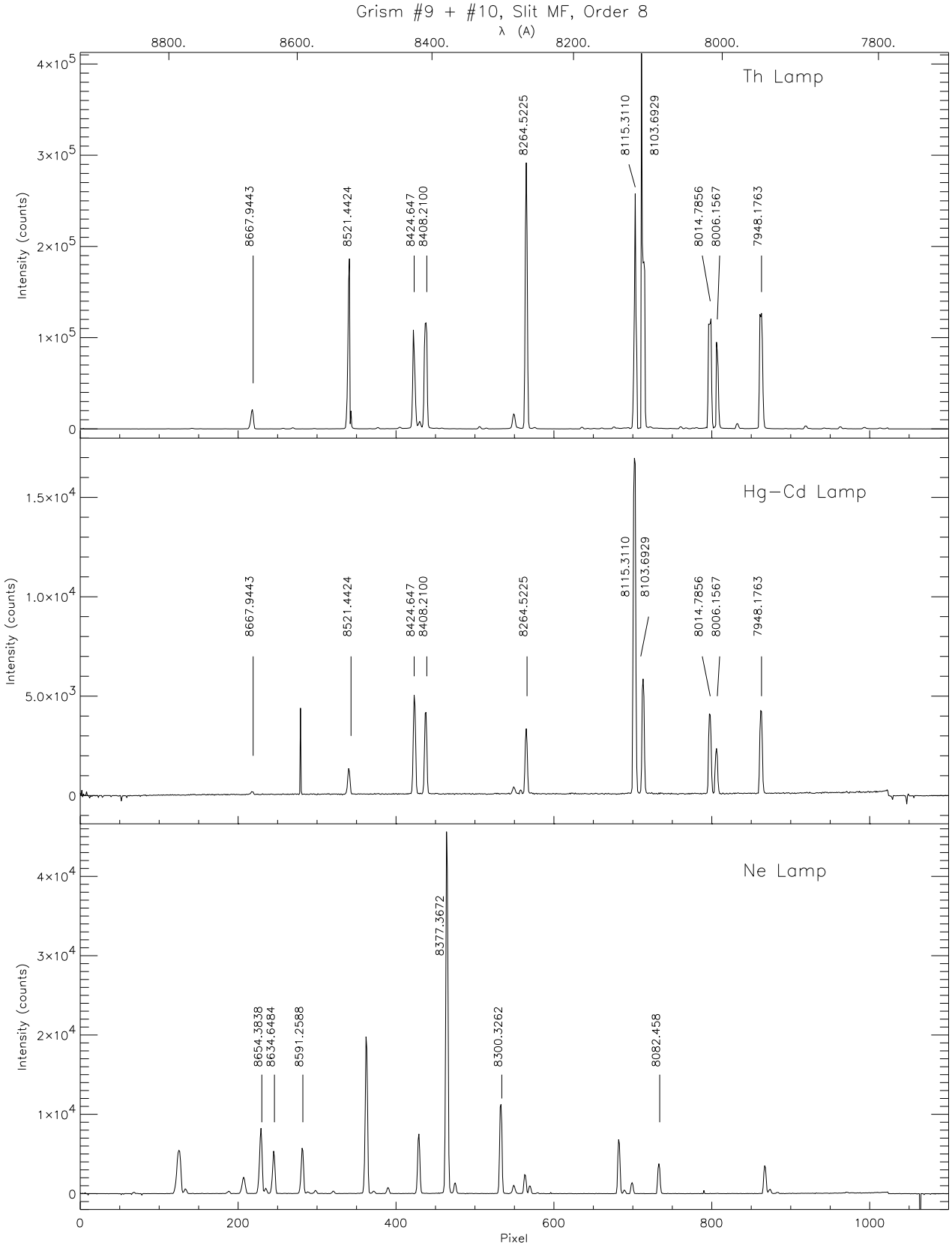

Figure C.20: Calibration spectra of Grism #9 + #10: order 8.

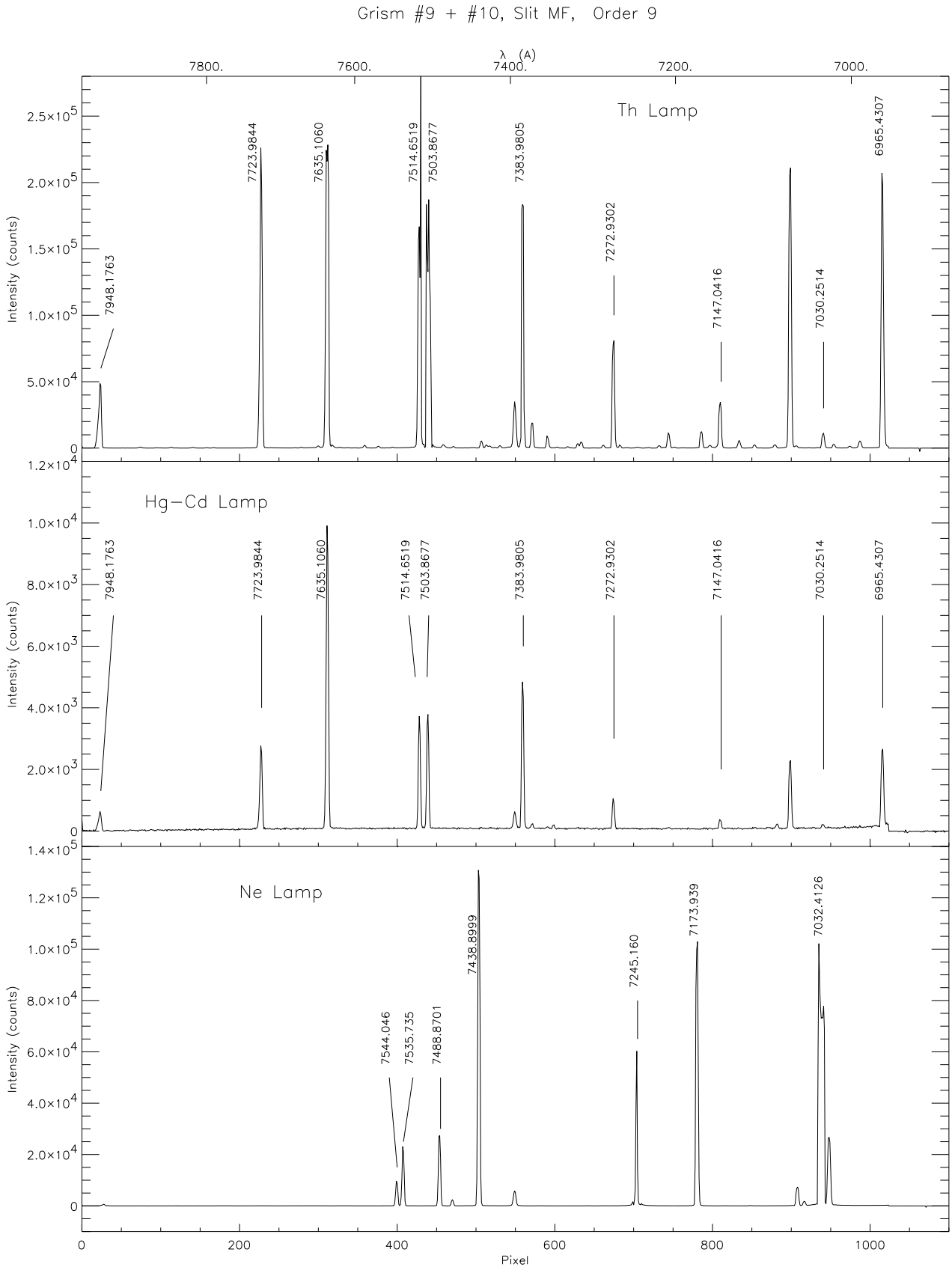

Figure C.21: Calibration spectra of Grism #9 + #10: order 9.

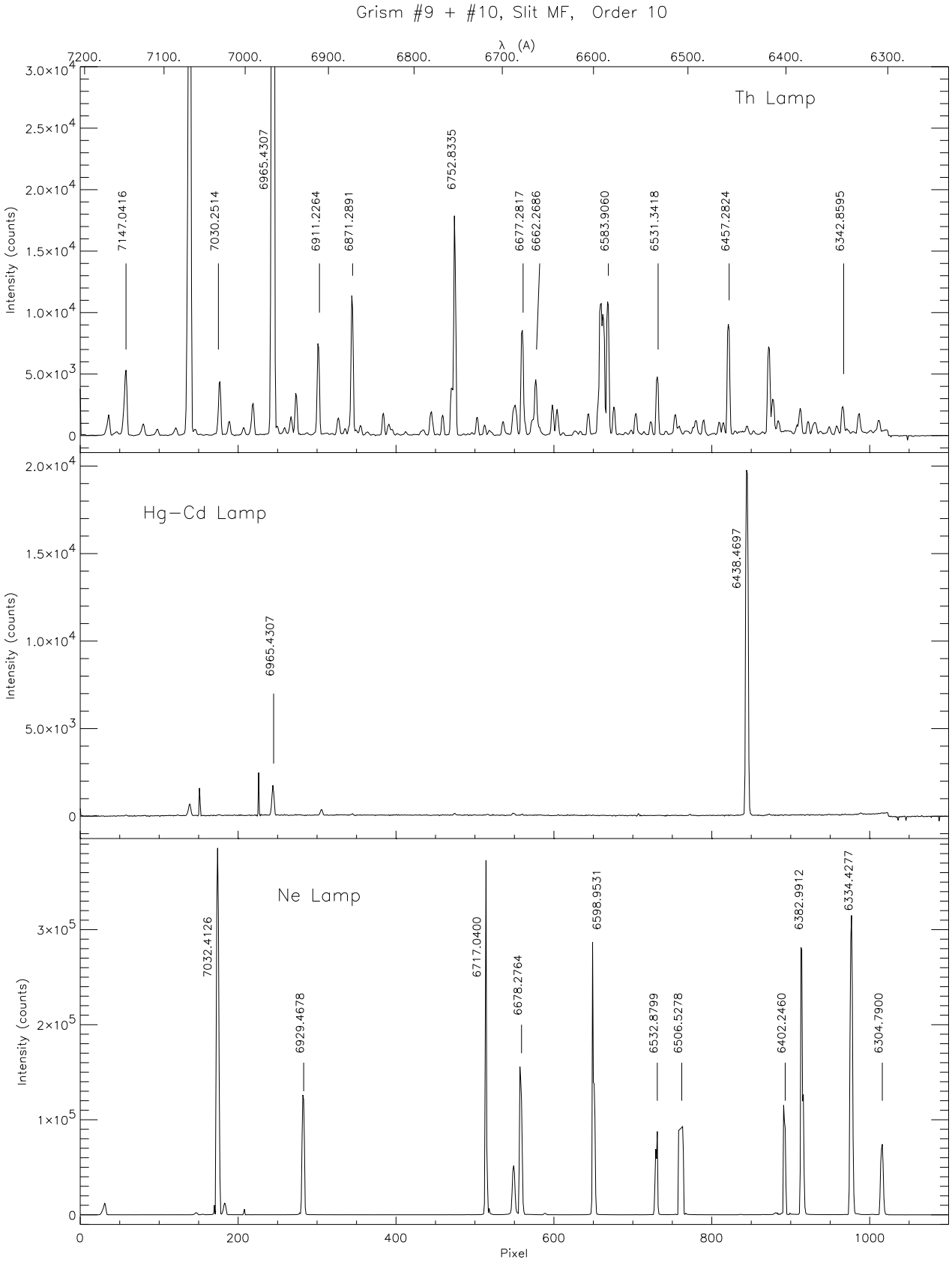

Figure C.22: Calibration spectra of Grism #9 + #10: order 10.

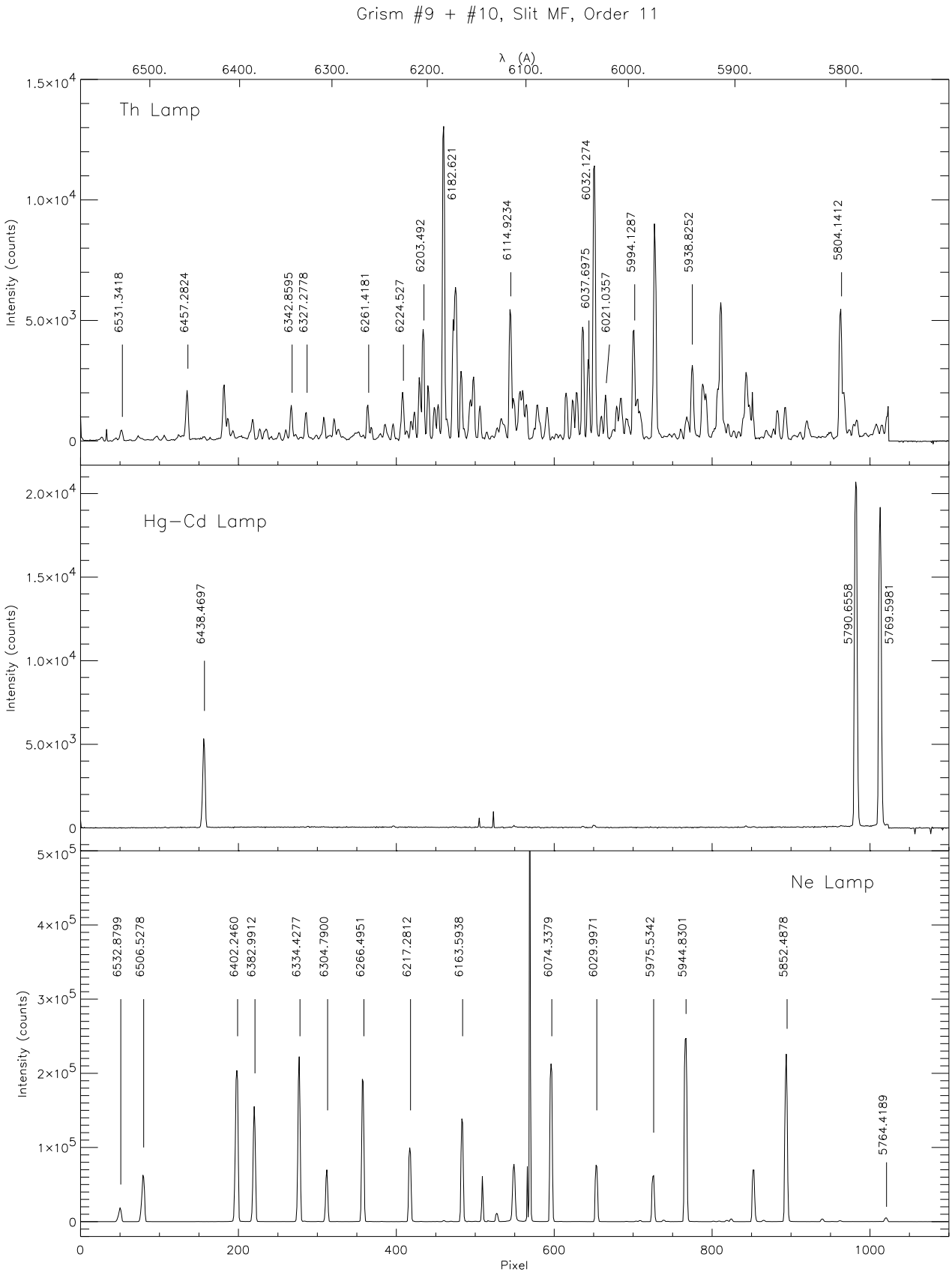

Figure C.23: Calibration spectra of Grism #9 + #10: order 11.

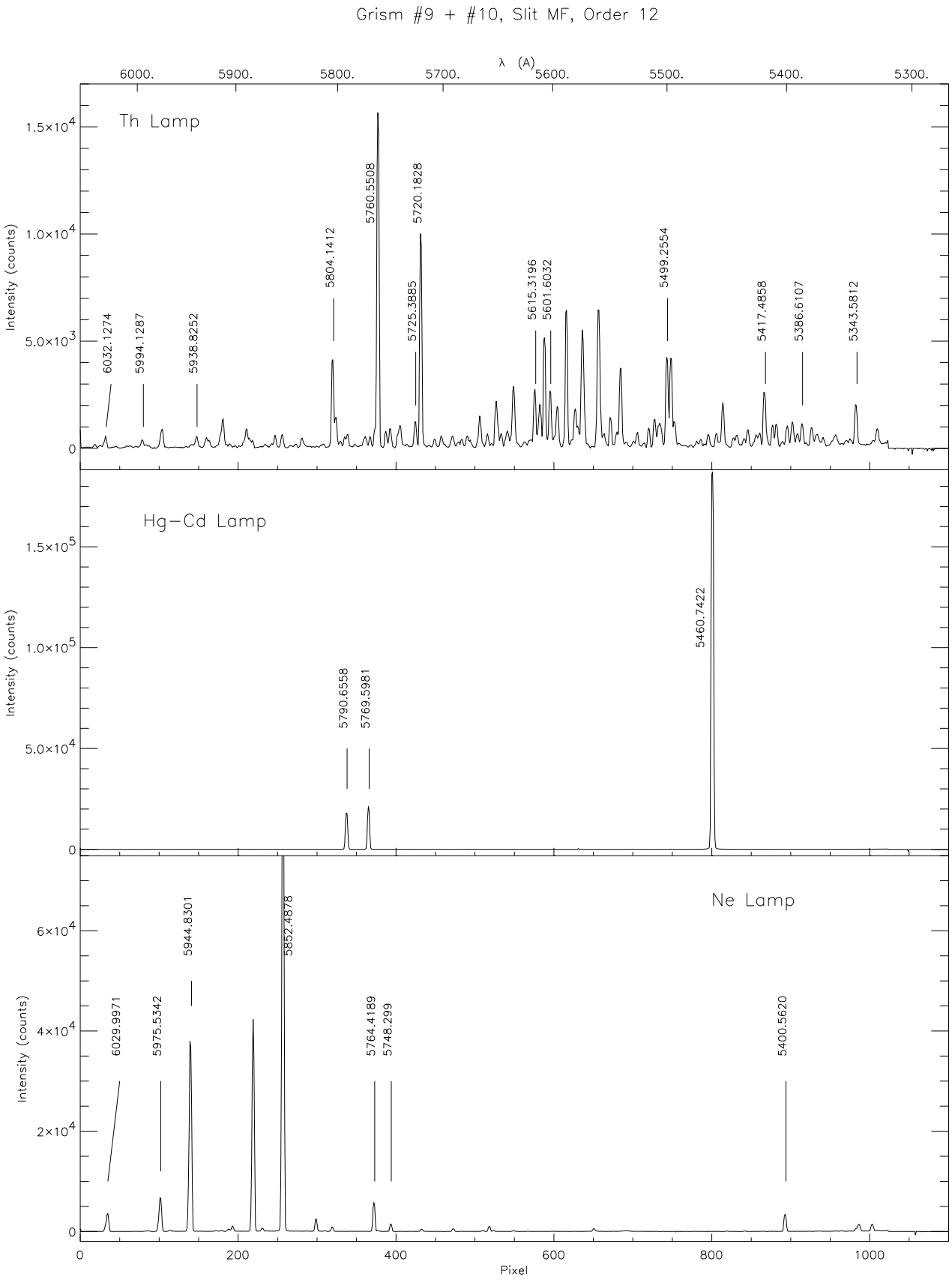

Figure C.24: Calibration spectra of Grism #9 + #10: order 12.

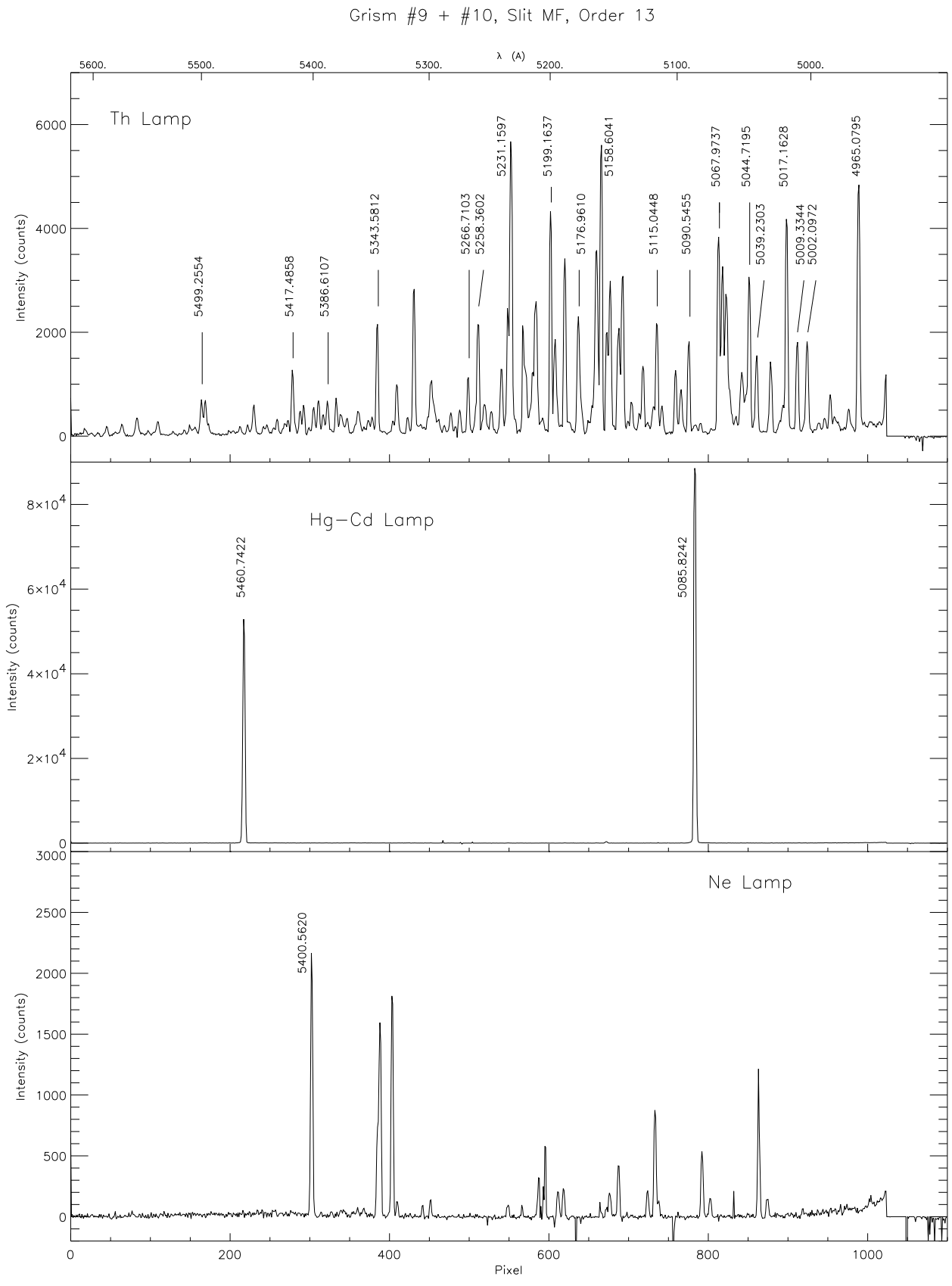

Figure C.25: Calibration spectra of Grism #9 + #10: order 13.

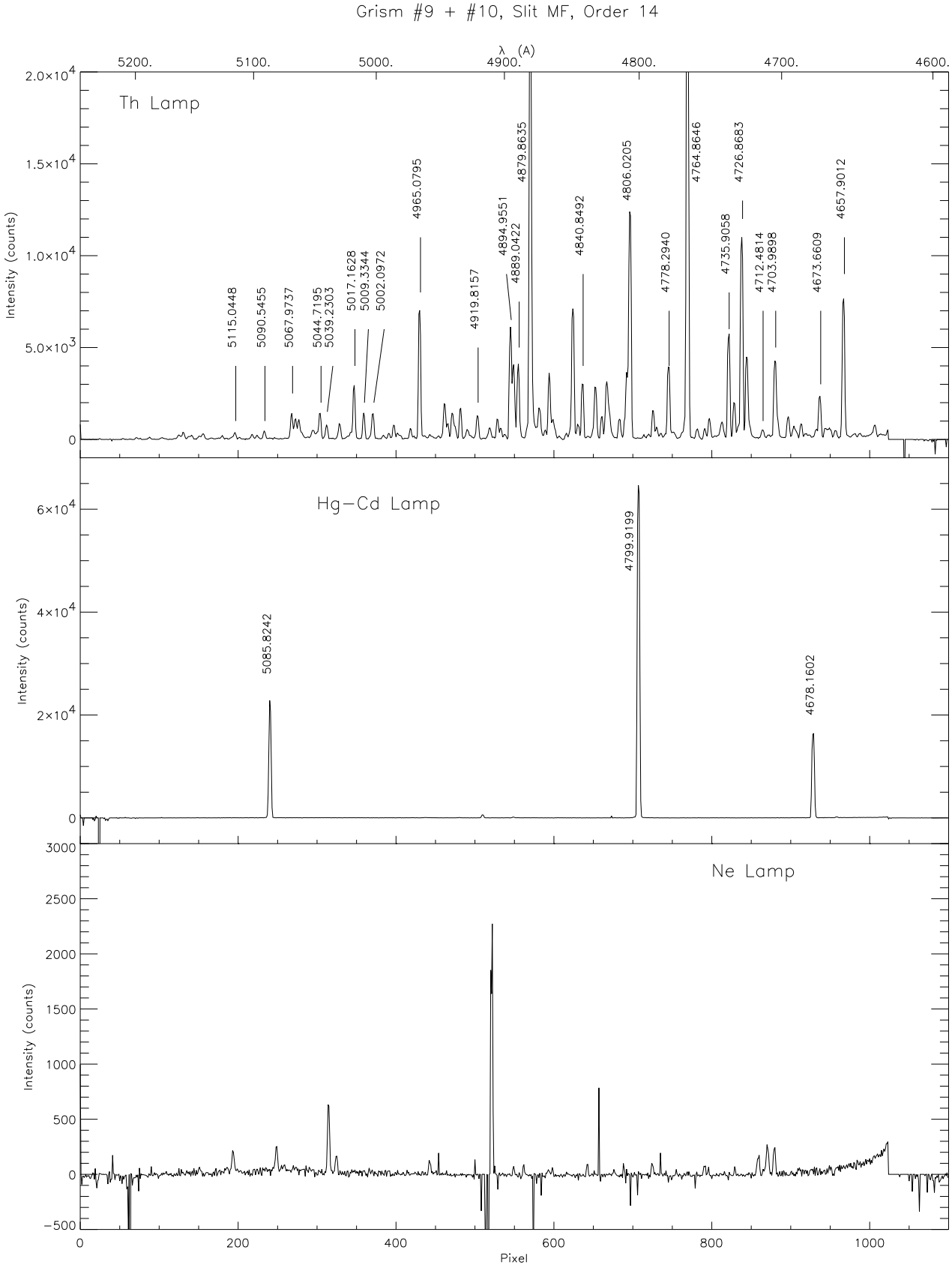

Figure C.26: Calibration spectra of Grism #9 + #10: order 14.

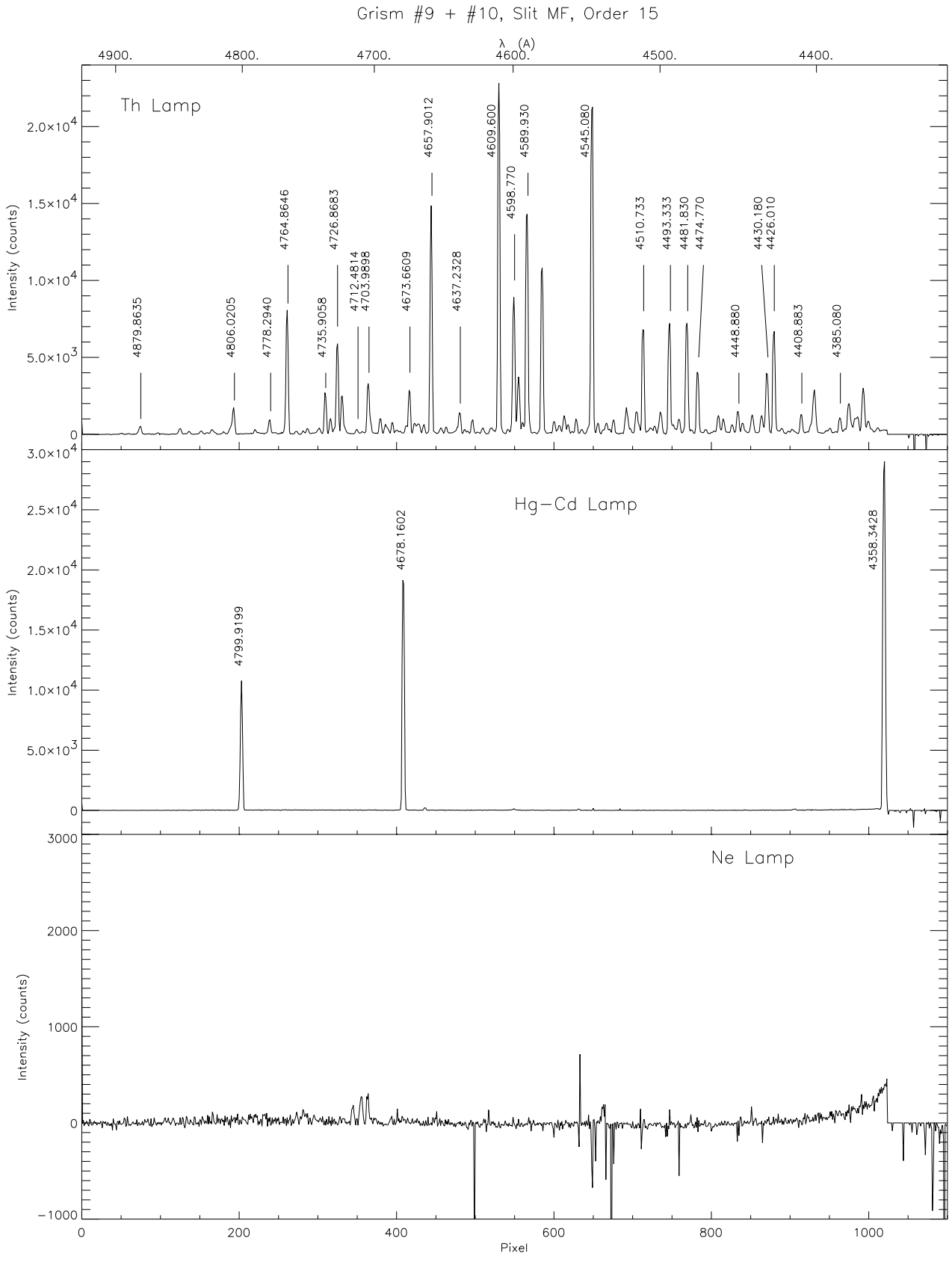

Figure C.27: Calibration spectra of Grism #9 + #10: order 15.

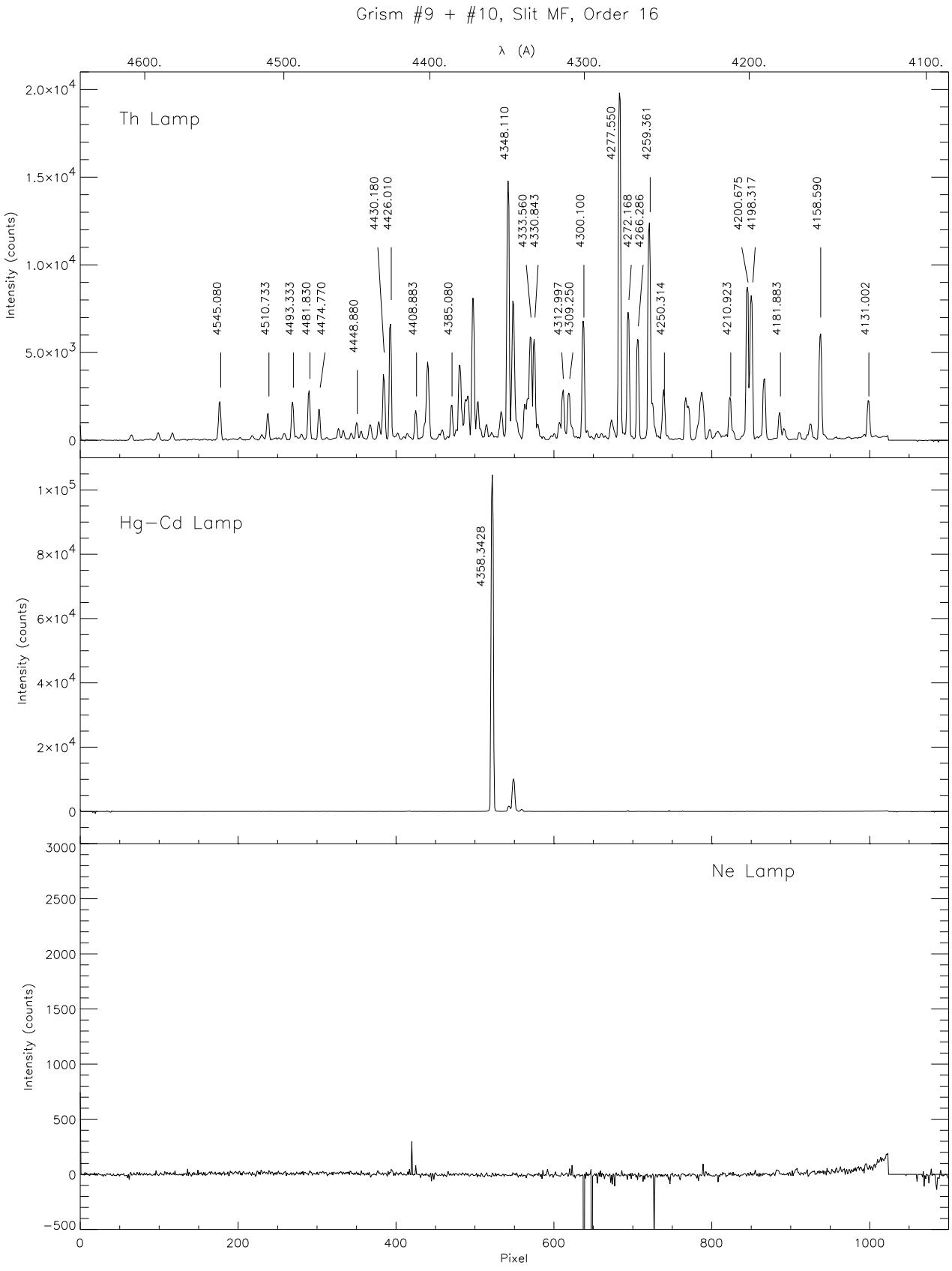

Figure C.28: Calibration spectra of Grism #9 + #10: order 16.

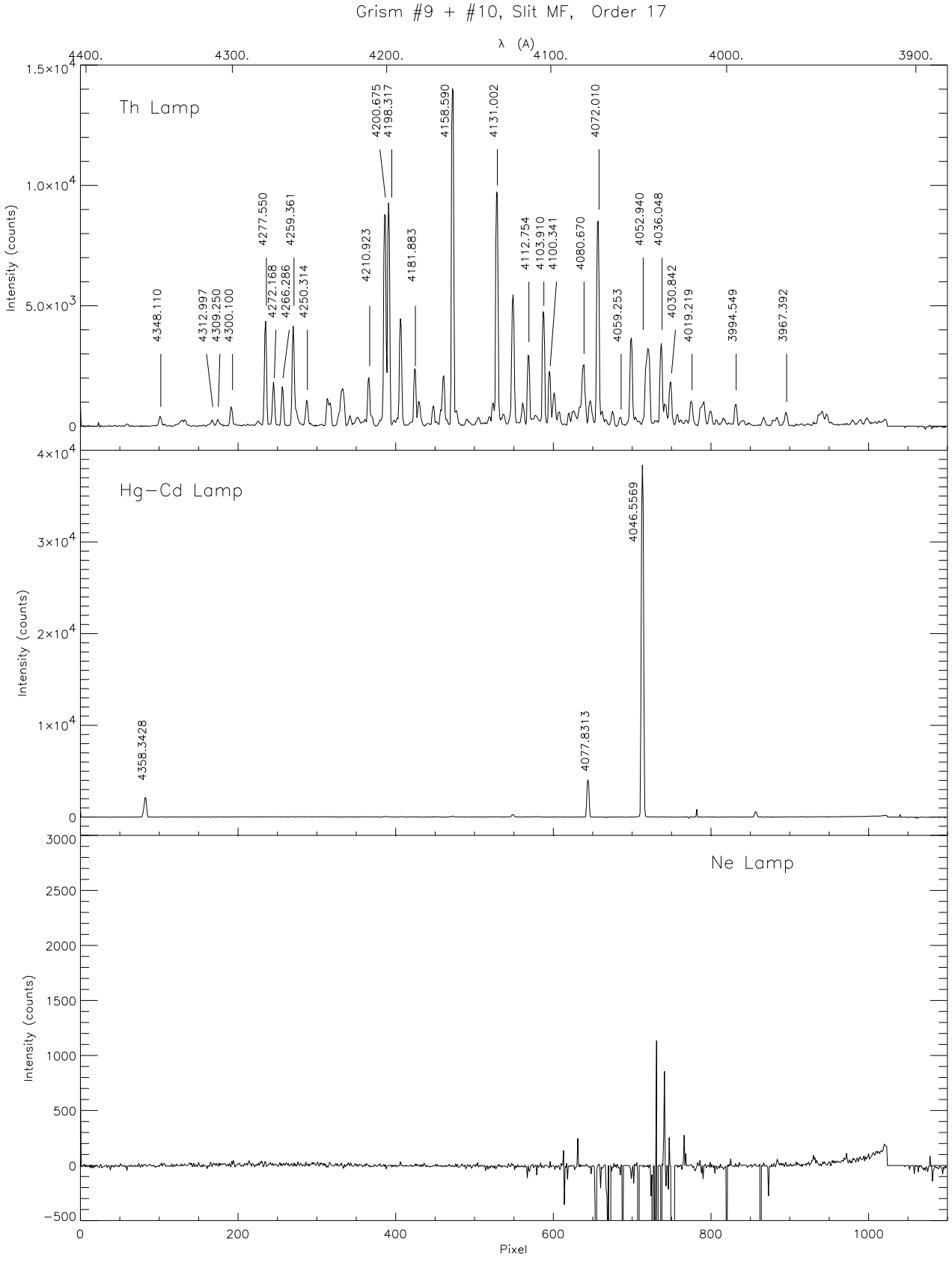

Figure C.29: Calibration spectra of Grism #9 + #10: order 17.

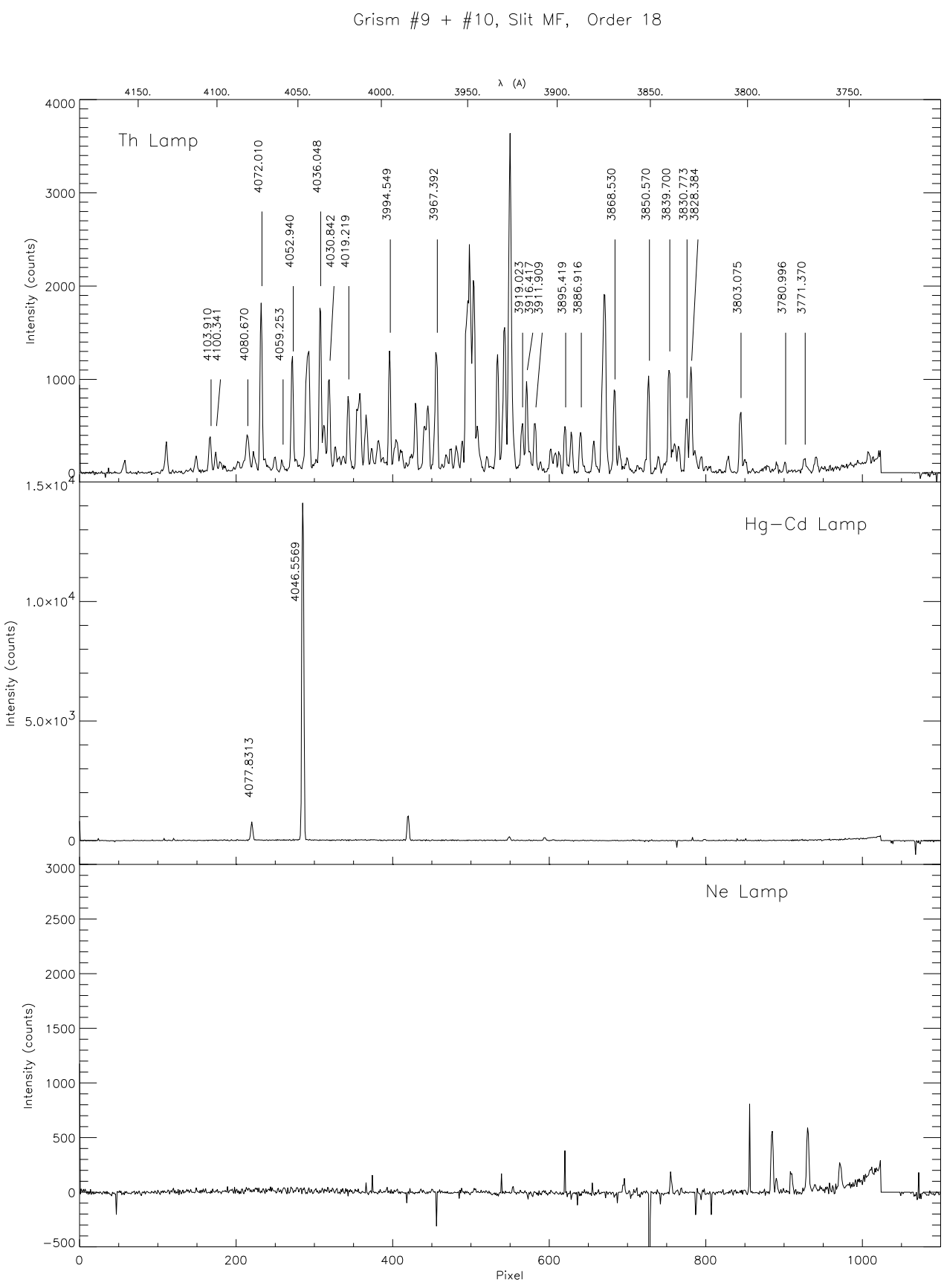

Figure C.30: Calibration spectra of Grism #9 + #10: order 18.

Appendix D

The FITS Header

```
SIMPLE  =                    T / Written by IDL: Tue Jan 8 02:18:51 2002
BITPIX  =                   16 /
NAXIS   =                    2 /
NAXIS1  =                 1100 /
NAXIS2  =                 1100 /
DATE-OBS= '08/01/02'             / Date of data acquisition
DATE    = '2002-01-08'           / Date file was written
EXPSTART= '01:16:46'             / UT at start exposure
JD      = '2452282.55331'        / JD at start exposure
SID-TIME= '09:12:46'             / ST at start exposure
EXPTIME =                 60.0 / exposure time in seconds
RA      = '10:28:01.19'          / Telescope position R.A.
DEC     = '+48:47:56'            / Telescope position Dec
AIRMASS =              2.569295 / Telescope airmass
TELESCOP= 'Mt. Ekar 182 cm. Telescope' /
INSTRUME= 'Afosc Camera'         /
ORIGIN = 'Padova Astronomical Observatory' /
IMAGETYP= 'OBJECT'               /
POSTNRA = '10.466997222222'      / Telescope position R.A.
OBJECT = 'HD90508/sp/pol/g8/0' /
OBSERVER= 'Giro E.'              /
FILTER = 'POL'                   /
GRAT_ANG= ''                     /
GRAT_TYP= 'GR08'                 /
SLIT    = 'SP25'                 /
CAMERA =                  15300 /
POS-ANG =               0.00000 /
DETECTOR= 'tektronix 1kx1k' /
COMMENT1= ''                     /
COMMENT2= ''                     /
COMMENT3= ''                     /
CRPIX1  =                    1 /
CRVAL1  =                    1 /
```

```
CRPIX2  =                    1 /
CRVAL2  =                    1 /
BS01    =          13.022181 /vrd
BS04    =          23.078432 /vdd
BS06    =         0.51316601 /vlg
CCD_TEMP=         -85.569008 /CCD temperature
AFTEMP  = ' 2.4'             /AFOSC temperature (C)
SERRTEMP= ' 0.3'              /Serrourier temperature (C)
M1TEMP  = ' 3.0'             /Primary mirror temperature (C)
OUTTEMP = ' -1.6'             /outdoor temperature (C)
HUMIDITY= ' 25.0'             /Outdoor humidity (%)
END
```

WARNING: The AIRMASS keyword is not reliable

Appendix E

Empty Fields

Field	α (2000)	δ (2000)	Remarks
BLANK 1	04 29 44.9	+54 15 35.5	
9090–7	09 12 00.2	-07 50 47.0	
CT1	10 06 59.3	-02 33 40.0	
CT5	12 28 43.3	-06 55 03.8	
SPKS 01	12 30 38.9	-08 03 27.8	one bright star
CT2	12 57 33.0	-02 23 16.0	
SPKS 11	13 06 55.9	+29 34 47.9	
SER 1	15 15 48.1	-00 42 49.8	
SPKS 12	16 52 33.2	-15 25 56.6	no stars
SPKS 09	18 04 40.0	-04 32 21.4	
SPKS 13	19 21 28.9	+12 27 49.0	
SPKS 14	21 29 34.4	-08 38 30.8	
2345+007	23 48 19.5	+00 57 20.4	
BLANK 6	23 56 40.3	+59 44 59.8	

Table E.1: Empty fields for sky flats.

Appendix F

Target Observability

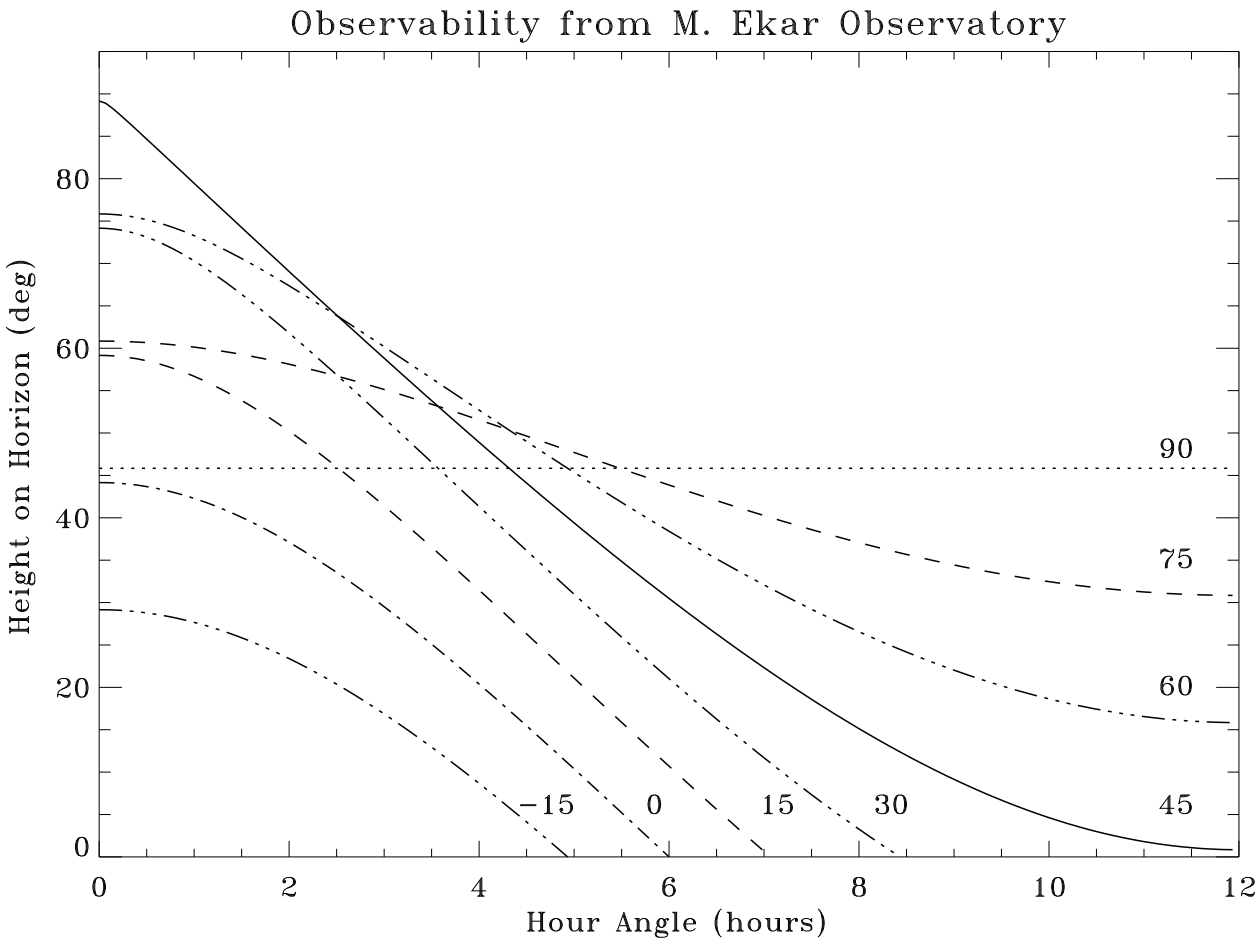

Figure F.1: Height of the horizon at M. Ekar Observatory for targets of declination $\delta = -15, 0, +15, +30, +45, +60, +75, +90$ as a function of the hour angle.

Appendix G

Almanacs and Manuals in Control Room

The following astronomical almanacs, manuals, technical documents are available in control room:

- The AFOSC User Manual (this manual)
- The Astronomical Almanac of the current year
- A list of photometric standards (Landolt 1992)
- A list of spectrophotometric standards
  (from www.eso.org/observing/standards/spectra)
- A list of polarimetric standards
  (from http://www.jach.hawaii.edu/JACpublic/UKIRT/instruments/irpol/irpol_stds.html)
- 9599-3200 Å atlas for the Asiago Echelle spectrograph (Munari & Zwitter 1994)

References

- Andersen M.I., Freyhammer L., Storm J., 1995, in *Proceedings of an ESO/ST-ECF workshop on calibrating and understanding HST and ESO instruments* P. Benvenuti ed., pag. 87
- Barbieri C. & Galazzi L., 1973, in *Atti delle celebrazioni del V Centenario della nascita di Nicoló Copernico*
- Bonanno G., Bruno P., Cosentino R., Scuderi S., Bortoletto F., D'Alessandro M., Bonoli C., Fantinel D., Carbone A., Evola, G., 2000, in *Optical Detectors for Astronomy II: State-of-the-Art at the Turn of the Millenium. 4th ESO CCD Workshop*, Amico P. and Beletic J.W. eds., pag. 389
- Claudi R.U., 1998, Document AFOSC-007
- Giro E., Pernechele C., Desidera S., Chiomento V., Frigo A., Traverso L., Molinari E., Conconi P., Crimi G., Bianco A., 2002, *First tests with VPH Grisms from AFOSC*, Padova and Asiago Observatories, Technical Report n. 20
- Landolt A.U., 1992, AJ 104, 340
- Munari U., 1988, Technical Report, Padova and Asiago Observatories
- Munari U. & Zwitter, 1994, *9599-3200 Å atlas for the Asiago Echelle spectrograph*, Technical Report n.4, Padova and Asiago Observatories
- Pernechele C., Bortoletto F., Fantinel D., Giro E., 2000, PASP 112, 996
- Pernechele C. & Giro E., 2002, in Astronomical Telescopes and Instrumentation, SPIE Proc., in press

Acknowledgements

We thank Claudio Pernechele for the supervision of this work and the contributions on AFOSC optics; Maurizio D'Alessandro for many useful suggestions for CCD testing; Riccardo Claudi, who provided "historical" documentation on AFOSC; S. Benetti, R. Falomo and D. Bettoni for a careful reading of an earlier version of the manual and for many suggestions; S. Benetti for providing the list of empty fields; Alessandro Pizzella for providing the original files of DFOSC manual.

The whole M. Ekar Observatory staff (V. Chiomento, L. Contri, A. Frigo, A. Gianesini, G. Lessio, G. Martorana., M. Rebeschini, I. Rigoni, L. Rigoni, I. Stefani, D. Strazzabosco, L. Traverso) gave continuous support during the tests described in this manual.

Many observers gave useful suggestions about the content of this manual during its preparation.